Arab Academy for Science and Technology and Maritime Transport
College of Engineering & Technology
Electrical and Control

Power Quality Analysis of a Grid Connected PV System

M.Sc. thesis

By:

Eng. Basem Abd-El Hamid Rashad Abd-El Razek

This Thesis is submitted to the Faculty of Engineering- Arab Academy for Science and Technology and Maritime Transport in Partial Fulfillments of the Requirements for The Degree of Master of Science in Electrical and Control Engineering

Supervised by:

Prof Dr. Almoataz Y. Abdelaziz
Department of Electrical Power & Machines
Faculty of Engineering, Ain Shams University

Dr. Hadi Maged El- Helw

Department Electrical Power and Computer Control
Arab Academy for Science and Technology

Cairo 2014

Arab Academy for Science and Technology and Maritime Transport
College of Engineering & Technology
Electrical and Control

Power Quality Analysis of a Grid Connected PV System

M.Sc. thesis

By:

Eng. Basem Abd-El Hamid Rashad Abd-El Razek

This Thesis is submitted to the Faculty of Engineering- Arab Academy for Science and Technology and Maritime Transport in Partial Fulfillments of the Requirements for The Degree of Master of Science in Electrical and Control Engineering

Supervised by:

Prof Dr. Almoataz Y. Abdelaziz
Supervisor

Dr. Hadi Maged El- Helw
Supervisor

Examination committee:

Prof Dr. Ahmed Abd- Elsattar
Examiner

Prof Dr. Said M. Wahsh
Examiner

Cairo 2014

STATEMENT

This thesis is submitted to Arab Academy for Science and Technology and Maritime Transport in Partial Fulfillments of the Requirements for M.Sc. degree in Electrical and Control Engineering. The included work in this thesis has been carried out by the author at the Electrical and Control department, Arab Academy. No part of this thesis has been submitted for a degree or a qualification at other university or institute.

Name: Basem Abd-El Hamid Rashad Abd-El Razek

Signature:

Date: / /

DEDICATION

To my parents, my brothers, wife, and lovely kids

Basem Abd El-hamid Rashad Abd-el razek

ACKNOWLEDGMENTS

At the beginning, I thank **ALLAH** for giving me the strength and health to let this work see the light.

I wish to express my deepest gratitude to my advisors, **Prof Dr. Almoataz Y. Abdelaziz** & **Dr. Hadi Maged El- Helw** , for his professional assistance, support, advice and guidance throughout my thesis, and to my discussion committee, **Prof Dr. Ahmed Abd- Elsattar,** And **Prof Dr. Said M. Wahsh** for their acceptance to discuss my thesis.

Many thanks for head of Electrical and Control Department, **Prof Dr. Rania El- Sharkawy,** for their support and cooperation.

I would also like to extend my gratitude to my family, my brothers, and my wife, for providing all the preconditions necessary to complete my studies. They have been always behind me throughout my academic career.

I am extremely grateful and thankful to my wife and my lovely kids **Malak & Ahmed** for giving me their support, love and encouragement.

Abstract

Power Quality Analysis of a Grid Connected PV System

Recently, the use of a grid-connected photovoltaic (PV) system has increased in order to meet the rising demand of electrical energy. This needs to improve the materials and methods used to harness this power source. Several approaches are proposed in order to accomplish the maximum power point tracking for a PV array such as; Perturb and Observe, Incremental Conductance, open circuit voltage, short circuit current, fuzzy or neural based etc. Among all of these techniques those based on Artificial Inelegance are very efficient nevertheless they are more complicated. The controller may be conventional or intelligent such as Fuzzy Logic Controller (FLC). FLCs have the advantage to be relatively simple to design as they do not require the knowledge of the exact model and work well for nonlinear system. The advantage of FLC is that the linguistic system definition becomes the control algorithm.

In this thesis, a PV model is used to simulate actual PV arrays behavior, and then the performance of three maximum power point tracking techniques is evaluated for grid-connected PV system in order to control the DC-DC converter. The methods used for comparative study are (i) Perturb & observe (P&O) (ii) Incremental conductance technique (ICT) and (iii) Fuzzy logic based (FLC). Voltage-Sourced Converter (VSC) technique is applied on the three phase inverter so that the output voltage of the converter remains constant at any required set point which facilitates the maximum power point process.

A grid-connected complete PV model is generated to simulate the actual life case. The proposed FLC algorithm is compared with the conventional hill climbing based techniques. The grid disturbances effects on a grid connected PV array were studied while considering different maximum power point tracking algorithms. The grid disturbances involved in this thesis are the different types of faults, voltage sag, and voltage swell. A comparative study of the grid disturbances effect on the three maximum power point tracking algorithms is discussed.

Simulation results show that the proposed FLC algorithm gives least oscillations around the final operating point and gives faster response than the conventional hill climbing based techniques under rapid variations of operating conditions. Also the VSC inverter control scheme shows fast response and that facilitates the maximum power tracking process with the grid connection.

Furthermore, the simulation results under steady state condition show the effectiveness of the MPPT on increase the output power of the PV array for the three techniques. However the FLC algorithm offers accurate and faster response compared to the others. The simulation results under transient conditions show that, the output power injected to grid from PV array is approximately constant while utilizing the proposed FLC and the PV system can still connect to grid and deliver power to grid without any damage to the inverter switches.

Contents

List of Tables

List of Figures

List of Abbreviations

PV	**Photovoltaic**
R_s	**Array series resistance**
R_p	**Array parallel resistance**
N_s	**Number of series modules**
N_p	**Number of parallel modules**
I	**Output current of the array**
V	**Output voltage of the array**
I_m	**Module current**
a	**Diode ideality constant**
V_t	**Thermal voltage**
N_{cs}	**Number of cells connected in series**
q	**Electron charge**
k	**Boltzmann constant**
T	**Temperature of the P-N junction in Kelvin's**
I_{pv}	**Photovoltaic current**
I_o	**Reverse leakage current of the diode**
I_{pvn}	**Nominal photovoltaic current at 25°C and 1000 W/m^2**
K_i	**Current temperature confidents**
K_v	**Voltage temperature confidents**
G	**Irradiance (W/m^2)**
G_n	**Irradiance at nominal conditions**
I_{scn}	**Short circuit current at nominal conditions**
V_{ocn}	**Open circuit voltage at nominal conditions**
Δ T	**Difference between the actual and the nominal temperatures in Kelvin's**
D	**Duty-Cycle**
MPP	**Maximum Power Point**
MPPT	**Maximum Power Point Tracking**
FLC	**Fuzzy Logic Controller**
P&O	**Perturbation and Observation**
ICT	**Incremental conductance technique**
VSC	**Voltage Source Converter**
PWM	**Pulse Width Modulation**

CHAPTER 1

INTRODUCTIOIN

1.1 INTRODUCTION

The usage of the grid-connected photovoltaic (PV) system has improved in order to meet the rising request of electrical energy. The non-linear characteristics of the PV array and the dependency of its output power on the array terminal voltage for the same environmental conditions make the task of efficiently utilizing the power generated by PV array challenging. When many such PV modules are connected in series and parallel combinations we get a PV array, that suitable for obtaining higher power output.

The applications for PV energy are increased, and that need to improve the materials and methods used to harness this power source. Main factors that affect the efficiency of the collection process are PV efficiency, intensity of source radiation and storage techniques. The efficiency of a PV is limited by materials used in PV manufacturing. It is particularly difficult to make considerable improvements in the performance of the cell, and hence controls the efficiency of the overall collection process. Therefore, the increase of the intensity of radiation received from the sun is the most attainable method of improving the performance of solar power.

There are two major methodologies for maximizing power extraction in solar systems. They are sun tracking, maximum power point (MPP) tracking or both. These methods need controllers which may be intelligent such as fuzzy logic controller or conventional controller such as Perturb & Observe method and Incremental Conductance method. The advantage of the fuzzy logic control is that it does not strictly need any mathematical model of the plant. It is based on plant operator experience, and it is very easy to apply. Hence, many complex systems can be controlled without knowing the exact mathematical model of the plant. In addition, fuzzy logic simplifies dealing with nonlinearities in systems. The most popular method of implementing fuzzy controller is using a general-purpose microprocessor or microcontroller.

Later on in this thesis, three tracking algorithms are studied and compared on steady-state and transient conditions. The first algorithm is based on P&O, the second is based on ICT and the third is based on FLC algorithm. Also a complete grid connected structure is proposed along with a DC-AC inverter control technique based on VSC (Voltage-Sourced Converter).

1.2 MOTIVATION

Renewable energy is the energy which is collected from the natural resources like sunlight, wind, tides, geothermal heat etc. As these resources can be naturally replaced, for all practical purposes, these can be considered to be limitless unlike the narrowing conventional fossil fuels. The global energy crisis has provided a renewed impulsion to the growth and development of clean and renewable energy sources. Another advantage of utilizing renewable resources over conventional methods is the significant reduction in the level of pollution associated. The cost of conventional energy is rising and solar energy has emerged to be a promising alternative. They are abundant, pollution free, distributed throughout the earth and recyclable. PV arrays consist of parallel and series combination of PV cells that are used to generate electrical power depending upon the atmospheric specifies (e.g. solar insolation and temperature). Nowadays, fuzzy logic controllers have an efficient performance over the traditional controller researches especially in nonlinear and complex model systems. Modern manufactures began to apply these technologies in their applications instead of the traditional ones, due to the low cost and widely features available in these controllers.

In Egypt we have a big problem in electrical power generation, since our sources don't cover all consumer requirements, electrical power have high cost and many daily interruptions, so we need clean renewable energy sources such as solar energy. This motivated to implement FLC techniques to control the MPP of a grid connected photovoltaic systems.

1.3 OBJECTIVES

The main objectives of the thesis are building an FLC for maximizing the power output of the solar arrays and comparing the FLC technique with the hill climbing techniques. Then the grid disturbances effects on a grid connected PV array were studied while considering different maximum power point tracking algorithms.

The specific objectives include**:**

- Modeling of the PV array using the MATLAB/SIMULINK.

- Using model to obtain the MPPT of grid connected PV array considering different techniques.
    - P&O method.
    - ICT method.
    - Fuzzy logic method.
- The grid disturbances effects on a grid connected PV array are studied while considering different maximum power point tracking algorithms. The grid disturbances involved in this thesis are the different types of :
    - Faults.
    - Voltage sags.
    - Voltage swells.

1.4 OUTLINE OF THE THESIS

The thesis consists of six chapters in which the MPPT problem is discussed in details and the proposed control schemes are fully explained. Also the grid disturbances effects on a grid connected PV array are studied while considering different maximum power point tracking algorithms. The grid disturbances involved in this thesis are the different types of faults, voltage sag, and voltage swell. A comparative study of the grid disturbances effect on the three maximum power point tracking algorithms is discussed.

Chapter two handles some basic principles of solar energy and especially on PV's and their types , equivalent circuits and characteristics. From which the MPPT problem originates.

Chapter three discusses the MPPT problem in details and shows different MPPT algorithms. Three MPPT techniques are discussed in details in this chapter (P&O, ICT and the proposed FLC) and also the role of **DC-DC** converters and **DC-AC** inverters is explained.

Chapter four In light of this definition of power quality, this chapter provides an introduction to the more common power quality terms. Along with definitions of the terms, explanations are included in parentheses where necessary. This chapter also attempts to explain how power quality factors interact in an electrical system.

Chapter five shows the simulation results for the grid connected PV system using P&O algorithm, ICT algorithm and the proposed FLC method, and the comparison between these algorithms is discussed. The grid disturbances effects on a grid connected PV array are studied while considering different maximum power point tracking algorithms. All the simulations are made using the **MATLAB/SIMULINK** computer software.

Finally in chapter six, an overall conclusion is presented and the outcomes of the thesis are stated.

CHAPTER 2

INTRODUCTION TO PHOTOVOLTAIC ENERGY

2.1 BACKGROUND

Renewable energy sources perform a significant role in electric power generation. There are various renewable sources which used for electric power generation, such as wind energy, PV energy, geothermal etc. P V energy is a good choice for electric power generation, since the PV energy is directly converted into electrical energy by photovoltaic modules. These modules are made up of semiconductor cells. When many such cells are connected in series and parallel combinations we get a solar PV module. The current rating of the modules increases when the area of the individual cells is increased, and vice versa. The increase of world energy request and the environmental concerns lead to an increase of the renewable energy production over the last decade. Energy sources such as solar, wind or hydro became more and more popular mainly because they produce no emissions and are limitless. PV energy is the fastest growing renewable source with a history dating since it has been first used as power supply for space satellites. The increased efforts in the semiconductor material technology resulted in the appearance of commercial PV cells and consequently made the PVs an important alternative energy source [1]. One of the major advantage of PV technology is the lack of moving parts which offers the possibility to obtain a long operating time (>20 years) and low maintenance cost. The main drawbacks are the high manufacturing cost and low efficiency (15-20 %). As one of the most promising renewable and clean energy resources, PV power development has been boosted by the favorable governmental support [2].One of the most important problems facing the world today is the energy problem. This problem is resulted from the increase of demand for electrical energy and raised of fossil fuel prices. Another problem in the world is the global climate change has increased. As these problems alternative technologies for producing electricity have received greater attention. The most important solution was in finding other renewable energy resources [3], [4].

2.1.1 Renewable Energy

Each year, the addition of persons to world will increase and the resources required to support them will also increase. Of the resources, one of the most dynamic to support the technological advancing population is energy.

The energy crisis became transparent in the late 1900's and birthed the desire to find additional energy resources to meet rising energy demands [5].One choice was to increase generation of currently used energy sources such as nuclear, fossil fuel, etc. The other was to explore new renewable energy alternatives. Many different renewable energy sources have appeared as feasible solutions and each one of them has their own positive and negative attributes. As a whole, renewable energy sources all share the fact that their fuel is primarily free and they produce minimal to no waste. These factors are the main motivation for countries to begin incorporating renewable into their energy collection.

A predictable 19% of global energy consumption in 2013 was supplied by renewable energy [6]. One more analysis of where the world's energy came from in 2013 is shown in Fig.2.1. Only 19% of global energy coming from renewable may not seem to be a vast amount; however in 2013 nearly half of the new electric power capacity installed was from renewable alone. The percentage of energy from renewable has increased every year for the past several years, and is predicted to continue with this trend in the future.

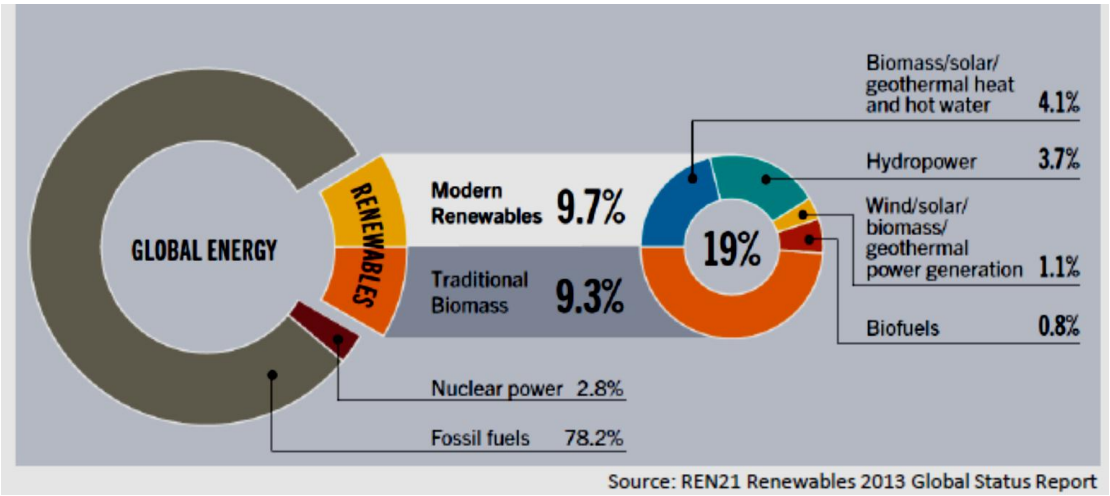

Fig. 2.1: Renewable energy share of global electricity production, 2013 [6].

Further analyzing Fig. 2.1, the largest source of energy used globally is fossil fuels [7]. Two of the largest other sources of energy are nuclear and hydropower. Fossil fuels are non-renewable and generate harmful pollution when burned for energy. Nuclear power plants have the potential to be a great energy source. However, they generate toxic nuclear waste that has to be buried and also always poses the risk of a meltdown, which could be catastrophic for the neighboring environment.

Hydropower generation requires damming a river or body of water, disrupting its natural flow, and completely changing the surrounding ecosystem. A form of renewable energy gaining recent popularity is solar [8]. Solar energy is one of the cleanest forms of energy available, converting energy from the sun to electricity without any waste or harmful by products.

2.1.2 Solar Energy

It's the energy which derivative from the sun through the form of solar radiation. Solar powered electrical generation relies on photovoltaic. A partial list of other solar applications includes space and water heating, solar cooking, and high temperature process heat for industrial purposes.

2.1.2.1 The Photovoltaic Resource

The PV energy is an extremely powerful energy; actually the earth's surface receives enough energy from the sun in one hour to meet its energy requirements for one year [8]. PV technology was originally created to power some of the first satellites used in space in the 1950's [7]. When the technology was in its early form its uses were limited, to such applications as space, due to economic practicality. However, in the last five years the PV market has experienced rapid growth. From 2010 to 2012 an additional 60 GW of new PV capacity was added globally, bringing the total world capacity to 100 GW [6]. Fig.2.2 shows the exponential increase, especially over the last five years of PV capacity.

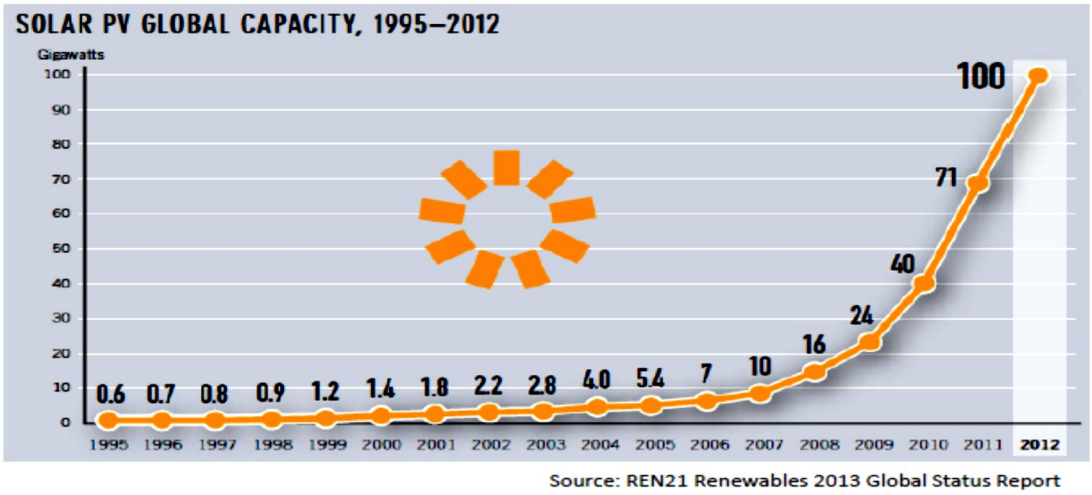

Fig.2.2: Total World Capacity of PV (1995-2012) [6].

The growth of installed PV can be recognized to many factors but the main reasons are increases in environmental considerations, new state laws and regulations, purchase incentives, increases in PV cell technology and efficiency, and decreases in overall system cost [7].

2.2 PHOTOVOLTAIC BACKGROUND

Solar panels are made up of photovoltaic cells; it means the direct conversion of sunlight to electricity by using a semiconductor, usually made of silicon [9], [10]. The word photovoltaic comes from the Greek meaning “light” (photo) and “electrical” (voltaic); the common abbreviation for photovoltaic is PV [11]. Then PV efficiency increased continuously in the following years, and costs have decreased significantly in recent decades. The main material used in the construction of PV cells is still silicon, but other materials have been developed, either for their potential for cost reduction or their potential for high efficiency [11]. Over the last 20 years the world-wide demand for PV electric power systems has grown steadily. The need for low cost electric power in isolated areas is the primary force driving the world-wide photovoltaic (PV) industry today. PV technology is simply the least-cost option for a large number of applications, such as stand-alone power systems for cottages and remote residences, remote telecommunication sites for utilities and the military, water pumping for farmers, and emergency call boxes for highways and college campuses [9]. PV cells are converting light energy, to another form of energy, electricity. When light energy is reduced or stopped, as when the sun goes down in the evening or when a cloud passes in front of the sun, then the conversion process stops or slows down. When the sunlight returns, the conversion process immediately resumes, this conversion without any moving parts, noise, pollution, radiation or constant maintenance. These advantages are due to the special properties of semiconductor materials that make this conversion possible. PV cells do not store electricity; they just convert light to electricity when sunlight is available. To have electric power at night, a solar electric system needs some form of energy storage, usually batteries, to draw upon [12].

2.3 PRINCIPLE OF PHOTOVOLTAIC SYSTEMS

Photovoltaic systems employ semiconductor cells, usually several square centimeters in size [13]. Semiconductors have four electrons in the outer shell, on average.

These electrons are called valence electrons [11]. When the sunlight hits the photovoltaic cells, part of the energy is absorbed into the semiconductor. When that happens the energy loosens the electrons which allow them to flow freely. The flows of these electrons are a current and when you put metal on the top and bottom of the photovoltaic cells. We can draw that current to use it externally, as shown in Fig. 2.3.

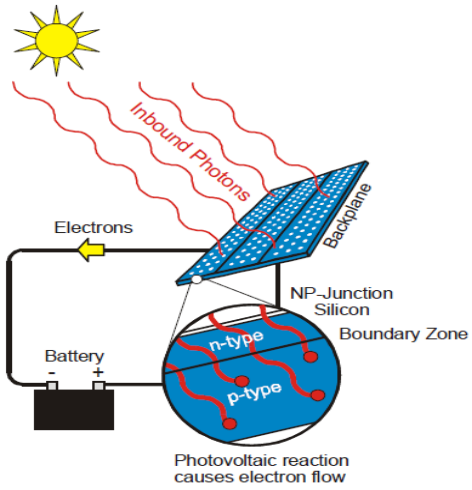

Fig.2.3: Principle of Photovoltaic cells.

Many cells are collected in a module to generate required power [13]. When many such cells are connected in series and parallel combinations we get a solar PV module, the current rating of the modules depends on the area of the individual cells. For obtaining higher power output the solar PV modules are connected in series and parallel combinations forming solar PV arrays.

2.4 TYPES OF PV CELLS

Over the recent decades, silicon has been used for manufacturing more than 80% of solar cells although other materials and techniques are developed. There are different types of solar cells which differ in their material, price, and efficiency, since the efficiency is the percentage of solar energy that is captured and converted into electricity. The efficiency values are an average percentage of efficiency, because it's difficult to give an exact number for the different types of solar panels output [10].

- Mono-crystalline Solar cells: They are made from a large crystal of silicon, see Fig.2.4. These types of solar cells are the most efficient as in absorbing sunlight and converting it into electricity. However they are the most expensive. They do somewhat better in lower light conditions than the other types of solar cells. Also, their efficiency is around 15% - 18%.

Fig.2.4: Mono-crystalline Solar Panels

- Polycrystalline Solar cells: This type of solar cell consists of multiple amounts of smaller silicon crystals, see Fig.2.5.This type is instead of one large crystal have efficiency approximately 15%.

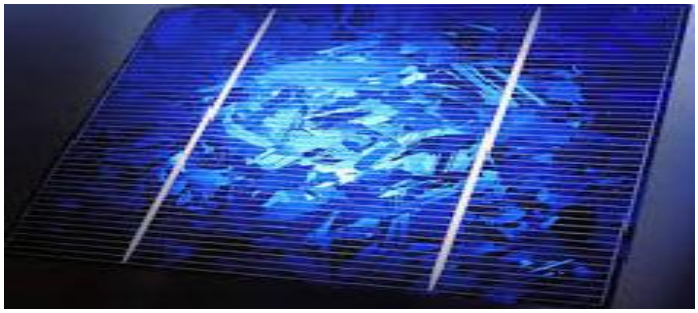

Fig.2.5: Polycrystalline Solar Panels.

They are the most common type of solar panels on the market today. They look a lot like shattered glass. They are slightly less efficient than the mono-crystalline solar cells and less expensive to produce.

- Amorphous Solar cells: This type is consisting of a thin-like film made from molten silicon that is spread directly across large plates of stainless steel or similar material, see Fig.2.6. One advantage of amorphous solar cells over the other two is that they are shadow protected.

That means when a part of the solar panel cells are in a shadow the solar panel continues to charge. These types of solar panels have lower efficiency than the other two types of solar panels, and the cheapest to produce. These work great on boats and other types of transportation [10]. The efficiency of this type is around 8-10%.

Fig.2.6: Amorphous Solar Panels.

2.5 EQUIVALENT CIRCUIT AND MATHEMATICAL MODEL

There are different mathematical models that can be used to model a PV array. From the solid-state physics point of view, the cell is basically a large area p-n diode with the junction positioned close to the top surface [13], [14]. So a practical solar cell may be modeled by a current source in parallel with a diode that mathematically describes the I-V characteristic.

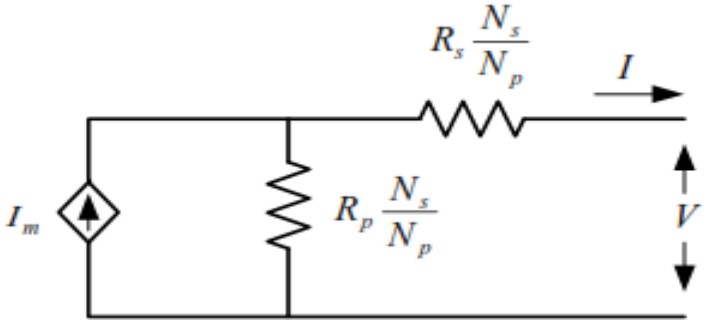

Fig. 2.7: Equivalent Circuit of PV module.

Where R_S is the array series resistance, R_p is the array parallel resistance [14], [15]. N_s and N_p are the number of series and parallel modules respectively, I and V are the output current and voltage of the array and I_m is the module current and can be obtained from the following equation:

$$I_m = I_{PV}N_p - I_0 N_p \left[exp\left(\frac{V + R_s\left(\frac{N_s}{N_p}\right)I}{V_t a N_s} \right) - 1 \right] \quad (2.1)$$

Where a is the diode ideality constant, V_t is the thermal voltage of the array and can be obtained from the equation [15]:

$$V_t = \frac{N_{cs} k T}{q} \quad (2.2)$$

N_{cs} is the number of cells connected in series, q is the electron charge, k is Boltzmann constant and T is the temperature of the P-N junction in Kelvin's. I_{pv} is the photovoltaic current and can be expressed by:

$$I_{pv} = (I_{pvn} + K_i \Delta T)\frac{G}{G_n} \quad (2.3)$$

and, Io is the reverse leakage current of the diode and can be calculated from [15]:

$$I_0 = \frac{I_{scn} + K_i \Delta T}{\exp\left(\frac{V_{ocn} + K_v \Delta T}{a V_t}\right) - 1} \quad (2.4)$$

Where: I_{pvn} is the generated current at 25°C and 1000 W/m^2 (nominal conditions). K_i, K_v the current and voltage temperature coefficients respectively, G is the irradiance and G_n is the irradiance at nominal conditions, I_{scn} ,V_{ocn} are the short circuit current and open circuit voltage respectively at nominal conditions and Δ T is the difference between the actual and the nominal temperatures in Kelvin's [15].

2.6 NON LINEAR CHARACTERISTICS VERIFICATION

The parameters of the PV model used in this thesis are adjusted according to a real PV module (Kyocera KC 200 GT) manufactured by Kyocera [16]. Fig.2.8 shows the I-V and P-V characteristics of the PV module at different irradiances and constant temperature (25°C) and Fig.2.9 shows the I-V and P-V characteristics of the PV module under constant irradiance and different temperature.

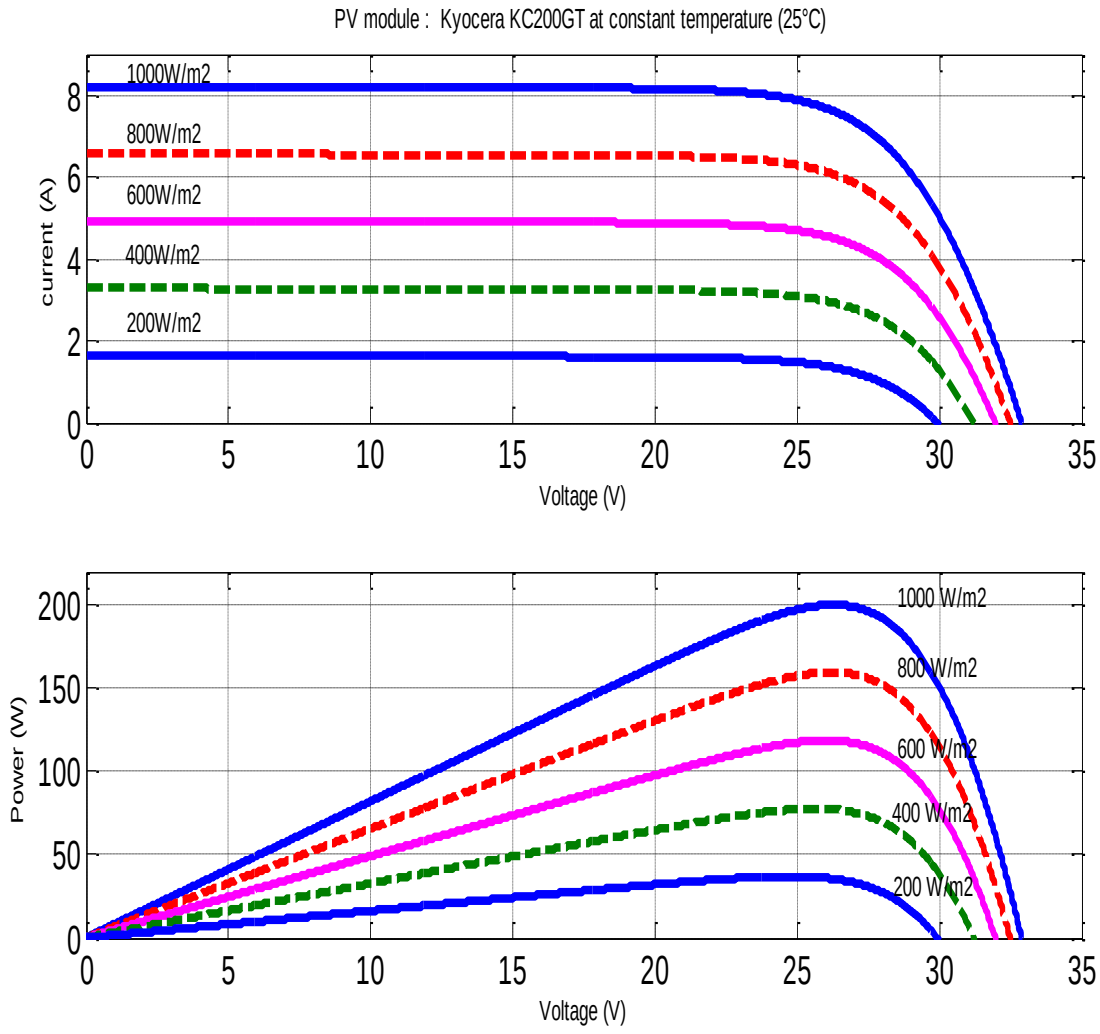

Fig.2.8: I-V and P-V characteristics of the PV module at constant temperature 25°C and various irradiances.

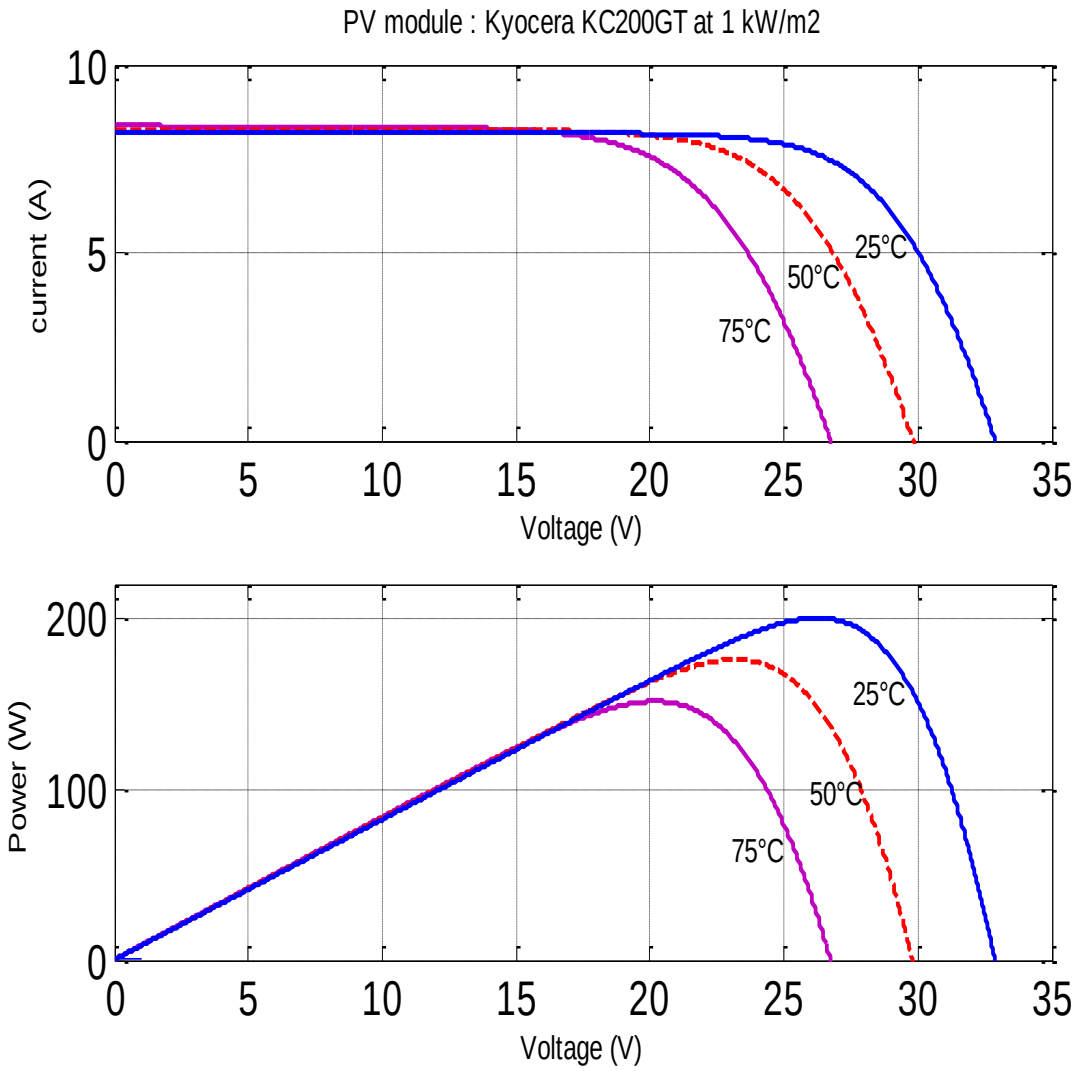

Fig.2.9: I-V and P-V characteristics of the PV module under constant irradiance and different temperature.

Fig. 2.8 and Fig. 2.9 are obtained by simulation and the results are similar to that shown in the PV module datasheet [16]. (See appendix A for the parameter and I-V curves of the PV module datasheet).

Fig.2.10 shows The I-V and P-V characteristics of the PV array (Kyocera KC200GT; 8 series modules; 63 parallel strings) at different irradiance (200,400,600,800,1000W/m^2) and constant temperatures (25°C).

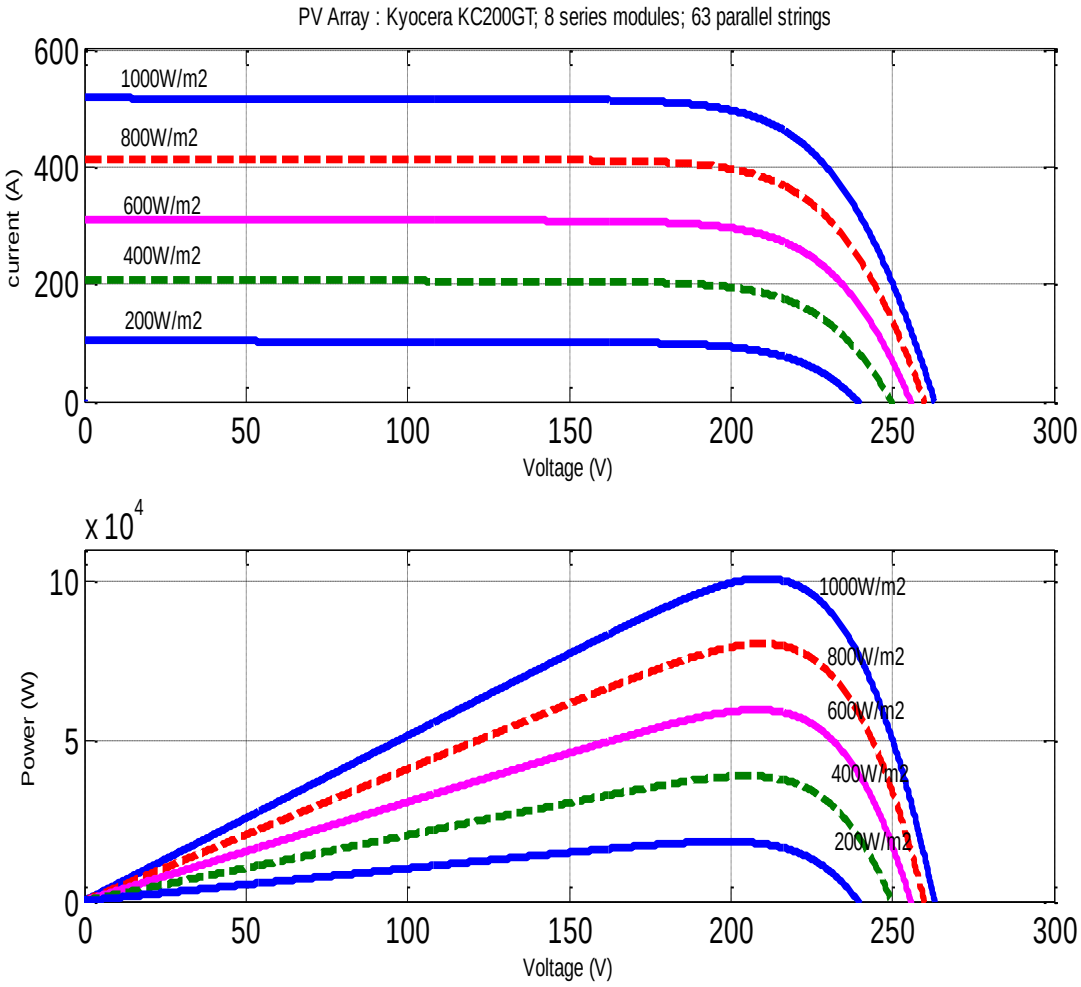

Fig.2.10: I-V and P-V characteristics at constant temperature 25^{o}C and various irradiances for the PV array. (Kyocera KC200GT; 8 series modules; 63 parallel strings)

Photovoltaic's have nonlinear characteristics, where the performance and output power are directly affected with the change of the operating conditions. It is clear from the previous figures that the output power of PV's is directly proportional with the amount of solar irradiance falling on it, and inversely proportional with its temperature. With the change of temperature and solar irradiance the point at which maximum power point can be obtained also changes.

This means that the array terminal voltage must be varied using DC-DC converters in order to track the maximum power point. Maximum power point tracking algorithms will be discussed in details in chapter 3.

2.7 PV APPLICATIONS

A photovoltaic application varies from solar farms that can generate hundreds of megawatts [9] to small residential rooftop systems that only generate a few kilowatts. The ability for PV systems to vary greatly in magnitude is a demonstration of how scalable and modular solar systems are looking at every type of solar application, at the highest level each one can be lumped into one of the two main types of PV system categories, either grid tied or off grid.

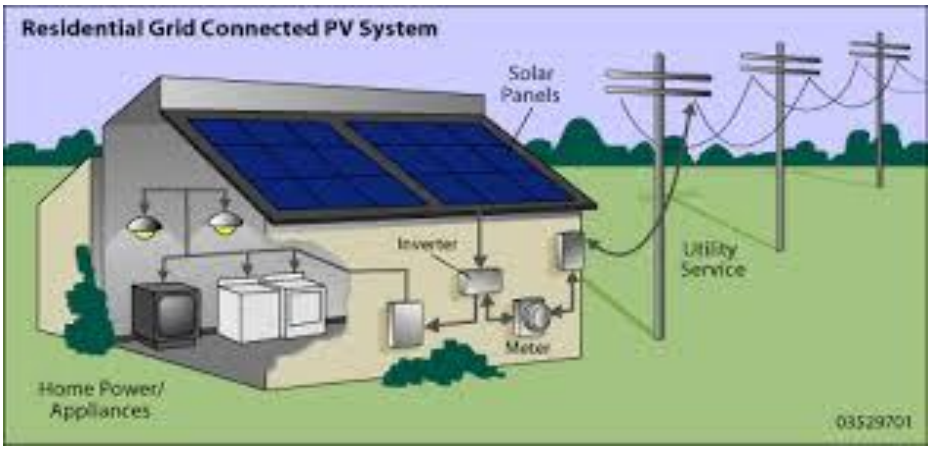

Fig.2.11: Typical grid - connected PV systems.

Off grid systems supply a local load and when the panel's generation exceeds the load the excess energy is usually stored in a battery system for later use. Grid tied systems are connected to the local utility network and can supply power back to the power grid when the panels generation exceeds the local loads demand. Some grid connected systems still have battery storage capability. For a residential system the local load is a home and everything inside consuming power. Both off grid and grid tied systems can help offset a customer's net energy consumption, but grid tied systems have the potential for the customer to sell back generated power at cost to the utility. Grid connected PV systems represent around 90 % of the total PV installed power. Grid connected distributed systems gained popularity in the last years, as they can be used as power generators for grid connected customers or directly for the grid. Different sizes are possible since they can be mounted on public or commercial buildings [17]. Grid connected systems produce and transform the power directly to the utility grid. The configuration is usually ground mounted and the power rating is above kW order [18].

The typical configuration of a PV system can be observed in Fig.2.11. Depending on the number of the modules, the PV array converts the solar irradiation into specific DC current and voltage. A DC/DC boost converter is used when the voltage required by the inverter is too low and to achieve the MPP. Energy storage devices can be included in order to store the energy produced in case of grid support connection. The power conversion is realized by a three-phase inverter which delivers the energy to the grid [19].

2.8 ADVANTAGES OF PV SYSTEMS

The advantages of photovoltaic [4] systems are**:**

- PV systems are considered static electricity generators as they create electricity directly from sunlight. They come prepackaged, ready to be mounted and wired. Modules contain no moving parts, eliminating service and maintenance needs.

- PV systems come in a range of sizes and output suitable for different applications. They are lightweight, allowing for easy and safe transportation.

- PV system can be easily expanded by adding more modules either in series to expand the system's voltage or in parallel to enlarge the current.

- PV systems are manufactured to withstand the most rugged conditions. Modules are designed to endure extreme temperatures, at any elevation, in high winds, and with any degree of moisture or salt in the atmosphere. Systems can be designed with storage capabilities to provide consistent, high-quality power even when the sun isn't shining.

- PV systems cause no noise or carbon emissions i.e. no pollution.

The drawbacks of photovoltaic [4] systems are**:**

- Very high manufacturing cost compared to other renewable resources.
- Maximum power point problems.
- Requires regular cleaning of its outer surfaces from dust.
- Significantly low in efficiency.

2.9 SUMMARY

In this chapter, an overview of the importance of renewable energy, and photovoltaic background and principle of photovoltaic systems are presented. The photovoltaic energy in particular is reviewed with cell type, equivalent circuit, mathematical model and model verification. The main PV system of a grid connected is also discussed and their advantages and disadvantages are mentioned.

CHAPTER 3

MPPT ALGORITHMS

3.1 REVIEW OF MAXIMUM POWER POINT TRACKING

A set of photovoltaic cells called the solar panel. Photovoltaic cells are devices which detect electromagnetic radiation and generate a current or voltage, or both, upon absorption of radiant energy. The output power of PV arrays is mainly influenced by the irradiance (amount of solar radiation) and temperature. Moreover for a certain irradiance and temperature, the output power of the PV array is function of its terminal voltage and there is only one value for the PV's terminal voltage at which the PV panel is utilized efficiently. The procedure of searching for this voltage is called maximum power point tracking MPPT. Recently, several algorithms have been developed to achieve MPPT technique such as; Perturb and Observe (P&O), incremental conductance, open circuit voltage, short circuit current, fuzzy or neural based etc [20], [21],. However, the insulation levels and the cell temperature determine only the limits of the best obtainable matching. The array voltage determines the real matching. This mismatch can be improved by the use of a MPPT controller to locate the local maximum power point in the **p-v** response range of the solar panel [22], Fig.3.1 shows the P-V characteristics of a practical PV array showing MPP.

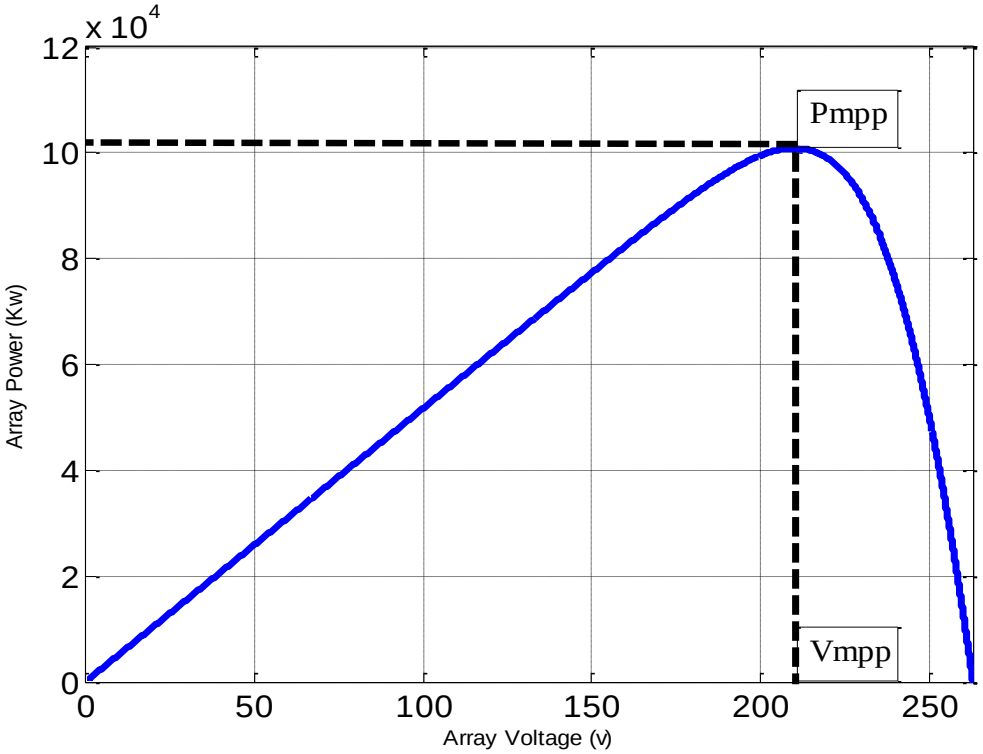

Fig.3.1: P-V characteristics of a practical PV array showing MPP.

From the simulation results, the PV array under constant temperature 25^{o}C and irradiances 1000 W/m^{2} for PV array. The maximum readings appear to be 210.4V, 479A and 100.8 kW. The absolute maximum current (short circuit current) is 517A and the absolute maximum voltage (open circuit voltage) is 263V.

3.2 MAXIMUM POWER POINT TRACKING

A PV panel has a nonlinear characteristics and its output power depends mainly on the irradiance (amount of solar radiation) and the temperature. Moreover for the same temperature and irradiance the output power of a PV panel is function of its terminal voltage. There is only one value for the terminal voltage that corresponding to maximum output power for each particular case. The procedure of searching for this voltage is called maximum power point tracking. Maximum power point tracking of a PV panel can be obtained either in a single stage or in a double stage. In the case of single stage, a DC/AC converter is utilized. On the other hand in case of double stage a DC/DC and DC/AC converters are utilized. The characteristics of PV shown in Fig.3.1 shows that the maximum power point for this particular panel lays at the values between approximately 75-80% of array's open circuit voltage. Consequently, in this thesis the maximum power point tracking algorithm scans the P-V curve at predefined voltage of 75% from the array's open circuit voltage. The MPPT techniques are accomplished through the DC/DC converter which interfacing the PV array to the inverter [23]. This can be achieved by controlling the input voltage of the DC/DC converter. Fig.3.2 shows the Maximum power point tracker (MPPT) system as a block diagram.

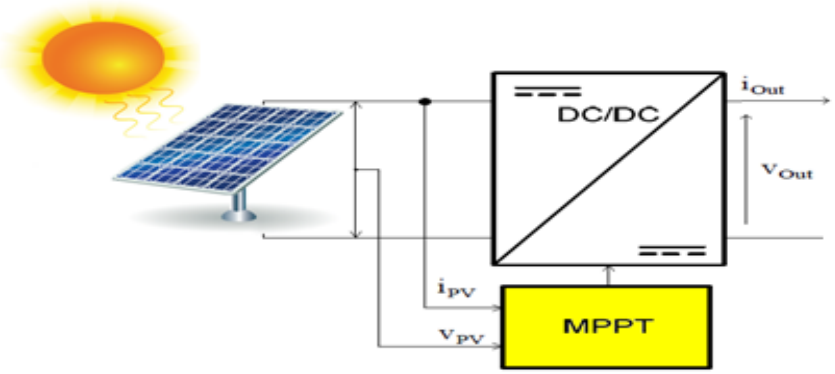

Fig.3.2: Maximum Power Point Tracker (MPPT) system as a block diagram.

Maximum power point tracker (MPPT) tracks the new modified maximum power point in its corresponding curve whenever temperature and/or insolation variation occurs. MPPT is used for extracting the maximum power from the solar PV array and transferring that power to the grid. A DC/DC (step up/step down) converter acts as an interface between the inverter and the array. The MPPT changing the duty cycle to keep the transfer power from the solar PV array to the grid at maximum point [22], [23].

The function of the inverter is to convert the output DC voltage of the PV into AC and to keep the output voltage of the DC/DC converter constant. In order to accomplish that, two controllers are required; one for the DC/DC converter, and the other for the inverter.

3.3 CONTROL ALGORITHMS

There are two algorithms which are used in this thesis for MPPT [24], [25]:

- Hill Climbing methods
- Fuzzy Based Algorithm

3.3.1 Hill Climbing Method

The hill climbing based techniques are so named because of the shape of the power-voltage (P-V) curve. This technique is sub-categorized in two types:

- Perturb & Observe Algorithm (P&O)
- Incremental Conductance Algorithm (ICT)

3.3.1.1 Perturb and Observe method (P&O)

Perturb and Observe is a widely used method. It is common because of the simple feedback structure and the fewer control perimeters. The basic idea is to give a trial increment or decrement in the voltage, and if this result in an increase in the power, the subsequent perturbation is made in the same direction or vice versa. This method is easy enough to handle and manipulate. However, this method of monitoring the perimeter causes a delay and therefore tracking a real time maximum power point is difficult [26-28].

Usually voltage or duty ratio will be the parameter used to perturb the system. This algorithm is not suitable when the variation in the solar irradiation is high. The voltage never actually reaches an exact value but perturbs around the maximum power point (MPP) as in this method, after obtaining the approximate maximum power point by scanning the entire P-V curve, the slope of the P-V curve dP/dV is determined by giving the step change in duty ratio of boost converter. If due to increase in duty cycle, the dP/dV decreases then next perturbation in duty cycle is kept unchanged otherwise the sign of the perturbation step is changed [26]. Fig.3.3 shows the flow chart for maximum power point tracking based Perturb and Observe algorithm.

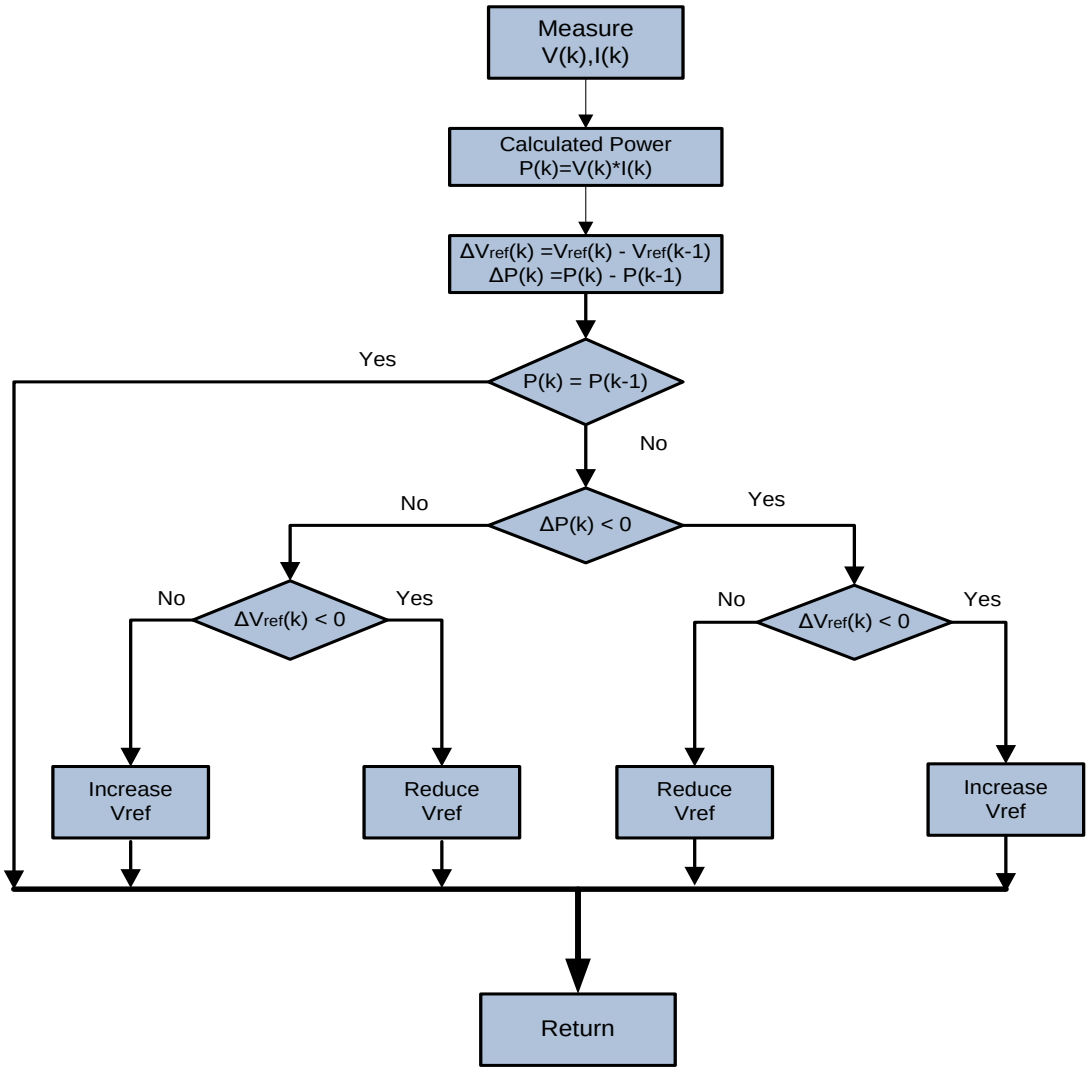

Fig.3.3: Flowchart for maximum power point tracking for (P&O) Algorithm.

3.3.1.2 Incremental Conductance method (ICT)

The incremental conductance method [27-29] is based on the fact that the slope of the PV array power curve is zero at the MPP, positive on the left of the MPP, and negative on the right, as given by eq.(3.1).

$$\frac{dP}{dV} = 0 \quad \text{, at MPP} \tag{3.1}$$

$$\frac{dP}{dV} > 0 \quad \text{, left of MPP} \tag{3.2}$$

$$\frac{\mathrm{dP}}{\mathrm{dV}} < 0 \quad \text{, right of MPP} \tag{3.3}$$

Since,

$$\frac{dP}{dV} = \frac{d(IV)}{dV} = I + V\frac{dI}{dV} \approx I + V\frac{\Delta I}{\Delta V} \tag{3.4}$$

Using (3.4), the location of tracking point represented by equations (3.1, 3.2 & 3.3) is given by eq. (3.5, 3.6, 3.7).

$$\frac{\Delta I}{\Delta V} = -\frac{I}{V} \quad \text{, at MPP} \tag{3.5}$$

$$\frac{\Delta I}{\Delta V} > -\frac{I}{V} \quad \text{, left of MPP} \tag{3.6}$$

$$\frac{\Delta I}{\Delta V} < -\frac{I}{V} \quad \text{, right of MPP} \tag{3.7}$$

The flow chart for maximum power point tracking for Incremental Conductance Algorithm is shown in Fig.3.4.

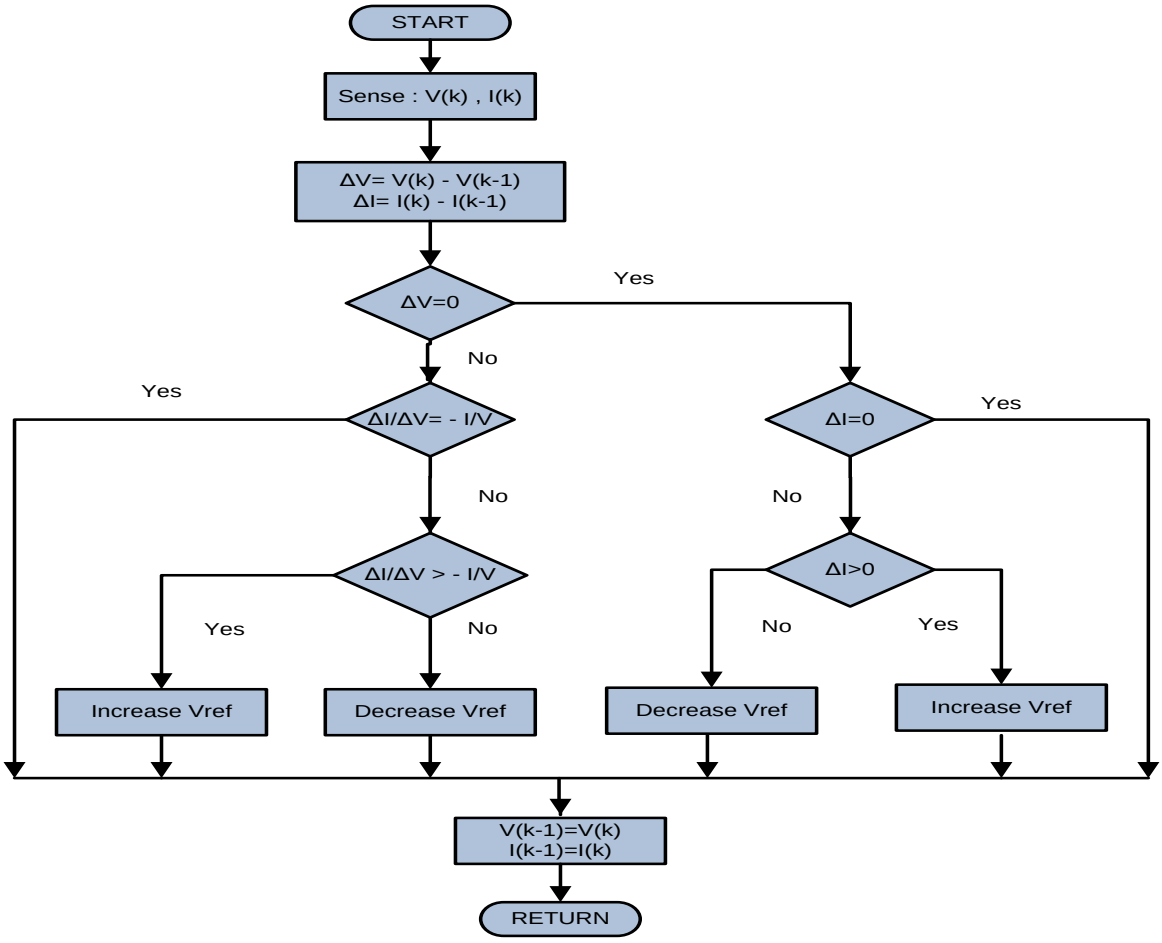

Fig.3.4: Flow Chart for maximum power point tracking for ICT Algorithm.

From eq. (3.8), the MPP can thus be tracked by comparing instantaneous conductance I/V to the incremental conductance ΔI/ΔV as shown in the flow chart in Figure 3.4. The Incremental Conductance Algorithm based tracking adjusts the duty cycle D of boost converter which adjusts the operating voltage of PV array to operate at MPP. It is very unlikely for the ICT algorithm to stop exactly on the MPP. Hence, practical ICT algorithm considers the MPP reached when the operating point is within a certain error margin which is given by eq. (3.8):

$$I + V\frac{\Delta I}{\Delta V} < e \qquad (3.8)$$

This method gives a very good and accurate performance under rapidly varying conditions. However, the drawback is that the actual algorithm is very complicated to handle. It requires sensors to carry out the computations and high power loss through the sensors.

3.3.2 Proposed Fuzzy Logic Controller Based Algorithm (FLC)

The maximum power point tracking speed is greatly reduced by performing the scanning in larger steps and using the proposed fuzzy controller that gives faster convergence around the final operating point [30], [31]. MPP fuzzy logic controller measures the values of the voltage and current at the output of the solar cell, then calculates the power from the relation (P=V*I) to extract the inputs of the controller. The crisp output of the controller represents the duty cycle of the pulse width modulation to switch the DC/DC converter. The block diagram of the proposed fuzzy logic controller (FLC) is shown in Fig.3.5.

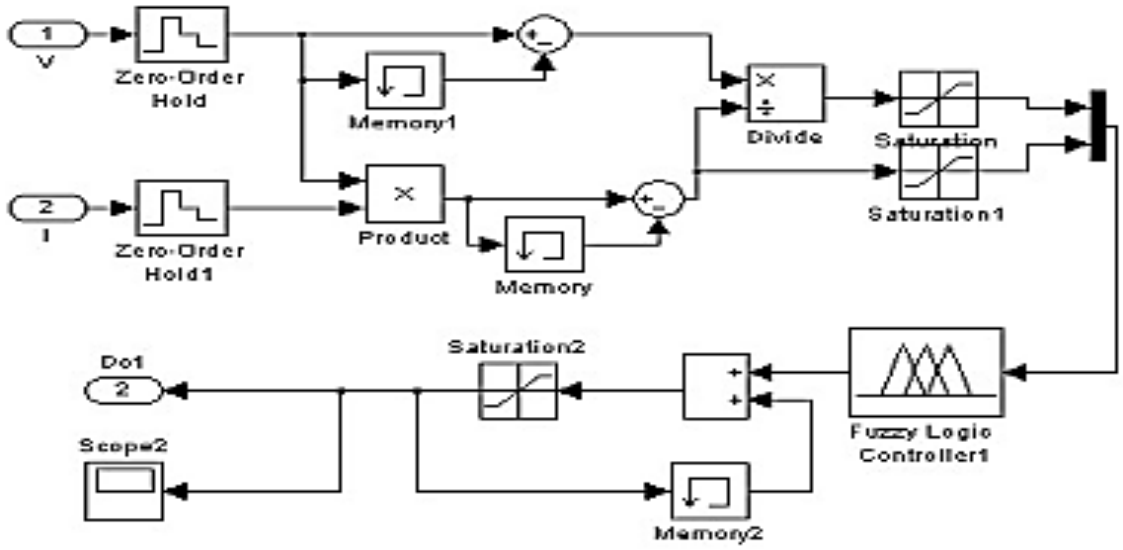

Fig.3.5. Block diagram of Proposed Fuzzy (FLC) Based Tracking.

3.3.2.1 MPPT Fuzzy Logic Controller

The FLC examines the output PV power at each sample (time-k), and determines the change in power relative to voltage (dp/dv). If this value is greater than zero the controller changes the duty cycle for switching the boost converter to increase the voltage until the power is maximum or the value (dp/dv) =0, if this value is less than zero the controller changes the duty cycle for switching the boost converter to decrease the voltage until the power is maximum [32] as shown in Fig.3.6.

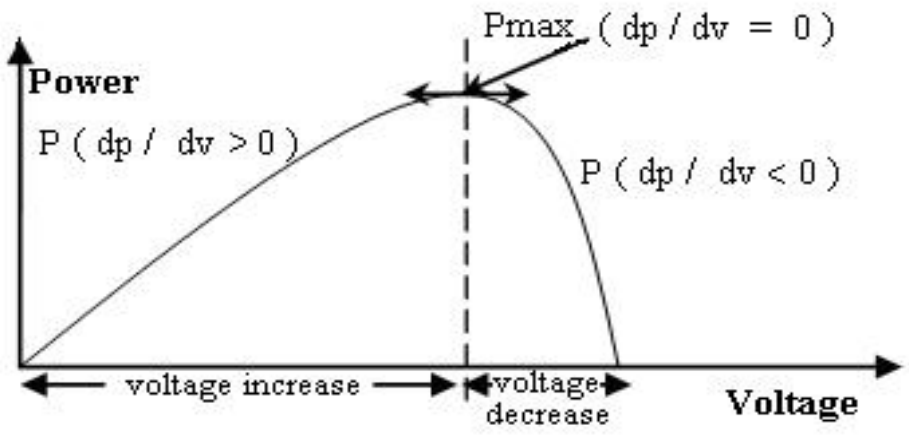

Fig.3.6: Power-voltage characteristic of a PV module.

FLC has two inputs which are: the error and the change in error, and one output feeding the switching of the boost converter. The two FLC input variables are error (E) and change of error (CH-E) at sampled times (k). FLC consists of three functional blocks described as follows:

- **Fuzzification**

The fuzzification process divides the input and output into some linguistic fuzzy sets from the previous knowledge of inputs and outputs range. The proposed FLC takes only one input that is the slope of the P-V curve and gives the duty cycle for switching the boost converter as an output. After taking voltage and current samples of the PV array, ΔP (k) and ΔV (k) are determined as follows:

$$\Delta P(k) = P(K) - P(k-1) \tag{3.9}$$

$$\Delta V(k) = V(k) - V(k-1) \tag{3.10}$$

Where, P (k) and V (k) are the power and voltage of PV array, respectively. Hence, the slope of the PV array power curve is zero at MPP. The ΔP (k)/ΔV (k) is given as an input to the FLC that generates the duty cycle D as an output for providing the switching pulses to the boost converter in order to operate the PV array at maximum power point (MPP).

The proposed FLC divides the input and output into seven linguistic fuzzy sets, Negative Big (NB), Negative Medium (NM), Negative Small (NS), Zero (ZO), Positive Big (PB), Positive Medium (PM) and Positive Small (PS). FLC has two inputs which are: error (E) and the change in error (CH-E), and one output feeding to the DC-to-DC converter. The membership functions of the input and output variables are shown in Fig. 3.7, Fig.3.8 and Fig.3.9 respectively.

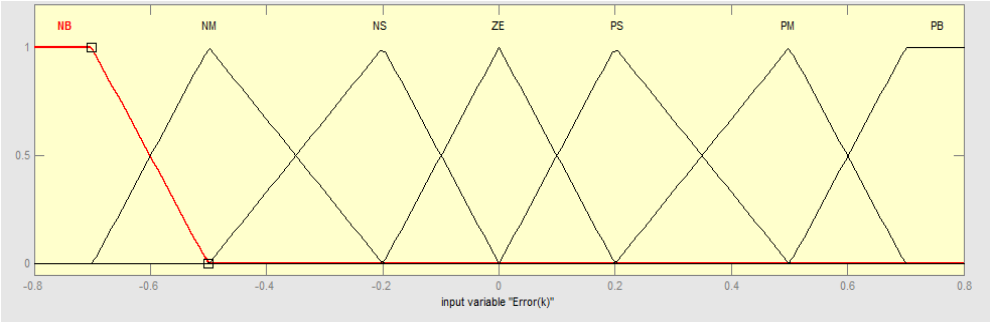

Fig.3.7: Membership functions for input variable (E).

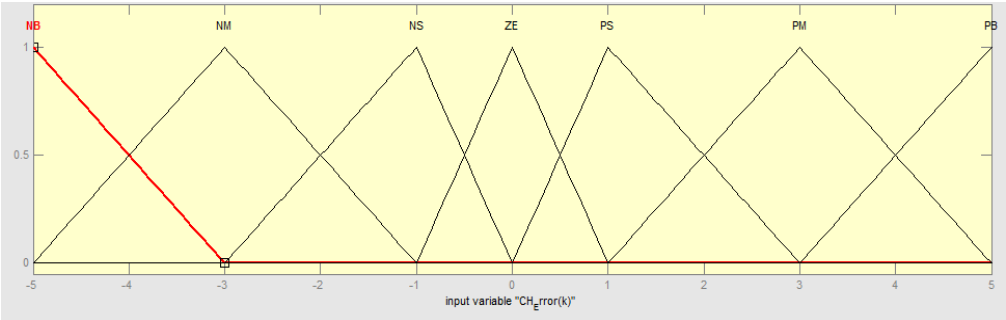

Fig.3.8: Membership functions for input variable (CH-E).

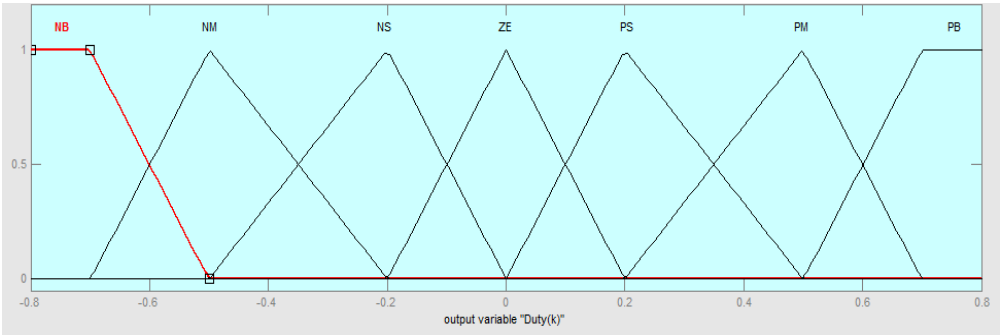

Fig.3.9: Membership functions for output variable (D).

- **Fuzzy rule base**

Based on the previous knowledge, the fuzzy rules should be precisely defined in order to generate an output duty cycle as per the magnitude the slope of P-V curve to operate the PV array at maximum power point. When the slope of P-V curve is positive then to reach towards MPP, the duty ratio of boost converter is decreased in order to increase the PV operating voltage.

Similarly, if the slope of P-V curve is negative then to move the operating point at MPP, the duty cycle is increased. The seven rules used for tracking the MPP in the proposed technique are listed in Table 3.1.

E↓ / CE→	NB	NM	NS	ZE	PS	PM	PB
NB	ZE	ZE	ZE	NB	NB	NB	NB
NM	ZE	ZE	ZE	NM	NM	NM	NM
NS	NS	ZE	ZE	NS	NS	NS	NS
ZE	NM	NS	ZE	ZE	ZE	PS	PM
PS	PM	PS	PS	PS	ZE	ZE	PS
PM	PM	PM	PM	PM	ZE	ZE	ZE
PB	PB	PB	PB	PB	ZE	ZE	ZE

Table3.1. Fuzzy Rules.

- **Defuzzification**

The deffuzification process generates the single crisp value of output duty cycle D from the aggregated fuzzy set that includes a range of output values. The widely used centroid method [33], [34] is used to convert the fuzzy subset of duty cycle D to real number. It computes the center of gravity from the final output fuzzy set which is mathematically represented by,

$$Z^* = \frac{\int \mu(Z).ZdZ}{\int \mu(Z)dZ} \tag{3.11}$$

Where, Z^* = D which is the output of fuzzy logic controller, ∫ denotes an algebraic integration and Z is the aggregated fuzzy Set of output. Thus, the proposed fuzzy logic controller inherently applies variable steps in duty ratio for controlling the boost converter as per the current operating point and hence, gives faster convergence to maximum point.

3.4 DC-DC CONVERTERS

DC-DC converters have wide applications in PV systems. Whether it is boost converter [35], [36], buck-boost converters or buck converters [37].

DC-DC converters are considered the main element in the maximum power point tracking process and without it the maximum power could not be achieved. In this thesis, the boost converter is used to change the terminal voltage of the PV array and from which maximum power point tracking can be obtained.

3.4.1 Boost Converters

The maximum power point tracking is essentially a load matching problem. A DC - DC converter is required for changing the input resistance of the panel to match the load resistance by varying the duty cycle. (See appendix B for details on boost converter's theory of operation). Since this thesis work deals with the boost converter, further discussions will be focused on this one [35], [36].The Boost converter circuit diagram is shown in Fig.3.10.

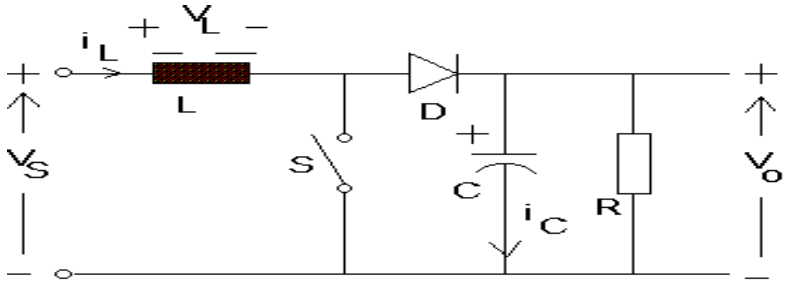

Fig.3.10: Boost Converter Circuit Diagram.

The relation between the output voltages over the input voltage is:

$$\frac{V_o}{V_s} = \frac{1}{1-D} \qquad (3.12)$$

Where, V_S is the input voltage to the boost converter Vo is the output voltage, and D is the duty cycle. In this thesis, Vo is fixed using the voltage -sourced converter (VSC), and V_S is at the same time the array terminal voltage which is controlled by varying the duty cycle D.

3.5 VOLTAGE SOURCE CONVERTER (VSC)

As previously mentioned in this chapter, the main function of the inverter is to interface the PV array with the grid. In the same time the inverter is used to maintain the voltage at the output side of the boost converter (the inverter's DC link). In order to obtain this voltage source converter (VSC) is used [38], [39].The VSC is controlled in the rotating d-q frame to inject a controllable three phase AC current into the grid. To achieve unity power factor operation, current is injected in phase with the grid voltage. A phase locked loop (PLL) is used to lock on the grid frequency and provide a stable reference synchronization signal for the inverter control system, which works to minimize the error between the actual injected current and the reference current obtained from the DC link controller [40], [41]. The overall scheme of vector based control is as shown Fig.3.11.

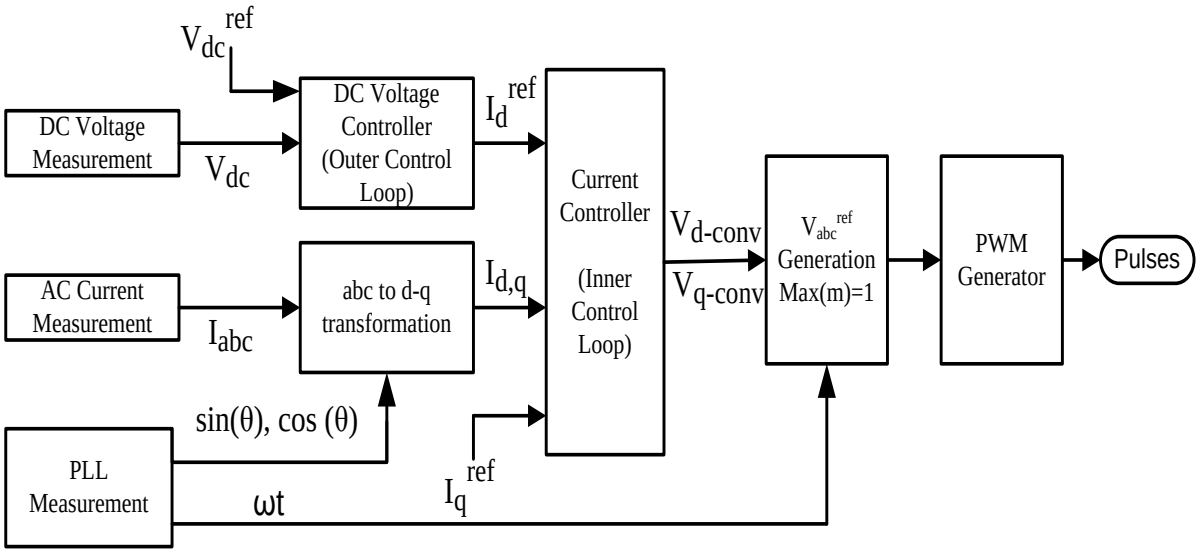

Fig.3.11: Functional control diagram of VSC using vector control.

The brief description of the controller components of the vector control system is discussed below.

3.5.1 DQ Transformation

DQ transformation is the transformation of coordinates from the three-phase stationary coordinate system to the d-q rotating coordinate system. This transformation is made in two Steps:

- A transformation from the three-phase stationary coordinate system to the two-phase, α-β stationary coordinate system and
- A transformation from the α-β stationary coordinate system to the d-q rotating coordinate system.

Clark and Inverse-Clark transformations are used to convert the variables (e.g. phase values of voltages and currents) into stationary α-β reference frame and vice-versa. Similarly, Park and Inverse-Park transformations convert the values from stationary α-β reference frame to synchronously rotating d-q reference frame, and vice versa. The reference frames and transformations are shown in Fig.3.12.

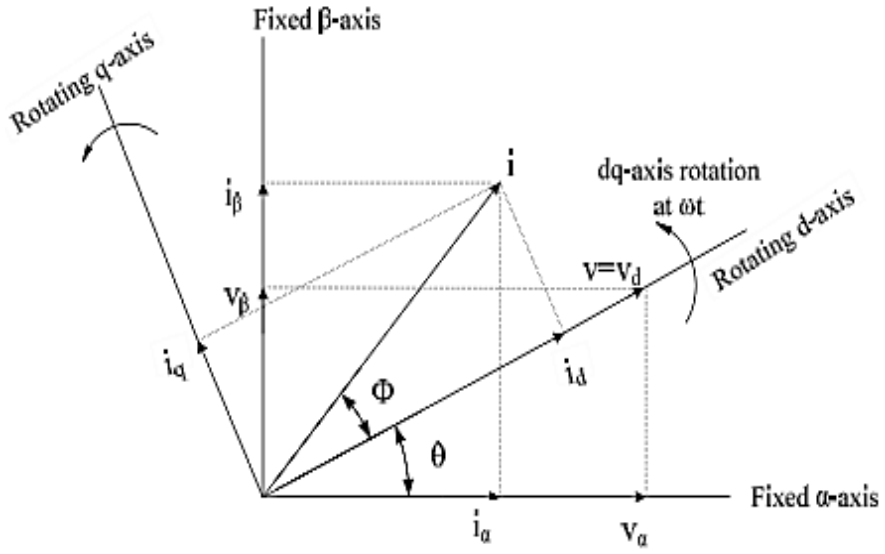

Fig.3.12: Transformation of axes for vector control.

The stationary α-axis is chosen to be aligned with stationary three phase a-axis for simplified analysis. The d-q reference frame is rotating at synchronous speed ω with respect to the stationary frame α-β, and at any instant, the position of d-axis with respect to α-axis is given by θ=ωt. The summary of the transformation is presented in tabular form in Appendix-C.

3.5.2 Phase Locked Loop (PLL)

The phase-locked loop technique [42] has been used as a common way to synthesize the phase and frequency information of the electrical system, especially when it's interfaced with power electronic devices. The Phase Locked Loop block [43] measures the system frequency and provides the phase synchronous angle θ (more precisely [sin (θ), cos (θ)]) for the d-q Transformations block. In steady state, sin (θ) is in phase with the fundamental (positive sequence) of the α component and phase A of the PCC voltage V_{abc}. In the three-phase system, the d-q transform of the three-phase variables has the same characteristics and the PLL system can be implemented using the d-q transform. The block diagram of PLL system can be described in Fig.3.13.

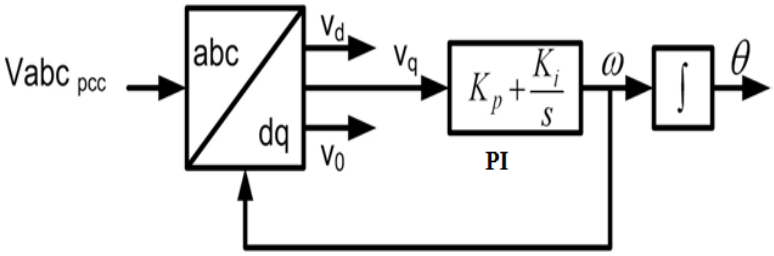

Fig.3.13: Schematic diagram of the phase locked loop (PLL).

3.5.3 Vector Control

For analysis of the voltage source converter using vector control, three phase currents and voltages are described as vectors in a complex reference frame, called α-β frame. A rotating reference frame synchronized with the AC-grid is also introduced, as in Figure.3.12. As the d-q frame, is synchronized to the grid, the voltages and currents occur as constant vectors in the d-q reference frame in steady state. For the analysis of the system, basic equations describing the system behavior are presented based on analysis done in [38], [39]. Considering the converter system connected to grid, and defining grid voltages as V_{abc} , currents I_{abc} , and converter voltages V_{conv} , and resistance (R) and inductance (L) between the converter and the grid. The voltage of the converter can be expressed as:

$$V_{abc} = V_{abc,conv} + R.i_{abc} + L\frac{d}{dt}i_{abc} \qquad (3.13)$$

Using the a-b-c to d-q transformations, the converter 3-phase currents and voltages are expressed in 2-axis d-q reference frame, synchronously rotating at given AC frequency ω.

$$\begin{bmatrix} V_d \\ V_q \end{bmatrix} = R \begin{bmatrix} i_d \\ i_q \end{bmatrix} + L \frac{d}{dt} \begin{bmatrix} i_d \\ i_q \end{bmatrix} + L \begin{bmatrix} 0 & -\omega \\ \omega & 0 \end{bmatrix} \begin{bmatrix} i_d \\ i_q \end{bmatrix} + \begin{bmatrix} V_{d,conv} \\ V_{q,conv} \end{bmatrix} \quad (3.14)$$

The voltage equations in d-q synchronous reference frame are,

$$L \frac{di_d}{dt} = -Ri_d + \omega L i_q - V_{d,conv} + V_d \quad (3.15)$$

$$L \frac{di_q}{dt} = -Ri_q - \omega L i_d - V_{q,conv} + V_q \quad (3.16)$$

The system equations of Eqn. (3.15, 3.16) are rewritten as follows,

$$V_d - V_{d,conv} = L \frac{di_d}{dt} + Ri_d - \omega L i_q \quad (3.17)$$

$$V_q - V_{q,conv} = L \frac{di_q}{dt} + Ri_q - \omega L i_d \quad (3.18)$$

3.5.3.1 DC-Voltage Controller

The dc voltage controller is discussed as the outer controller. Dimensioning of the dc link voltage controller is determined by the function between the current reference value to be given and the dc link voltage. The general Simulink model of the external controller can thus be given as in Fig.3.14. For the PI controller block of the function of K(s) the outer voltage control can be implemented based on Equation (3.19).

$$i_{d,ref} = \left(V_{dc} - V_{dc,ref}\right) * \left[K_P + \frac{K_I}{S}\right] \quad (3.19)$$

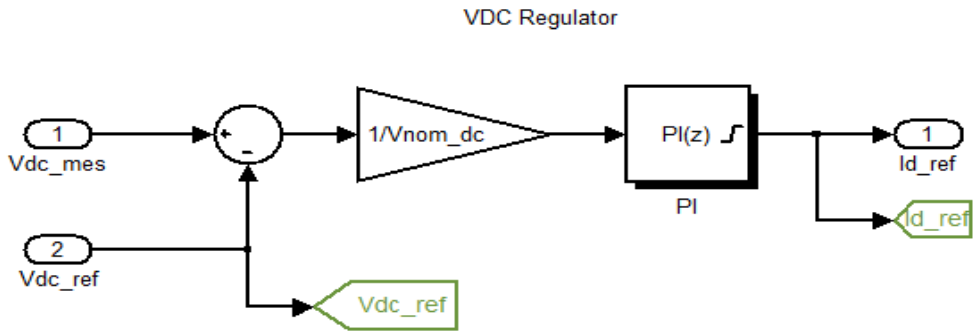

Fig.3.14: Simulink Model of the DC-Voltage Controller.

3.5.3.2 Inner Current Controller

The inner current control loop can be implemented in the d-q-frame, based on the basic relationship of the system model equations (3.17, 3.18). Inside the current controller as shown in Fig.3.15, the PI regulator for d and q axis current control which transform the error between the comparison of d and q components of current into voltage value.

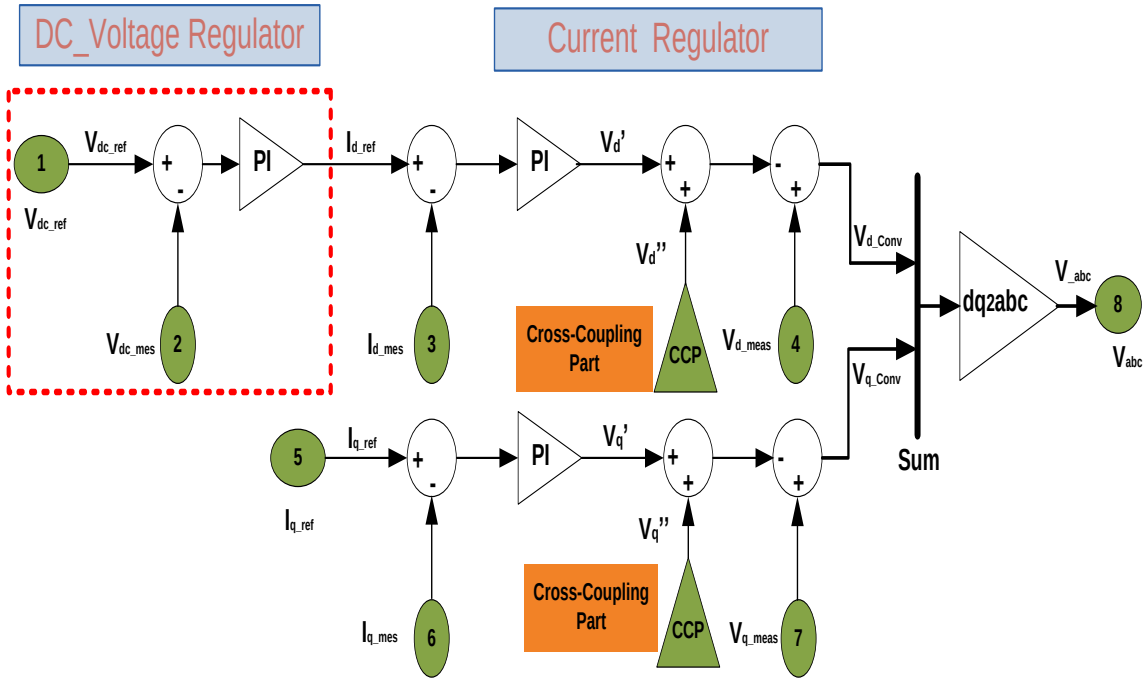

Fig.3.15: Total converter control scheme.

It's shown in Fig.3.15 that the control signal V_d' is the output of the PI regulator K(s) that processes the error signals $I_{d\text{-}ref}$ - I_d. Similarly, V_q' is the output of the PI regulator K(s) that processes the error signals $I_{q\text{-}ref}$ - I_q. In order to generate the converter voltage signals $V_d V_{q\,Conv}$, the PWM modulation pulses are produced by transformation the converter signals to pulses. The pulses for voltage source inverter are fired by using sine-triangular modulation.

3.6 SINUSOIDAL PULSE WIDTH MODULATION (SPWM)

The DC-AC inverters usually operate on Pulse Width Modulation (PWM) technique. The PWM is a very useful technique in which width of the gate pulses are controlled by various mechanisms. PWM inverter is used to keep the output voltage of the inverter at the rated voltage irrespective of the output load. The pulse width modulation inverter has been the main choice in power electronic for decades, because of its circuit simplicity and strong control scheme [44]. Depending on the switching performance and good characteristic features, Sinusoidal Pulse Width Modulation (SPWM) will be used and the modulating signal as illustrated in Fig.3.16. As mentioned in [45], the advantages of using SPWM include low power consumption, high energy efficient up to 90%, high power handling capability, no temperature variation-and aging-caused drifting or degradation in linearity and SPWM is easy to implement and control. SPWM techniques are characterized by constant amplitude pulses with different duty cycle for each period [46] .(see Appendix D for details on Sinusoidal Pulse Width Modulation (SPWM) theory of operation).

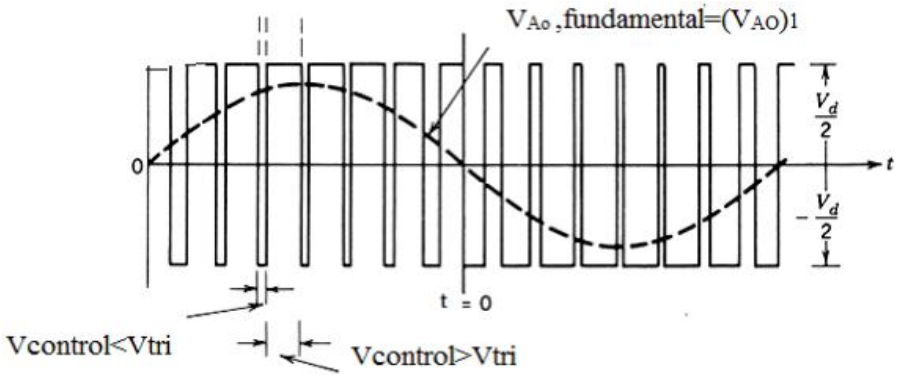

Fig.3.16: Pulse width modulation waveforms.

3.7 SUMMARY

In this chapter, the maximum power point tracking problem is discussed, and the boost type of DC-DC converters, which is the main tool used for obtaining the maximum power point are mentioned. The operation of the boost converter is also discussed. Further on, different famous MPPT algorithms are mentioned and their advantages and disadvantages are also highlighted, and then the three main algorithms used in this thesis (P&O, ICT and FLC) are discussed in more details along with the control scheme of the DC-AC inverter.

CHAPTER 4

POWER QUALITY TERMS AND DEFINITIONS

4.1 INTRODUCTION

With the dramatic increases over the last 20 years in energy conversion systems utilizing power electronic devices, we have seen the emergence of "power quality" as a major field of power engineering. Simply, power electronic technology has played a major role in creating “power quality” and simple control algorithm modifications to this same technology can often play an equally dominant role in enhancing overall quality of electrical energy available to end-users.

4.2 DEFINITION OF POWER QUALITY

"Power quality is a set of electrical boundaries that allows a piece of equipment to function in its intended manner without significant loss of performance or life expectancy" This definition embraces two things that we demand from an electrical device: performance and life expectancy. Any power-related problem that compromises either attribute is a power quality concern. Many sources in the literature have addressed the importance of power quality; however, there is no single agree definition for the term “power quality”, and various sources have different and sometimes inconsistent definitions for it. In addition, “power quality” is sometimes used loosely to express different meanings: “supply reliability”, “service quality”, “voltage quality”, and “current quality” [47]. The multiple meanings of power quality are the result of defining power quality from different perspectives. Power quality, in generation, relates to the ability to generate electric power at a specific frequency, 50 or 60 Hz, with very little variation; while power quality in transmission can be referred to as the voltage quality. At the distribution level, power quality can be a combination of voltage quality and current quality. From the marketing point of view, electricity is a product and the power quality is the index of the product quality [48].

Several engineering organizations and standard bearers in several parts of the world are spending a large amount of resources to generate power quality standards. Following some of power quality definition and related standards. The Institute of Electrical and Electronics Engineers (IEEE) defines power quality in the IEEE standard 1159-1995 as: “power quality is the concept of powering and grounding sensitive equipment in a matter that is suitable to the operation of that equipment” [49]. This definition limits the term power quality to only sensitive equipment, and this definition narrows down the impact of harmonic currents to consider it as affecting only that equipment [49].

It is hard to distinguish between voltage disturbances and current disturbances due to the close relationship between the two, and there is no common reference point that the disturbance can be seen from. For instance, starting a large induction motor leads to an over current; this is a current disturbance from the network perspective. However, the neighboring loads can suffer from a voltage dip, which is considered a voltage disturbance from another perspective. This action, starting an induction motor, leads to a disturbance that can be looked at from different perspectives: as a voltage disturbance from one point and a current disturbance from the other. The distinguishing complexity makes using the term "power quality disturbance" more preferable in general [50]. Much recent research has focused on classifying power quality disturbances according to the underlying causes [51], but it is still a difficult classification. However, the typical power quality disturbance classification is usually based on voltage magnitude and frequency variation for different time durations.

4.3 POWER QUALITY DISTURBANCES CLASSIFICATION

The effects of power disturbances vary from one piece of equipment to another and with the age of the equipment. Equipment that is old and has been subjected to harmful disturbances over a prolonged period is more susceptible to failure than new equipment. With the purpose of classify different types of power quality disturbances, the characteristics of each type must be known. In general, power quality disturbances are classified into two types: steady state and non-steady state. This classification is done in terms of the frequency components which appear in the voltage signals during the disturbance, the duration of the disturbance, and the typical voltage magnitude. These disturbances are mainly caused by [52]:

- External factors to the power system: for example, lightning strikes cause impulsive transients of large magnitude.
- Switching actions in the system: a typical example is capacitor switching, which causes oscillatory transients.
- Faults which can be caused, for example, by lightning (on overhead lines) or insulation failure (in cables). Voltage dips and interruptions are disturbances related to faults.
- Loads which use power electronics and introduce harmonics to the network.

Different power quality disturbances will be discussed below:

4.3.1 Transients

Transients are sudden but significant deviations from normal voltage or current levels. On the subject of describing a phenomenon or a quantity that varies between two consecutive steady states during a time interval that is short compared to the time scale of interest.

A transient can be a unidirectional impulse of either polarity or a damped oscillatory wave with the first peak occurring in either polarity [49]. Transients refer to variations in the voltage waveform, which results in over-voltage conditions for a fraction of a cycle of the fundamental frequency. Transients are classified as impulsive or oscillatory.

4.3.2 Short-Duration Variations

These are variations of the RMS (root mean square) value of the voltage from nominal voltage for a time greater than 0.5 cycles of the power frequency but less than or equal to 1 minute. Usually further described using a modifier indicating the magnitude of a voltage variation (e.g., sag, swell, or interruption), and possibly a modifier indicating the duration of the variation (e.g., instantaneous, momentary, or temporary) [49]. Table 4.1 shows the different characteristics of short-duration voltage variations.

4.3.2.1 Voltage Sag (Dip)

One of the most common power frequency disturbances is voltage sag. By definition, voltage sag is an event that can last from half of a cycle to several seconds. Common causes of voltage sags are short circuits (faults) on the electric power system, motor starting, customer load additions, and large load additions in the utility service area. Voltage sags well-defined as decrease to between 0.1 and 0.9 pu in RMS voltage or current at the power frequency for durations of 0.5 cycles to 1 minute.

4.3.2.2 Voltage Swell

A voltage swell is a short duration increase in voltage values. Voltage swells lasting longer than two minutes are classified as over voltages. Voltage swells are commonly caused by large load changes and power line switching. If swells reach too high a peak, they can damage electrical equipment. The utility's voltage regulating equipment may not react quickly enough to prevent all swells or sags. Voltage swells well-defined as increase in RMS voltage or current at the power frequency for durations from 0.5 cycles to 1 minute. Typical values are 1.1 – 1.8 pu.

4.3.2.3 Voltage Interruption

This is complete loss of voltage (< 0.1 pu) on one or more phase conductors for a time period between 0.5 cycles and 3 seconds (momentary), and between 3 seconds and 1 minute (temporary).

4.3.3 Long-Duration Variations

This is a variation of the RMS value of the voltage from nominal voltage for a time greater than 1 minute, usually further described using a modifier indicating the magnitude of a voltage variation (e.g., under-voltage, over-voltage, or voltage interruption). It is caused by load variations on the system or system switching operations.

4.3.3.1 Over-voltage

This is a measured voltage having a value greater than the nominal voltage for a period of time greater than 1 minute. Typical values are 1.1 – 1.2 pu.

4.3.3.2 Under-voltage

This is a measured voltage having a value less than the nominal voltage for a period of time greater than 1 minute. Typical values are 0.8 – 0.9 pu.

The general characteristics of over-voltage, under-voltage, and sustained interruptions are summarized in Table 4.1 as indicated in [49].

Table 4.1: Characteristics of Short-Duration Variations and typical causes.

Short-Duration Variations	Typical Spectral Content	Typical Duration	Typical Voltage Magnitude
A. Instantaneous			
Sag	-----	0.5 – 30 cycles	0.1 – 0.9 pu
Swell	-----	0.5 – 30 cycles	1.1 – 1.8 pu
B. Momentary			
Interruption	-----	0.5 – 3 sec.	< 0.1 pu
Sag	-----	30 cycles – 3 sec.	0.1 – 0.9 pu
Swell	-----	30 cycles – 3 sec.	1.1 – 1.4 pu
C. Temporary			
Interruption	-----	3 sec. – 1 min.	< 0.1 pu
Sag	-----	3 sec. – 1 min.	0.1 – 0.9 pu
Swell	-----	3 sec. – 1 min.	1.1 – 1.2 pu
Typical Sag causes	Remote system faults, large loads, and non-linear loads		
Typical Swell causes	Remote system faults, large loads, and non-linear loads		
Typical Interruption causes	System protection and maintenance		

4.3.4 Harmonics

Harmonics are sinusoidal voltages or currents having frequencies that are integer multiples of the frequency at which the supply system is designed to operate. Harmonics in conjunction with the fundamental voltage or current can produce waveform distortion. Harmonic distortion exists due to nonlinear characteristics of devices and loads on the power system. Voltage distortion results as these currents cause nonlinear voltage drops across the system impedance. Harmonic distortion is a growing concern for many customers and for the overall power system due to increasing application of power electronics equipment.

Harmonic distortion levels can be found throughout the complete harmonic spectrum. Furthermore, the phase angle of each component is unique. It is also common to use a single quantity, the total harmonic distortion (THD), as a measure of the magnitude of harmonic distortion.

Each classification category has its own technical features, which can be considered the key to detecting and identifying the different types of disturbances in electrical systems. For instance, voltage sags or voltage swells can be detected by noticing the variation in the voltage magnitude for a specific duration.

4.4 SIGNAL ANALYSIS

This is the step for monitoring power quality disturbances. It involves signal processing techniques in order to analyze the detected disturbance signals. The main objective of the analysis procedure is to justify the disturbance signal's features. These features can lead to the identification of the type of disturbance that occurred, and the more features justified from the signal analysis the more accurate disturbance identification. There are many signal processing techniques that have been used to analyze the disturbance signals; a quick review of some techniques is presented below.

- **Fast Fourier Transform (FFT)**

FFT is a basic method used widely in signal processing. FFT is applied to extensive data that has been selected based on various measurements. The FFT spectrum is normally used for detecting dominant harmonics, inter-harmonics and their related magnitudes.

- **Short-Time Fourier Transform (STFT)**

STFT provides time-frequency signal decomposition, which is equivalent to applying a set of equal-bandwidth sub-band filters. STFT is a Fourier-related transform used to determine the sinusoidal frequency and phase content of local sections of a signal as it changes over time.

Continuous STFT and discrete STFT are examples of short-Time Fourier Transform. There are other kinds of transforms and filters that have been applied to power quality problems; however, research on power quality problem analysis is still developing. After data have been analyzed, these data are characterized into specific classes to extract information about the type of power quality disturbance.

4.5 CONCLUSION

Utilities in deregulated systems can no longer deal with power quality problems as a single entity. Thus, identifying who is responsible for any power quality problem will be a very important task in mitigating that problem. Moreover, the increase in nonlinear loads, which are sources of harmonic currents, makes the identification too complex. In light of this definition of power quality, this chapter provides an introduction to the more common power quality terms. Along with definitions of the terms, explanations are included where necessary. This chapter also attempts to explain how power quality factors interact in an electrical system.

CHAPTER 5

SIMULAION RESULTS

5.1 INTRODUCTION

This chapter shows all the simulation of the photovoltaic array, the boost converter, the proposed fuzzy logical control (FLC), Perturb and Observe (P&O), and Incremental Conductance (ICT) algorithms. Also, in this thesis the grid disturbances effects on a grid connected PV array were studied while considering different maximum power point tracking algorithms. The grid disturbances involved are the different types of faults, voltage sag, and voltage swell. A comparative study of the grid disturbances effect on the three maximum power point tracking algorithms is discussed. All the simulation results are done using MATLAB/SIMULINK software.

5.2 SYSTEM UNDER STUDY

The complete system is to be simulated using the MATLAB/SIMULINK (as shown in Fig.5.1), and by varying the operating condition (solar irradiance and temperature), for the three different control algorithms, P&O algorithm, ICT algorithm and FLC proposed algorithm. The PV array is composed of (63 * 8) parallel and series modules respectively with a total output power of 100 kW.

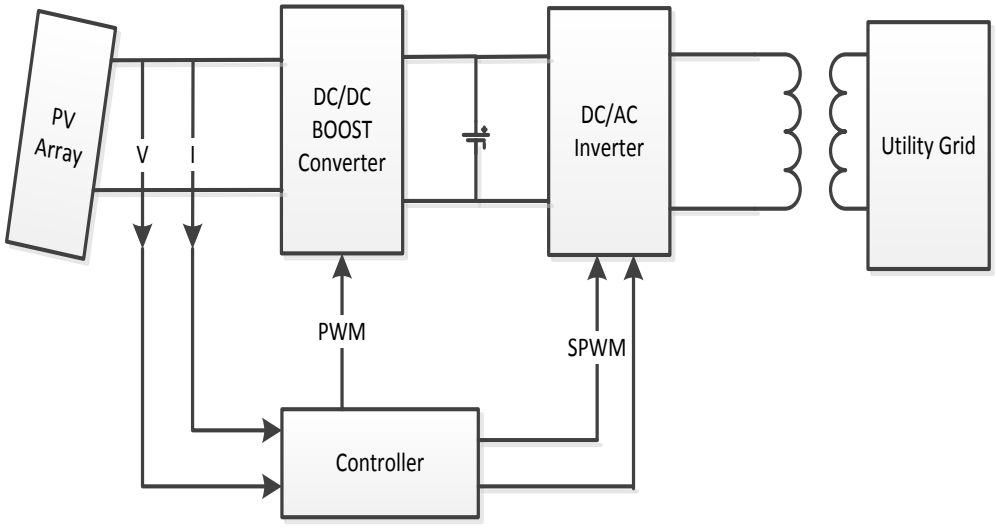

Fig.5.1: Block diagram of the grid connected photovoltaic system.

Table 5.1, shows the simulation parameters for the proposed system

Table 5.1: SIMULATION PRAMETERS

Quantity	Value
Grid voltage	**260V**
Frequency	**60 Hz**
Switching frequency	**5kHz**
DC link capacitor C	**100μF**
DC link Voltage	**500V**
Converter inductance	**5mH**
Converter Capacitor	**1.2mF**
Sampling period	**1μS**

5.3 PV MODELING FOR SIMULATION

The mathematical model used for this simulation is shown in equation (5.1)

$$I_0 = \frac{I_{scn} + K_i \Delta T}{\exp\left(\frac{V_{ocn} + K_v \Delta T}{aV_t}\right) - 1} \tag{5.1}$$

The various components used in developing the circuit design for a PV module are chosen from the MATLAB/SIMULINK library. The voltage measurement block, current measurement block, go to block, from block, and control current source block are used to model various outputs such as Shockley diode current, the light generated photovoltaic current, cell temperature equation, and power output.

Fig.5.2 shows the Simulink modeling for the reverse saturation current (I_0) at the reference temperature which is given by the equation (5.1).

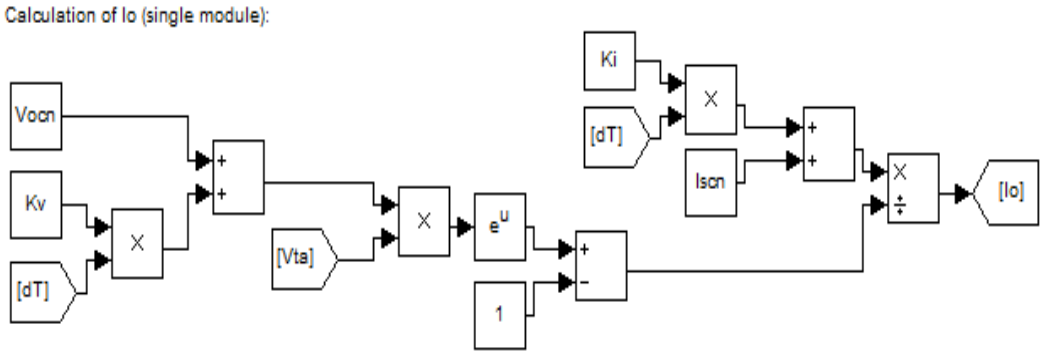

Fig.5.2: Simulink Model for Evaluating I_0

Fig.5.3 shows the Simulink model for the light generated current of the photovoltaic cell which is a linear function of temperature and solar radiation as shown in the equation (5.2) below:

$$I_{pv} = (I_{pvn} + K_i \Delta T)\frac{G}{G_n} \tag{5.2}$$

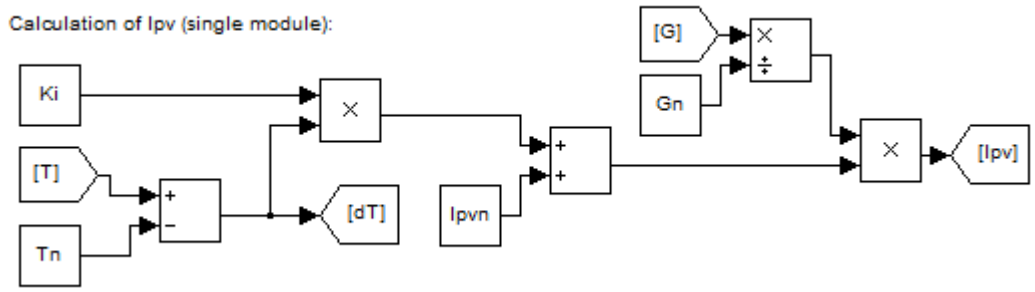

Fig.5.3: Simulink Model for Evaluating I_{pv}

Fig.5.4 shows the Simulink model to evaluate the model current I_m referring to the appropriate model circuit for which is given by the equation (5.3).

$$I_m = I_{PV}N_p - I_0 N_p \left[exp\left(\frac{V + R_s\left(\frac{N_s}{N_p}\right)I}{V_t a N_s} \right) - 1 \right] \tag{5.3}$$

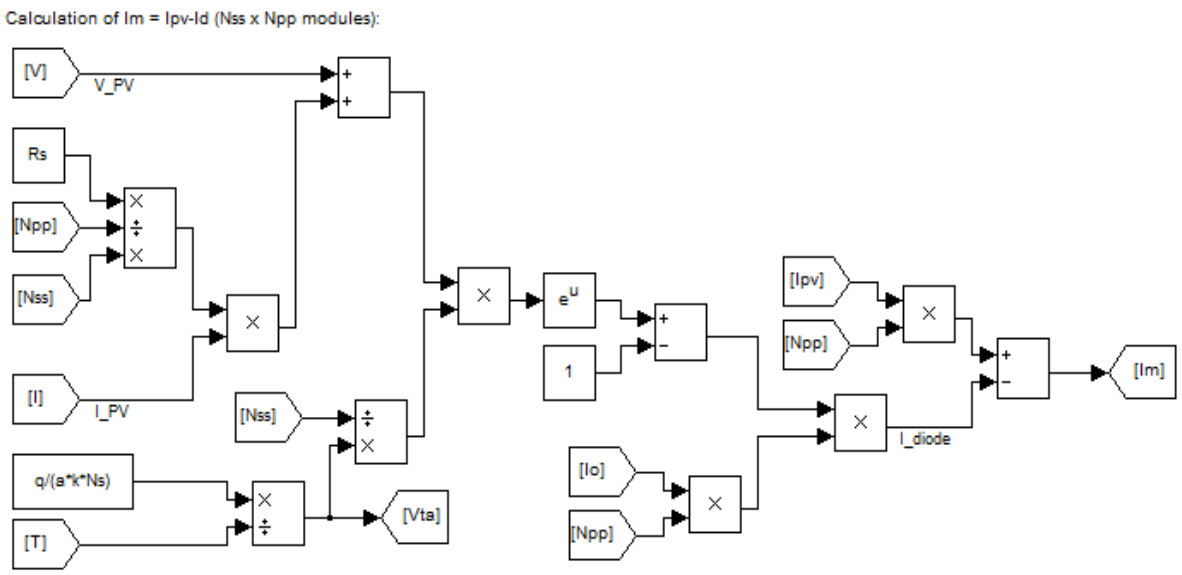

Fig.5.4: Mathematical Model Implementation for Model Current I_m

The MATLAB/SIMULINK model of the simulated PV is shown in Fig.5.5

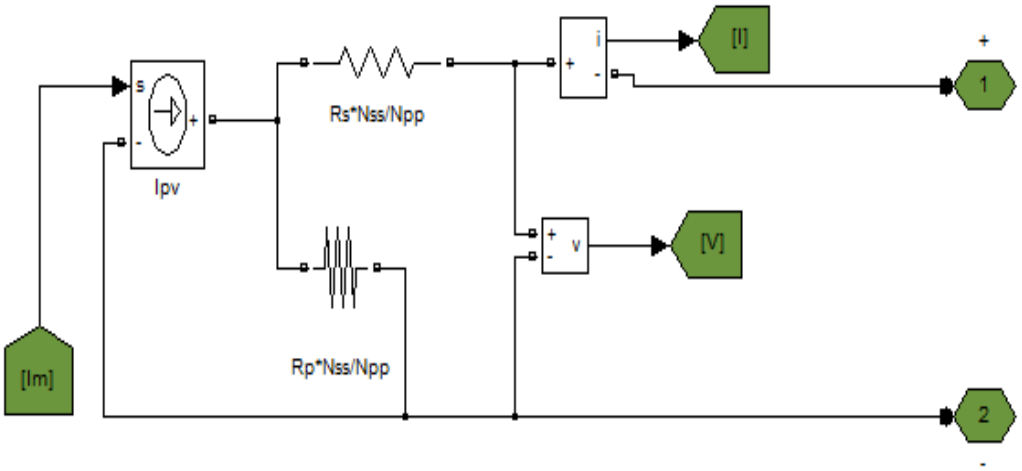

Fig.5.5: Simulation of the Photovoltaic Module.

The current I_m is passed through series and parallel resistors of the array as shown in Fig.5.5, and then all these blocks are converted to one sub system block with two inputs (Temperature, and Irradiation) as shown in Fig.5.6.

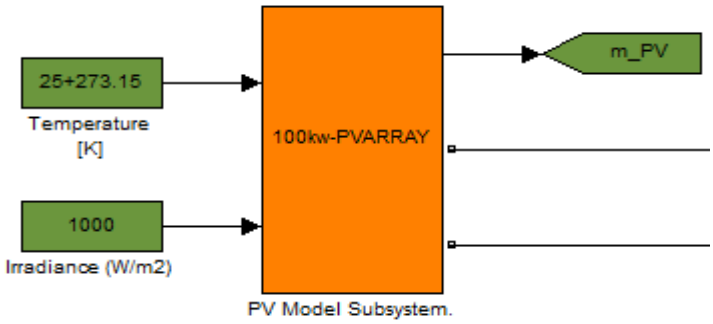

Fig.5.6: PV model Subsystem.

The MATLAB/SIMULINK model is tested by inserting all the required data shown in Table 5.2 to simulate the KYOCERA KC200 GT module. The data sheet [16] of the simulated module is shown in appendix A.

Table 5.2: KC200GT module parameters

Quantity	Value
I max power	7.61 A
V max power	26.3 V
P max	200.143 W
I short circuit	8.21 A
V open circuit	32.9 V
I leakage	$9.825*10^{-8}$ A
I photovoltaic	8.211 A
Diode ideality constant (a)	1.3
Parallel resistance	415.406 Ω
Series resistance	0.221 Ω

5.4 BOOST CONVERTER MODEL

As the name implies, the boost or step-up converter has an output voltage that is always greater than the input voltage. The boost converter also has the added advantage that the output can be isolated from the input.

The MATLAB/SIMULINK model of boost converter model is shown in Fig.5.7. The boost converter plays a very important role as it varies the PV array terminal voltage with the change of the duty cycle. The duty cycle will be determined depending on the signal of the maximum power point tracker whether it is P&O, ICT or FLC as it discussed in the following sections.

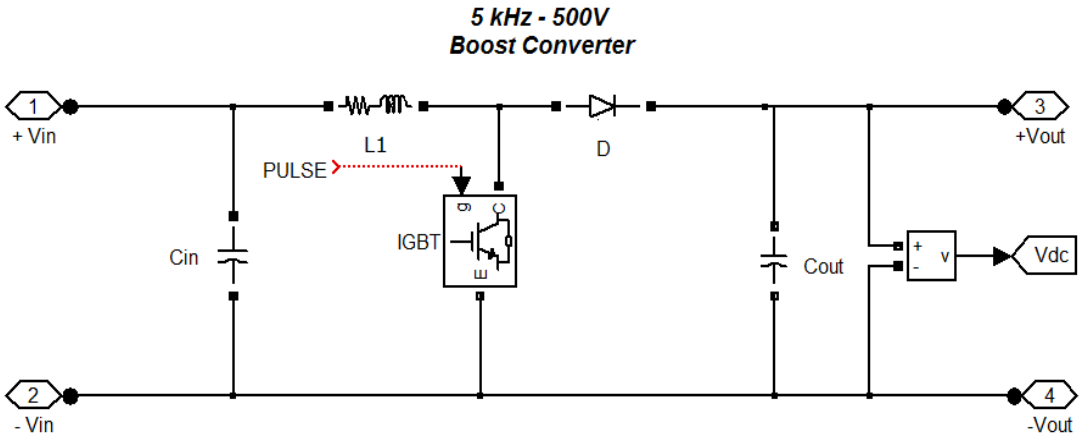

Fig.5.7: Block Diagram of Boost Converter Model.

5.5 PERTURB AND OBSERVE CONTROLLER

The perturb and observe algorithm discussed in chapter 3 is constructed using MATLAB M-FILE code within SIMULINK, the code is shown in appendix E and its output is connected to the boost converter to achieve the maximum power point tracking. Fig.5.8 shows the SIMULINK model of the MPPT using P&O method.

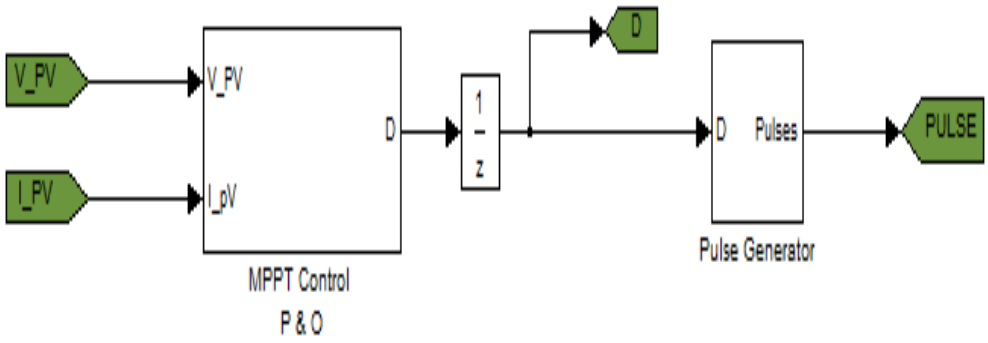

Fig.5.8: Maximum Power Point Controller Using P&O.

5.6 INCREMENTAL CONDUCTANCE CONTROLLER

The incremental conductance algorithm discussed in chapter 3 (section 3.4.1.2) is constructed using MATLAB/ SIMULINK TOOLBOX, and its output is connected to the boost converter to achieve the maximum power point tracking. Fig.5.9 shows the SIMULINK model of the MPPT using ICT method.

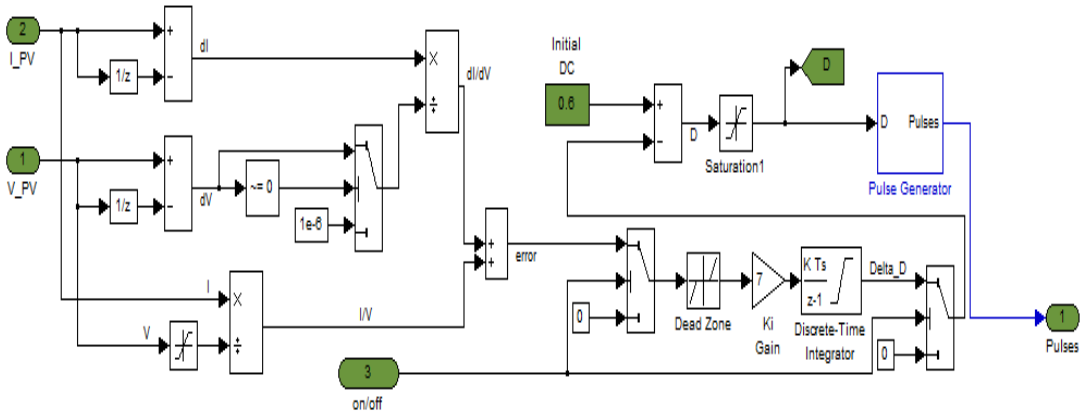

Fig.5.9: Maximum Power Point Controller Using ICT.

5.7 PROPOSED FUZZY LOGIC CONTROLLER

The designed fuzzy logic controller is connected between PV module and DC-to-DC converter module to track the MPP, as shown in Fig.5.10 which illustrates the sub-system using MATLAB/ SIMULINK, and its output is connected to the boost converter to achieve the maximum power point tracking.

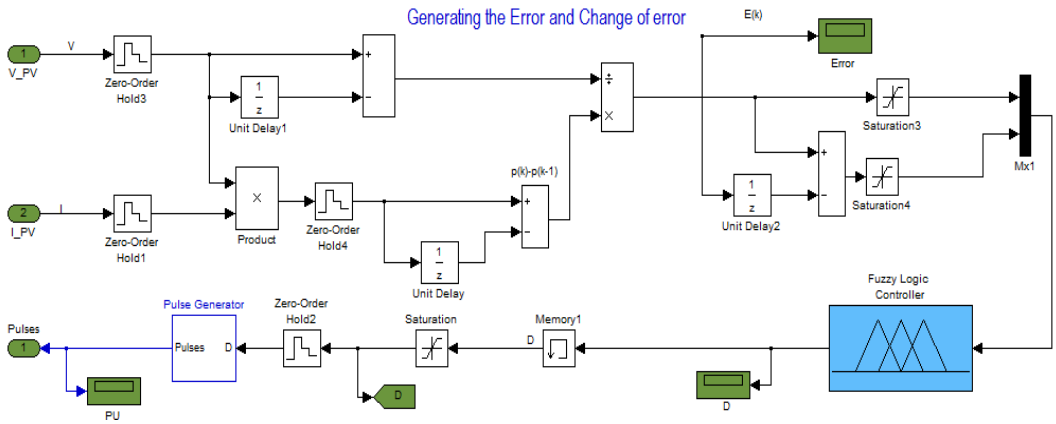

Fig.5.10: Controlling the PV power using FLC.

The purpose of learning mechanism is to learn the environmental parameters and to modify the fuzzy logic controller accordingly so that the response of the overall system is close to optimum operation point. The learning mechanism is composed of inverse fuzzy model and knowledge base modifier:

- **Inverse fuzzy model**

In this part, we use error (E) and change of error (CH-E) of system and control the knowledge base modifier to modify fuzzy parameter to optimize the operation of system. The fuzzy parameter can be adapted by this condition If error < ε (limit value) then knowledge base modifier will be done.

- **Knowledge base modifier**

In this part fuzzy parameter will be modifier as follow:

a) Scaling factor

Quite simple schemes for altering the scaling factor to meet various performance criteria can be devised. The range of the error, change of error and also output of fuzzy can be set like balance between proportional and integral control.

b) Fuzzy set membership function

In this part, tuning peak values, such as error, can improve both responsiveness and stability. The large error can improve responsiveness and small error can improve stability. The modification is performed by shifting the membership functions of both input and output.

Also we can show the three directions of the two inputs and output membership function as shown in Fig.5.11.

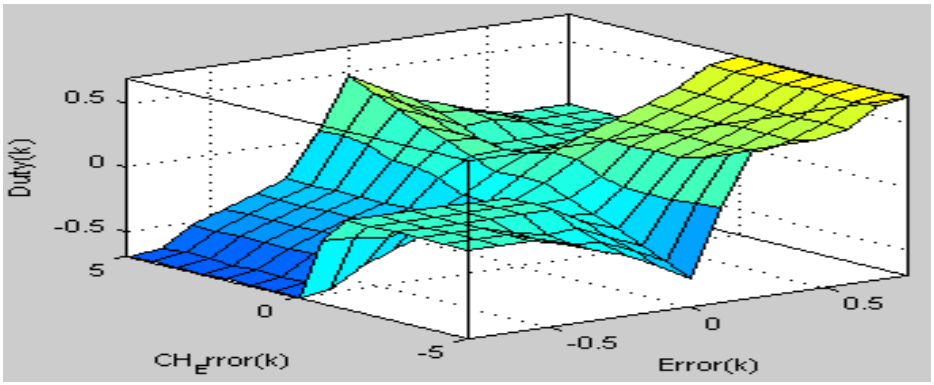

Fig.5.11: Fuzzy logic membership functions after tuning in three directions.

c) Tuning rule base

Modifying rule base can affect the control system such as overshoot, settling time, stability, responsiveness. Rule base and fuzzy set membership function have relationship with each other depending on the quantity of error and change of error like in Table 3.1.

5.8 INVERTER CONTROLLER

Voltage Source Converter Controller (VSC) is performed on the three phase inverter to keep the DC- link voltage constant at any required value. The whole process discussed before in chapter 3 (sections 3.6) is simulated on SIMULINK, as shown in Fig.5.12

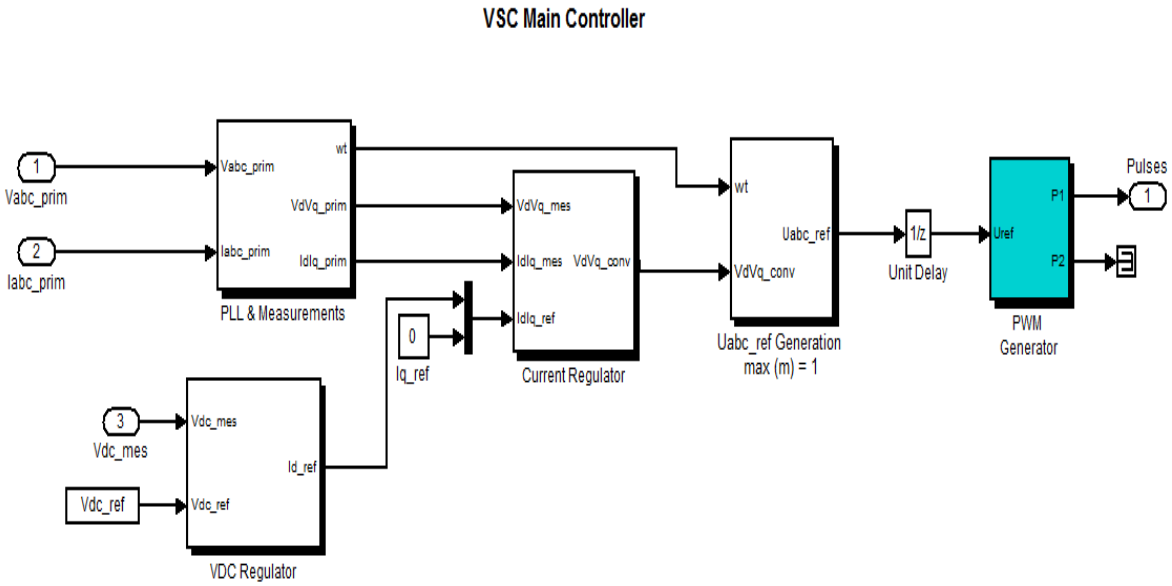

Fig.5.12: Control of three phase inverter.

The inverter succeeded to keep the DC link voltage at a constant value which makes the DC-DC converter's task of MPPT mush easier. At the same time the inverter converts the DC power into AC and that is its main task so that the PV system could be easily connected with the grid.

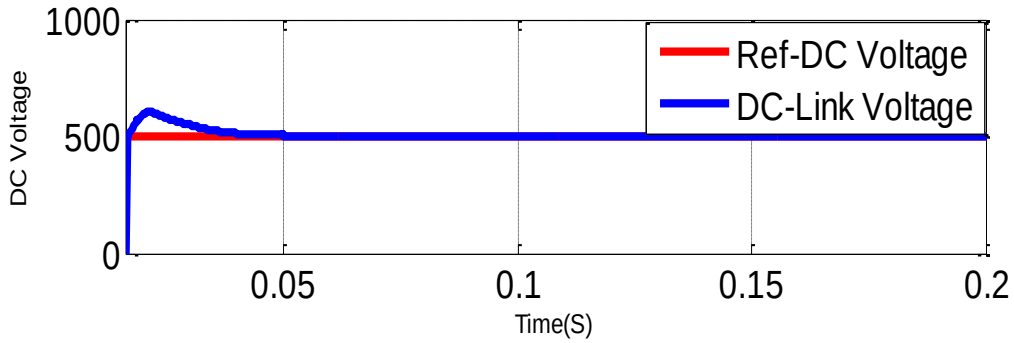

Fig.5.13: DC-link voltage VS Reference voltage.

5.9 SIMULATION RESULTS

All the discussed features in this chapter are to be bound together to form a complete grid-connected PV system as seen in Fig.5.14. The system shown in Fig.5.1 is modeled and simulated utilizing the Sim Power System toolbox under the MATLAB/Simulink. The MATLAB model is shown in Fig.5.14. This model is simulated under three conditions; First, by utilizing the Perturb & Observe (P&O) technique, second, by utilizing the Incremental Conductance technique, and finally by utilizing the Fuzzy logic based algorithm.

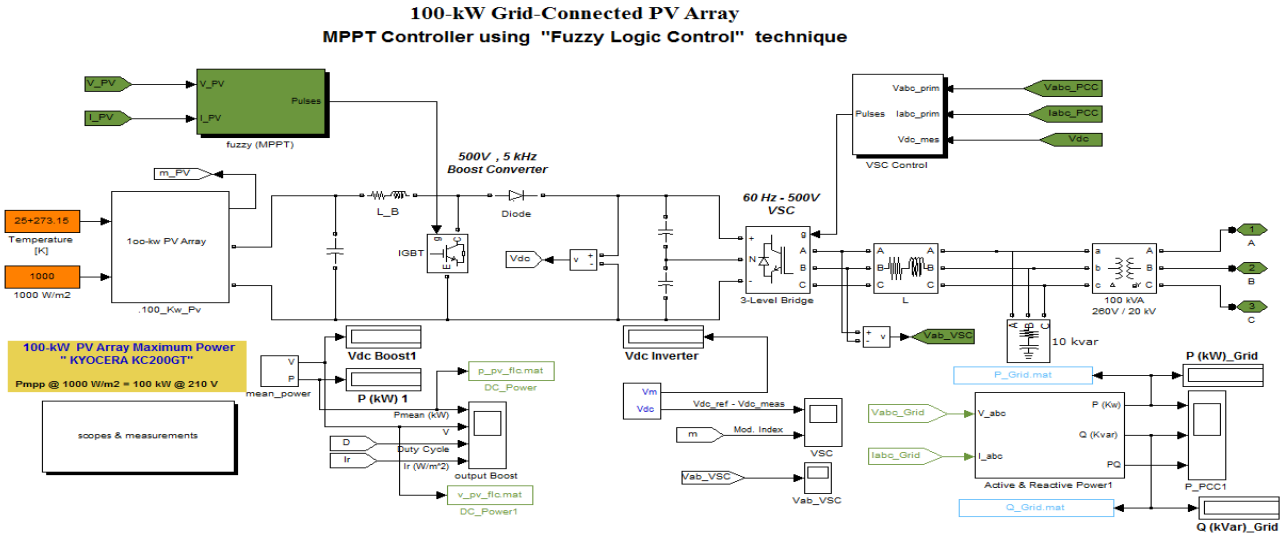

Fig.5.14: The MATLAB/ Simulink model of the system under investigation.

5.9.1 STEADY STATE ANALYSIS

The investigated system consists of a 100 kW PV array which is connected to a boost converter, and then the boost converter is connected to the grid via a three phase inverter. The PV panel utilized in this thesis is KYOCERA KC200GT. The MATLAB model of the PV Panel was described and verified in chapter 2 (section 2.5 and 2.6). In this study, the 100 kW array consists of 63 parallel string each comprise 8 series connected panel. The parameters of the investigated system are given in Table 5.1.

First the simulation is obtained while applying the P&O algorithm and set the irradiances to 1000 W/m^2 and the temperature to 25^{o}C. Fig.5.15 shows the output voltage, current, and power of the PV array terminal.

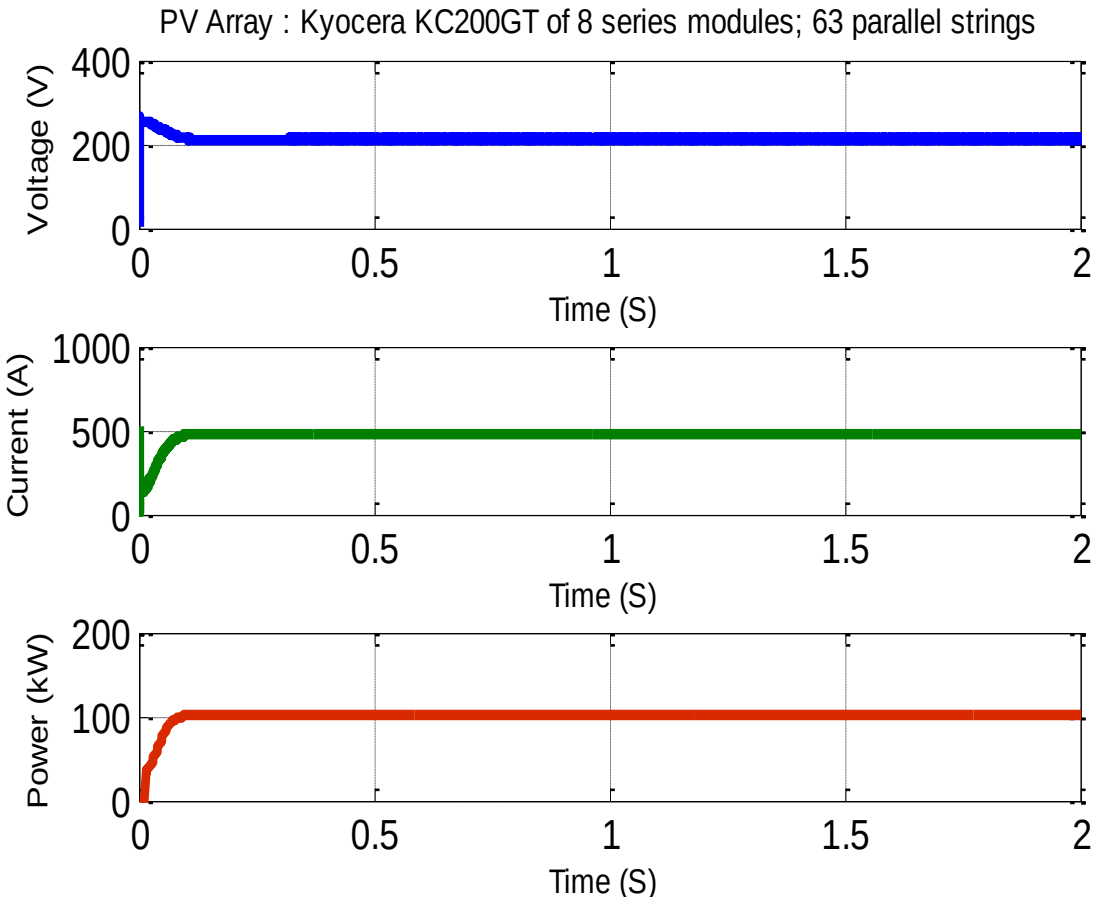

Fig.5.15. Voltage, Current and Power Output of PV array with MPPT Based P&O.

Then the simulation is achieved while applying the incremental conductance technique under the same condition. Fig.5.16 shows the output voltage, current, and power of the PV array terminal.

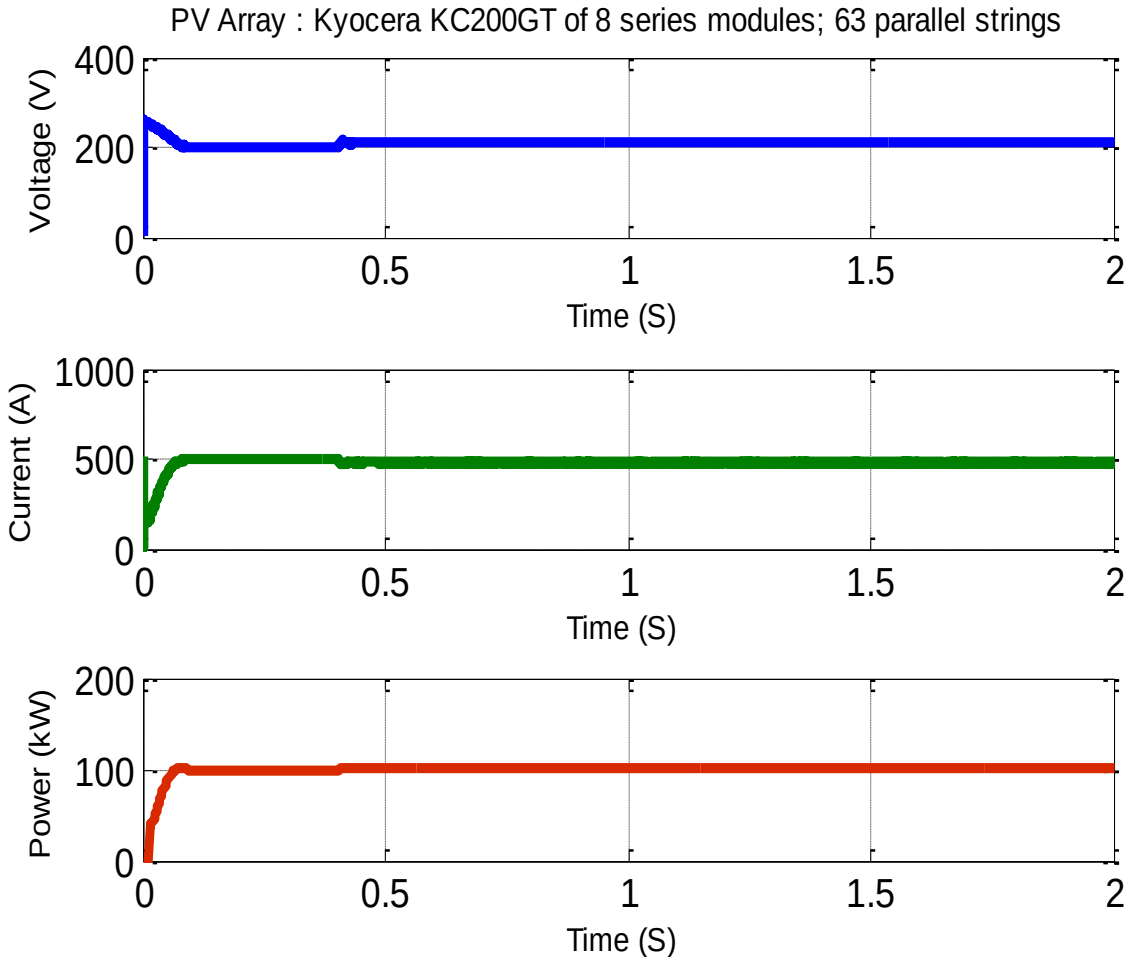

Fig.5.16: Voltage, Current and Power Output of PV array with MPPT Based ICT.

Finally, the simulation is accomplished under the same condition while applying the fuzzy logic based algorithm. Fig.5.17 shows the output voltage, current, and power of the PV array terminal.

It can be observed that PV array feeds 100 kW to the grid while utilizing the three algorithms but the proposed FLC is accurate and give a high response when compared with the others as shown in Fig.5.17 which illustrates the performance of the proposed FLC.

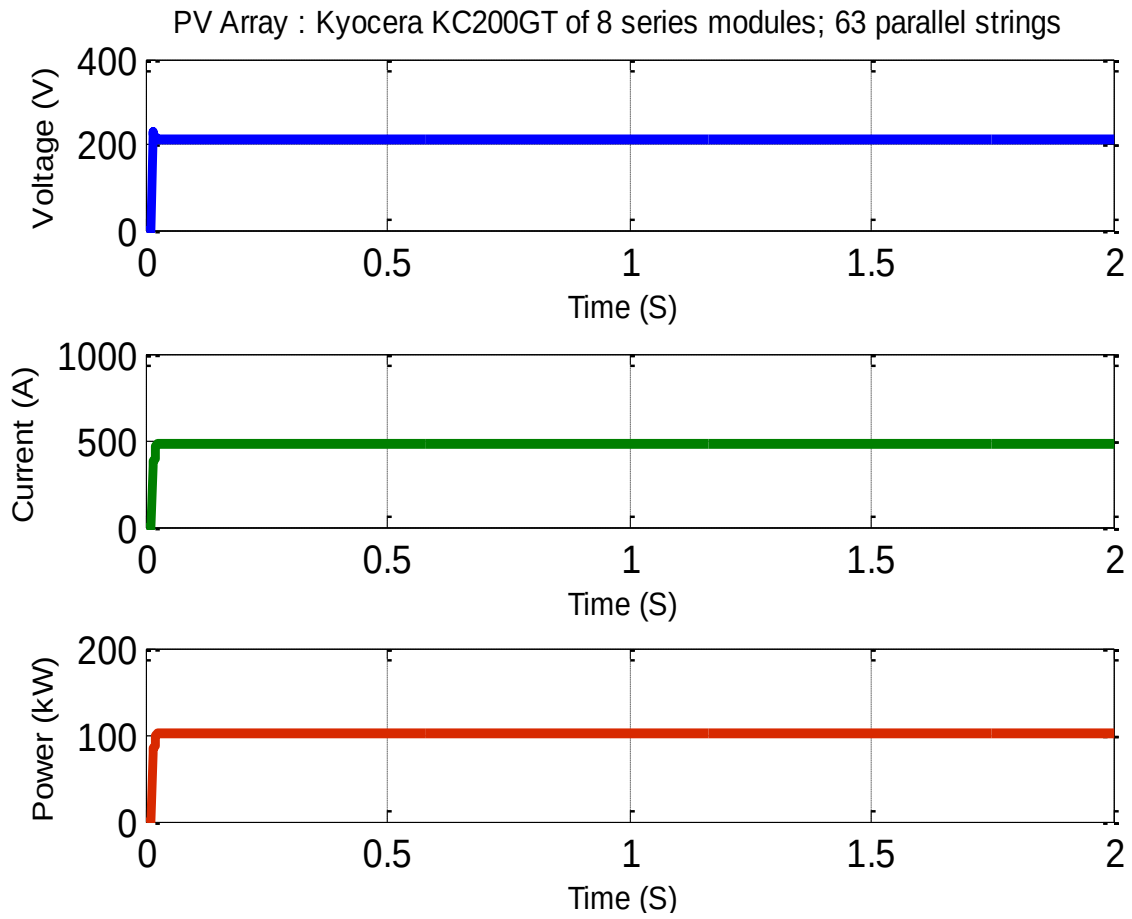

Fig.5.17: Voltage, Current and Power Output of PV array with MPPT Based FLC.

The array output power for the three techniques under constant irradiance (1000 W/m^2) is shown in Fig.5.18.

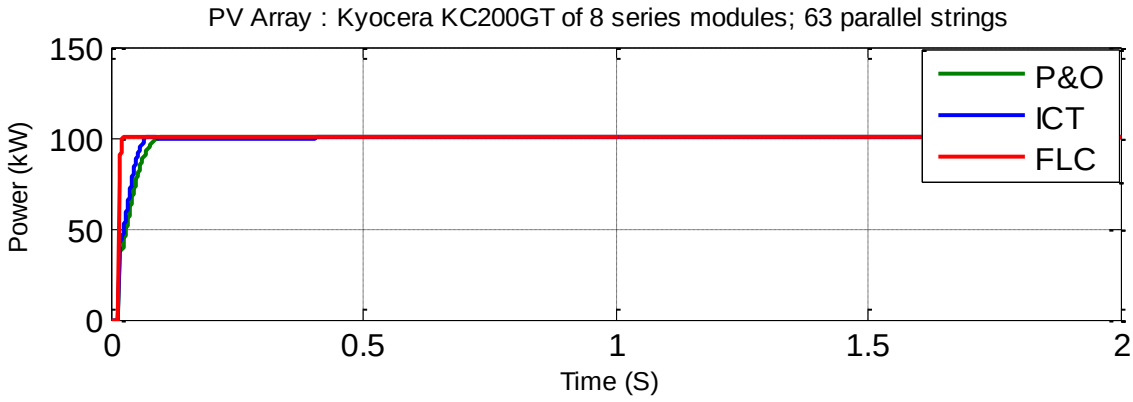

Fig.5.18: The output power of the PV array using the three different algorithms at constant irradiance.

The performance of rise time, settling time, and peak time of three different algorithms are summarized in Table 5.3, which show that the Fuzzy-controller is a best control system.

Table 5.3: The performance of three different algorithms

Type of Algorithm	The response of three different algorithms		
	Rise Time (sec)	Settling Time (sec)	Peak Time (sec)
With P&O controller	0.0510	0.0885	0.2360
With ICT controller	0.0377	0.0674	0.1834
With FLC controller	0.0032	0.0232	0.1525

The three techniques are compared by changing the irradiance from 1000 W/m^2 to 250W/m^2 then to 1000W/m^2 then to 250W/m^2 and then finally to 1000 again as seen in Fig.5.19.

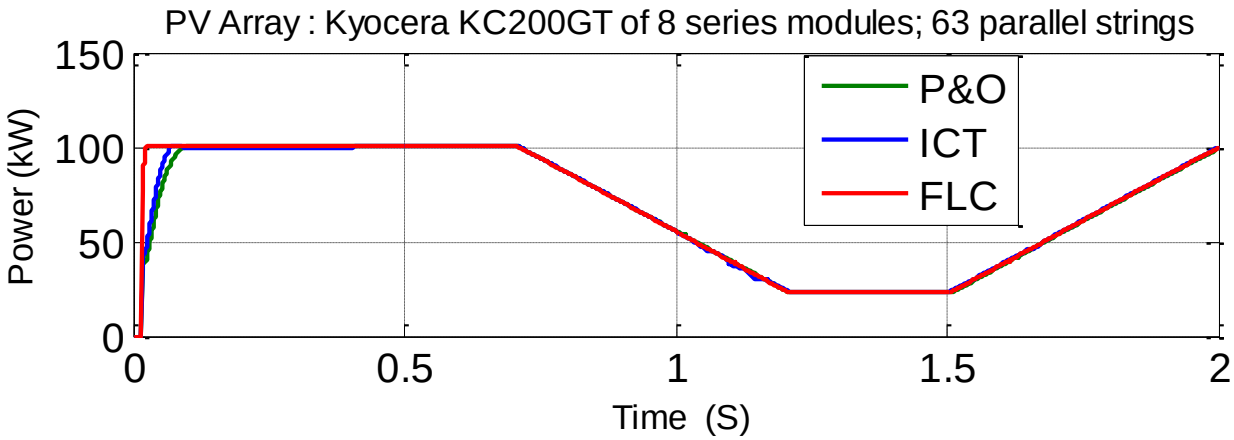

Fig.5.19: The output power of the PV array using the three different algorithms at variable irradiance.

It can be seen that the fuzzy based algorithm shows faster response in tracking the maximum power point under variable and constant irradiance and gives minimum oscillations around the final operating point compared to ICT and P&O based algorithm. It can be also seen from Fig.5.18, and Figure 5.19, that the P&O algorithm gives slower response, whereas the ICT algorithm gives relatively lower response as compared to the fuzzy based algorithm. Therefore the FLC gives relatively less oscillation and the highest response as compared to the P&O and ICT.

5.9.2 TRANSIENT ANALYSIS

In order to be able to categorize different types of power quality disturbances, the characteristics of each type must be known. In general, power quality disturbances are classified in terms of the frequency components which appear in the voltage signals during the disturbance, the duration of the disturbance, and the typical voltage magnitude. The power quality disturbances are classified in chapter 4.

5.9.2.1 FAULT ANALYSIS

In this section the MATLAB/SIMULINK model shown in Fig.5.20 is simulated under different fault conditions [53]. The simulation is accomplished under nominal condition (G = 1000 W/m^2 and T=25^{0}C). As shown in Figure 5.20 the fault is applied on the grid side. The fault duration is 0.1 seconds from 0.2 to 0.3 seconds. All types of faults will be discussed under the same condition. While applying three maximum power point tracking techniques. The simulation is run several times in order to study the effect of different disturbances on the three MPPT algorithms mentioned above.

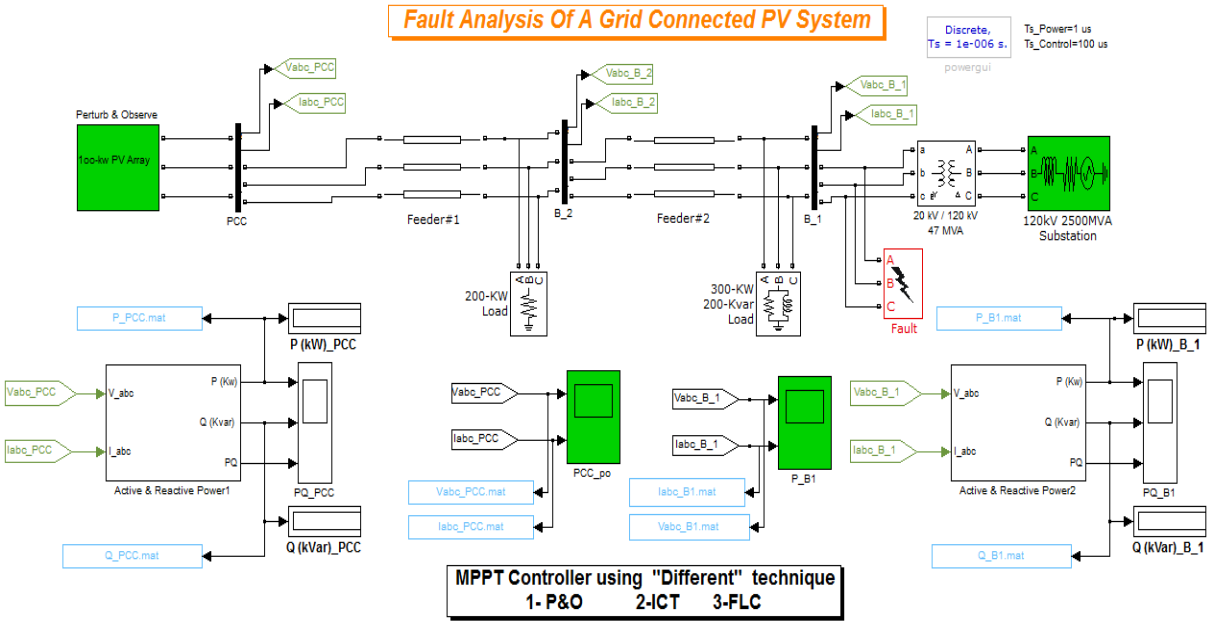

Fig.5.20: The MATLAB/SIMULINK model of the Grid Connected PV system.

- **Line-to-ground Fault**

The model shown in Fig.5.20 is simulated while applying single line to ground fault (1L-G) on phase A. the fault location is illustrated and the fault duration is 100 msec. The output voltage and current at the point of common coupling PCC is shown in Fig.5.21.

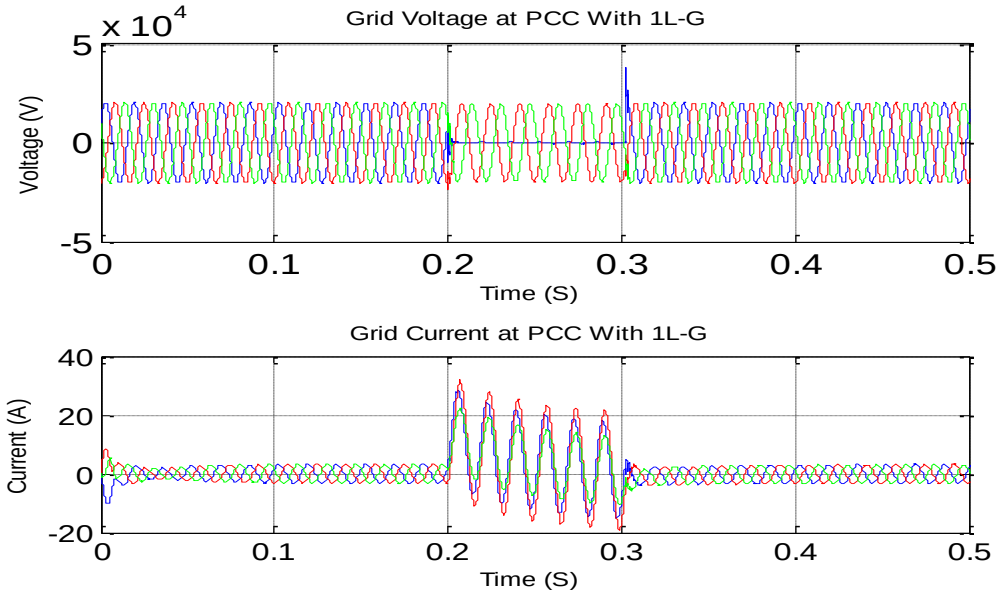

Fig.5.21: Output Voltage and current at the PCC with 1L-G fault.

The simulation was run three times under condition of applying a single line to ground fault while utilizing the three MPPT algorithms discussed in chapter 3. Fig.5.22 shows the output power at the array terminal for the three cases.

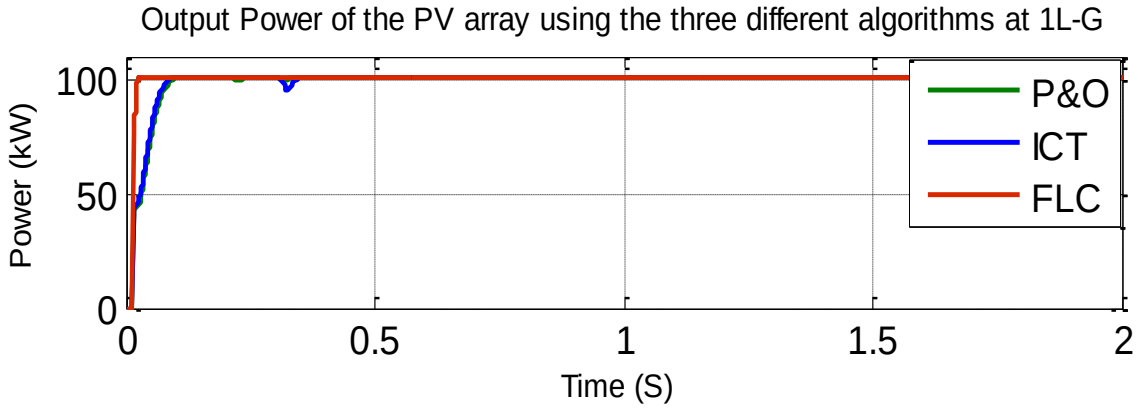

Fig.5.22: Output Power of the PV Array using the three different algorithms with 1LG fault.

- **Line-to-line Fault**

In this case, the model shown in Fig.5.20 is simulated with applying a line to line fault (L-L-F) between phases A and B. The voltage and the current at the PCC are shown in Fig.5.23.

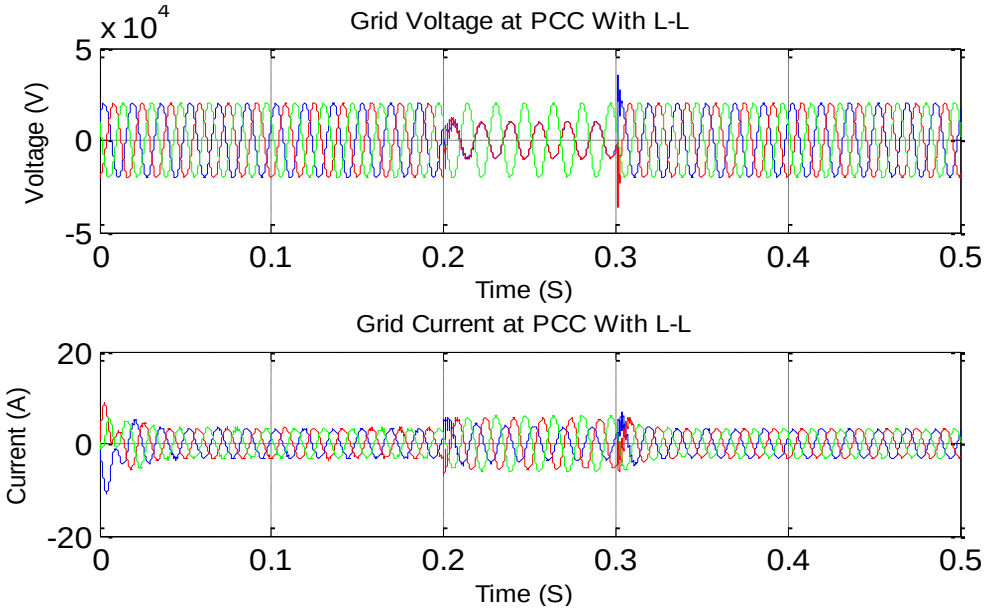

Fig.5.23: Output Voltage and current at the PCC with L-L fault.

In order of compare the performance of the three MPPT algorithms mentioned above to this type of fault, the model is run three times; each time one algorithm is implemented. The output power of the PV array under the three cases is in Fig.5.24.

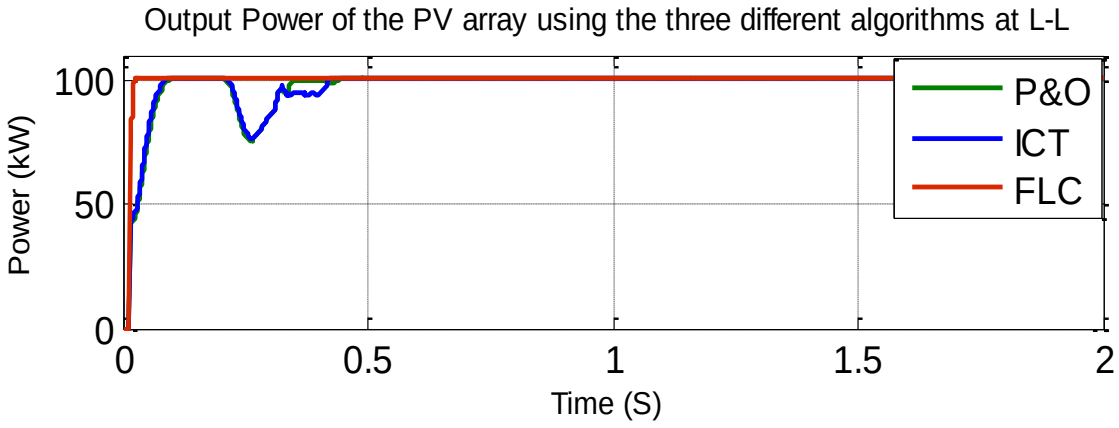

Fig.5.24: Output Power of the PV array using the three different algorithms with L-L fault.

- **Line-to-line-to-ground fault**

A line-to-line-to ground (L-L-G) fault is applied to the model shown in Fig.5.20. The voltage and current waveforms for this case at the point of common coupling is shown in Fig.5.25.

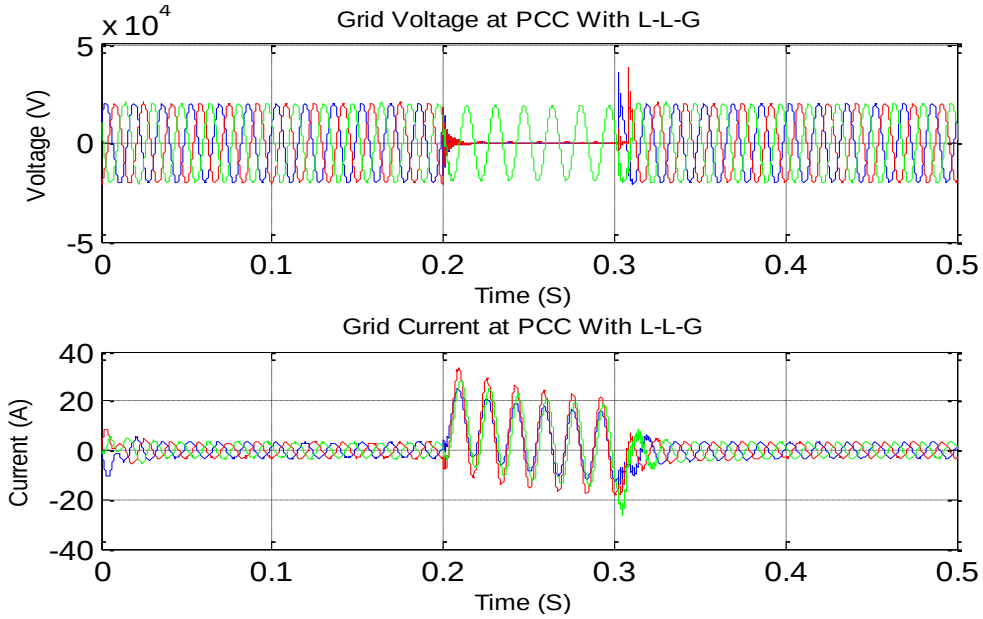

Fig.5.25: Output Voltage and current at the PCC with L-L-G fault.

The output power at the array terminal of the three different maximum power point tracking algorithms while applying this type of fault is shown in Fig.5.26.

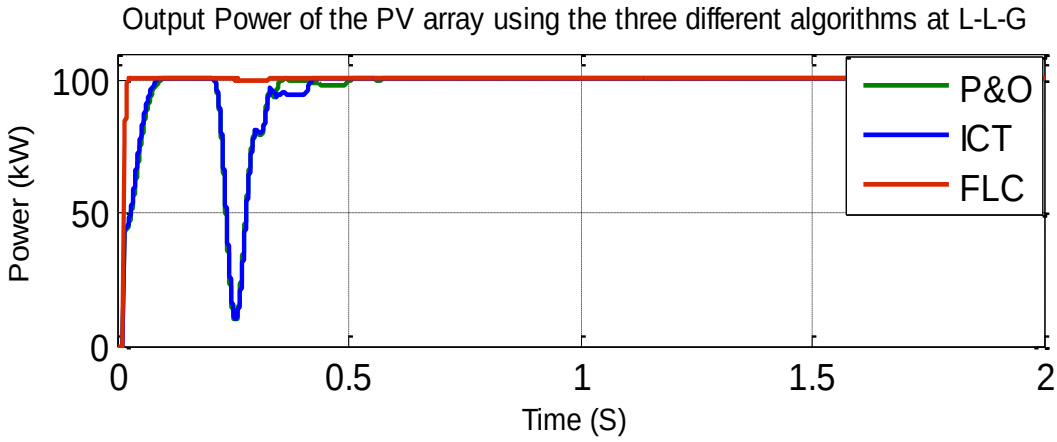

Fig.5.26: Output Power of The PV Array using the three different algorithms with L-L-G fault.

- **Three line to ground fault**

A three line to ground (L-L-L-G) fault is applied to the model shown in Fig.5.20. Fig.5.27 shows the output voltage and current at the PCC. Figure 5.28 shows the output power of the PV array while applying the three MPPT techniques for this type of fault.

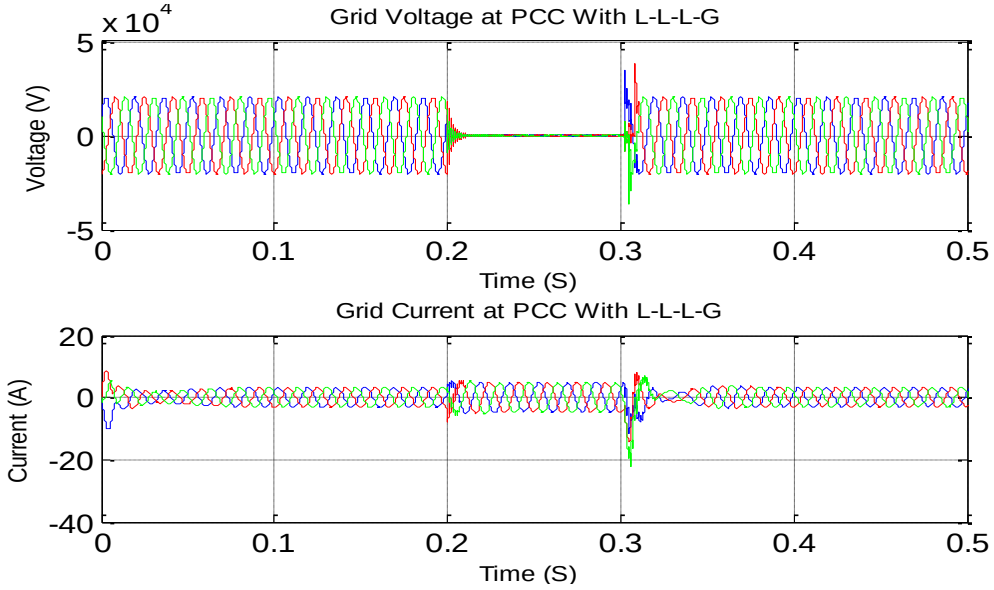

Fig.5.27: Output Voltage and current at Point of common coupling (PCC) with L-L-L-G fault.

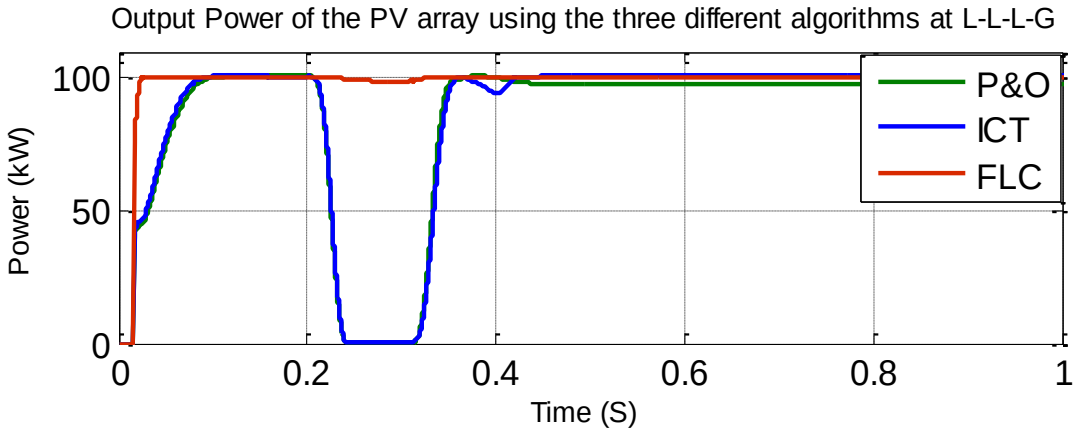

Fig.5.28: Output power of The PV Array using the three different algorithms with L-L-L-G fault.

5.9.2.2 SAG ANALYSIS

The decrease in the RMS value of the voltage between 0.9 to 0.1 p.u. for duration of 0.5 cycles to 1 minute is defined as voltage sag [54]. Voltage sags are generally caused by over loading or grid faults. The MATLAB/SIMULINK model shown in Fig.5.29 is utilized to conduct the analysis in this section. The model shown is simulated under condition of voltage sag at the point of common coupling for duration of 0.1 sec.

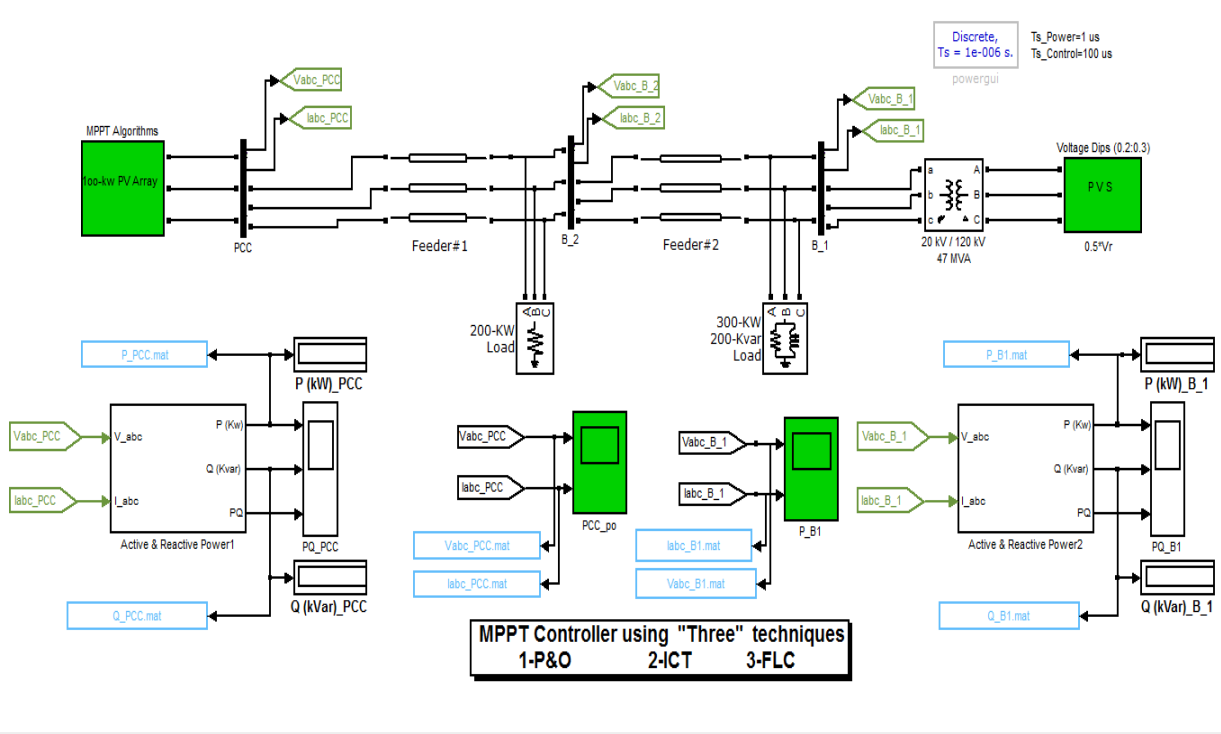

Fig.5.29: Grid Connected PV system under Sag Analysis.

In order to study the effect of voltage sag on the performance of the three MPPT algorithms under study in this thesis, the voltage at the PCC is reduced form 20 kV to 10 kV [55]. The output voltage and current at the PCC is shown in Fig.5.30.

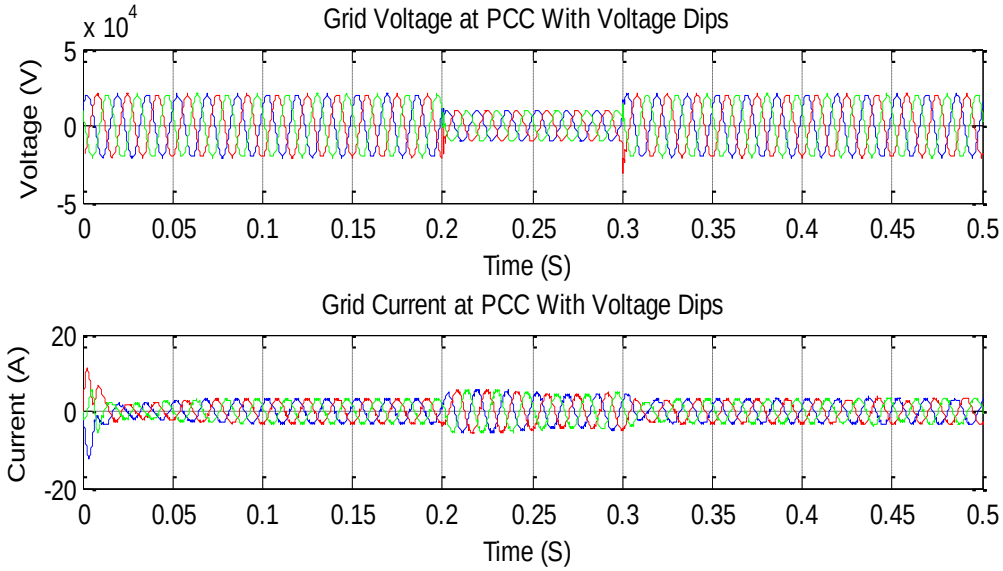

Fig.5.30: Output voltage and current at PCC in case of voltage decreased to 50%.

The simulation is run three times and each time one of the MPPT algorithms is employed while operating the PV array at normal condition. Fig.5.31 shows the output power of the PV array in the three cases.

It can be observed that FLC has a faster response and is not affected by the disturbances occurred on the grid side. In the same time the FLC gives the MPP during the period of voltage dip.

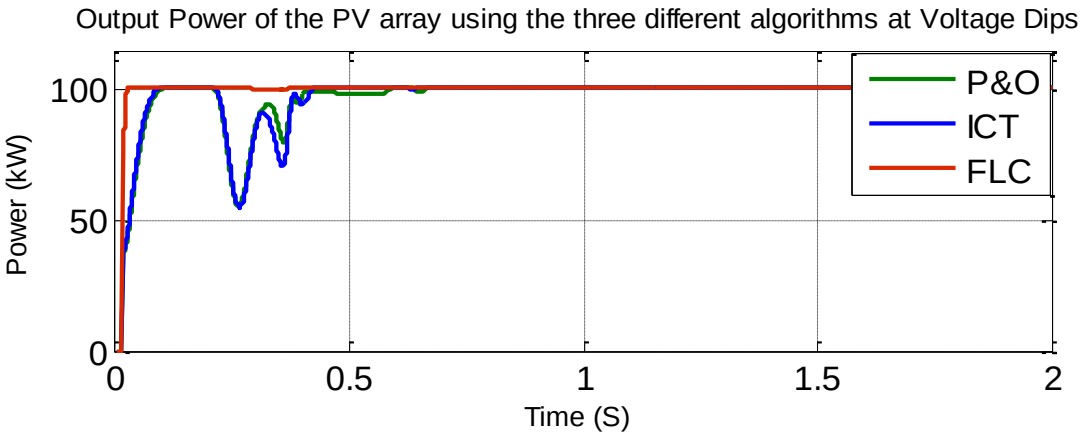

Fig.5.31: Output power of The PV Array using the three different algorithms Under voltage sag.

5.9.2.3 SWELL ANALYSIS

The increase in the RMS voltage between 1.1 to 1.8 p.u. for a duration of 0.5 cycle to 1 minute is defined as voltage swell. Voltage swells are normally initiated by the disconnection of a very large load, the energization of a large capacitor bank and voltage swells are usually associated with the system fault conditions. Fig.5.29 shows the grid connected PV array MATLAB/SIMULINK model which is utilized in this section. The system is studied under voltage swells of 0.1 sec. duration.

For the purpose of studying the effect of voltage swells, the voltage at the PCC is increased from 20 kV to 26 kV as shown in Fig.5.32.

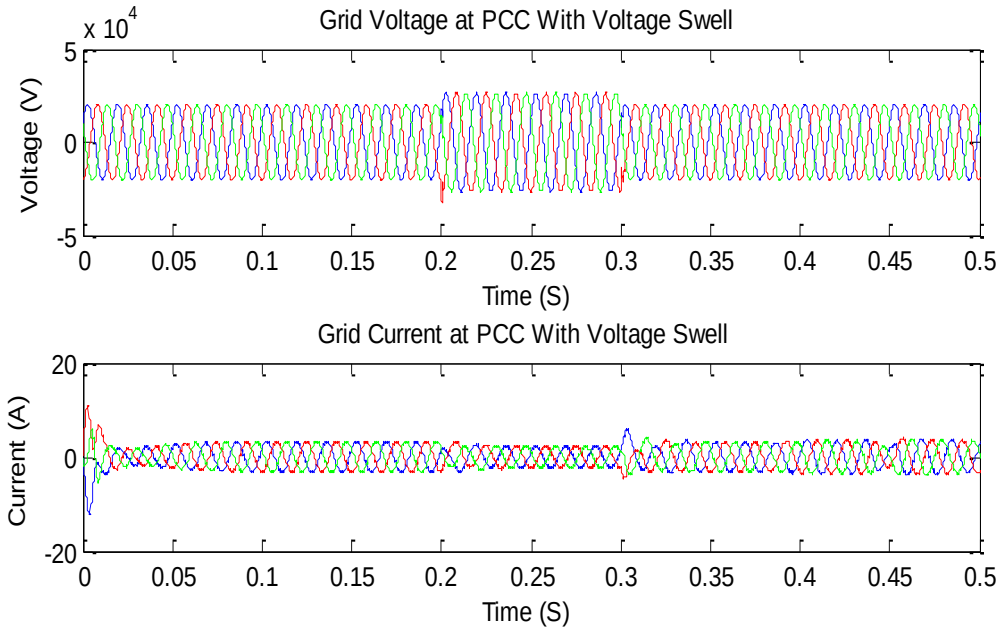

Fig.5.32: Output voltage at the PCC in case of voltage increased to 30%.

The PV array output power of the three MPPT algorithms in case of voltage swell is shown in Fig. 5.33. It can be observed that, the FLC has a good response and don't effect with the disturbances occurred on the grid side. Also, the FLC gives the MPP during the period of voltage swell.

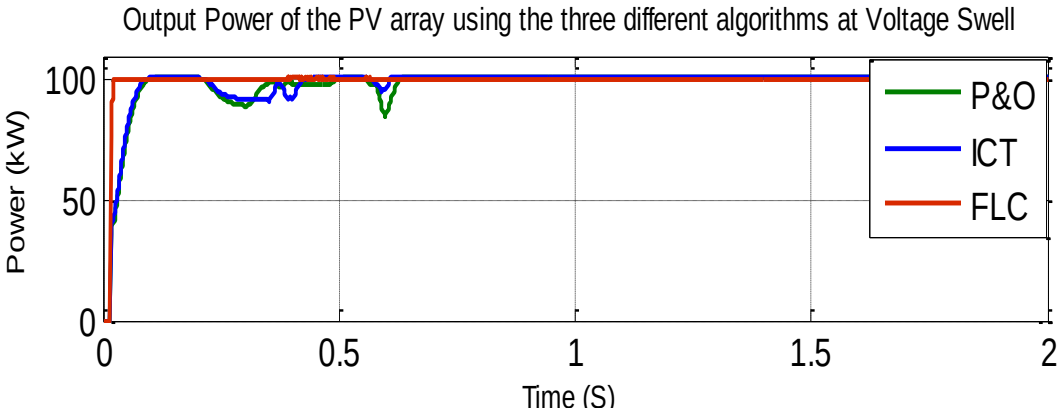

Fig.5.33: Output power of the PV Array using the three different algorithms Under voltage swell condition.

A 100 kW grid connected photovoltaic array is studied under steady state and transient conditions while utilizing three different maximum power point tracking algorithms. The simulation results under transient conditions show that, the output power injected to grid from PV array is approximately constant while utilizing the proposed FLC and the PV system is still connected to grid.

5.10 CONCLUSION

In this chapter, the simulation is made using MATLAB/SIMULINK software for a complete grid-connected PV system. Each component is simulated and discussed in details. The PV model was verified and it gives almost typical results like the ones supplied by the data sheet. The three maximum power point tracking algorithms are developed and compared together. The fuzzy logic control (FLC) algorithm shows faster response in tracking the maximum power point under variable and constant irradiance and gives minimum oscillations around the final operating point compared to ICT and P&O based algorithm. The simulation results under transient conditions show that, the output power injected to grid from PV array is approximately constant while utilizing the proposed FLC and the PV system is still connected to grid and deliver power to grid without any damage to the inverter switches.

.

CHAPTER 6

CONCLUSION AND SCOPE FOR FUTURE WORK

6.1 CONCLUSION

The renewable energy sources such as solar energy play an important role in electric power generation, it is clean and unlimited. A fuzzy logic controller (FLC) was designed to maximize the energy received from solar cells by tracking the maximum power point with the help of DC-DC converter, and then the system is connected to the grid with a DC-AC inverter.

The advantage of the fuzzy logic control is that it does not strictly need any mathematical model of the plant. It is based on plant operator experience, and it is very easy to apply. Hence, many complex systems can be controlled without knowing the exact mathematical model of the plant. In addition, fuzzy logic simplifies dealing with nonlinearities in systems. Also, in fuzzy logic control the linguistic system definition becomes the control algorithm.

The proposed algorithm is by implementing a maximum power point tracker controlled by fuzzy logic controller and using Boost DC-to-DC converter to keep the PV output power at the maximum point all the time. This controller was tested using Matlab/Simulink software, and the results were compared with a perturbation and observation controller and incremental conductance controller which were applied on the same system. The comparison shows that the fuzzy logic controller was faster response in tracking the maximum power point under variable and constant irradiance and gives minimum oscillations around the final operating point compared to the other algorithms.

In this thesis, a 100 kW grid connected photovoltaic array is studied under steady state and transient conditions while utilizing three different maximum power point tracking algorithms. The three algorithms employed are; the Perturb and Observe (P&O) algorithm, the Incremental Conductance (ICT) algorithm and the Fuzzy Logic Control (FLC) algorithm. The simulated results under steady state condition show the effectiveness of the MPPT on increase the output power of the PV array for the three techniques. However the FLC algorithm offers accurate and faster response compared to the others.

The simulation results under transient conditions show that, the output power injected to grid from PV array is approximately constant while utilizing the proposed FLC and the PV system can still connect to grid and deliver power to grid without any damage to the inverter switches.

The fuzzy logic control demonstrates good performance. Furthermore, fuzzy logic offers the advantage of faster design, and simulation of human control strategies. Also, fuzzy control worked well for nonlinear system and shown higher efficiency over the conventional controllers.

6.2 SCOPE FOR FUTURE WORK

- Implementation of a physical model for the fuzzy logic controller technique based MPP using microcontrollers and testing it on a real PV panel. The most popular method of implementing fuzzy controller is using a general-purpose microprocessor or microcontroller.

- Using optimization method to reduce the rules of the controller such as using Genetic Algorithm with Fuzzy controllers. They can be used in the control algorithm to tune the membership functions so that the inexact reasoning characteristics of the FLC are sufficient to control a system that requires precise control actions.

- Comparing between different inverter control strategies and its effect on power quality from the utility grid point of view.

- Studying the effect of power quality disturbances on the stability of maximum power point tracking controllers.

- Grid Connected Photovoltaic Systems with Smart Grid.

REFERENCES

REFERENCES

[1] A. Timbus, Grid Monitoring and Advanced Control of Distributed Power Generation Systems, 2007.

[2] M. Rashid, Power Electronics Handbook- Devices, Circuits and Application, Academic Press, 2011.

[3] S. Kalogirous, Solar Energy Engineering :Processes and Systems. Academic Press, 2009

[4] A. Goetzberger, Photovoltaic Solar Energy Generation. Springer, 2005.

[5] Governor Schwarzenegger Advances State's Renewable Energy Development, California Governor's Executive Order S-14-08, November 2008.

[6] Renewables 2013: Global Status Report, REN21, 2013.

[7] Solar Photovoltaics: Status, Costs, and Trends, EPRI, Palo Alto, 1015804, 2009.

[8] R. A. Messenger and J. Ventre, Photovoltaic Systems Engineering, CRC Press, 2010.

[9] U.S. Department of Energy, 2010 Solar Technologies Market Report, First Solar. [Online]. http://www.firstsolar.com/Projects/Topaz-Solar-Farm.

[10] The Solar Panel How To Guide, December, 2010. Retrieved from http://www.solarpanelsbook.com

[11] V. Quaschning, Understanding Renewable Energy Systems, London, Carl Hanser Verlag GmbH & Co KG, 2005.

[12] S. E. Evju, Fundamentals of Grid Connected Photovoltaic Power Electronic Converter Design. Specialization project, Department of Electric Engineering, Norwegian University of Science and Technology, December 2006.

[13] T.Burton, D.Sharpe, N.Jenkins and E.Bossanyi, Wind Energy Handbook. England, 2001.

[14] M.G.Villalva, J.R.Gazoli and E. Ruppert F, Comprehensive Approach to Modeling and Simulation of Photovoltaic Arrays, IEEE Transactions, vol. 25, no. 5, pp. 1198-- 1208, ISSN 0885-8993, 2009.

[15] M. Villalva, J. Gazoli, and E. Ruppert, Modeling and Circuit-Based Simulation Of Photovoltaic Arrays, IEEE Transactions' On Power Electronics, Vol. 24, No5. may 2009.

[16] KYOCERA [KC200GT], High Efficiency Photovoltaic Module Data Sheet.

[17] IEA International Energy Agency, Snapshot of International Electricity Utility Activities, survey report of selected IEA countries between 1992 and 2010 .

[18] A. S. Khalifa, Control and Interfacing of Three Phase Grid Connected Photovoltaic Systems, Master of Applied Science, Waterloo, 2010

[19] T. S. Basso, High-Penetration, Grid-Connected Photovoltaic Technology Codes and Standards, IEEE Photovoltaic Specialists Conference, 11-16 May 2008, pp.1-4.

[20] S. Wolf and J. Enslin, Economical, PV Maximum Power Point Tracking Regulator with Simplistic Controller, PESC'93

[21] S. Cardona and M. M. Lopez, Performance Analysis of A Grid-Connected Photovoltaic System. Energy. 24, 93-102, 1999.

[22] T. Esram and P. Chapman, Comparison of Photovoltaic Array Maximum Power Point Tracking Techniques, IEEE Trans. Energy Conversion, vol.22, No. 2, June 2007.

[23] A. M. Cheikh, and S. C.Larbes, Maximum Power Point Tracking using A Fuzzy Logic Control Scheme, Septembre 2007.

[24] S. Jain and V. Agarwal, Comparison of The Performance Of Maximum Power Point Tracking Schemes Applied To Single-Stage Grid-Connected Photovoltaic Systems, IETElectr. Power Appl., vol. 1, No. 756 (5), pp. 753-762, September 2007.

[25] F. Umeda, M. H. Ohsato, G. Kimura, and M. Shioya, New Control Method of Resonant DC-DC Converter in Small Scaled Photovoltaic System, Inpesc, '92 Record, v2, IEEE, Toledo, 29 Jun-3 Jul 1992, pp. 714 - 718 vol.1.

[26] M. G. Villalva, J. R. Gazoli and E. Ruppert F. Analysis and Simulation of The P&O MPPT Algorithm using Alinearized Array Model. Power electronics conference, Brazil, 2009.

[27] A. Safri and S. Mekhilef. Incremental Conductance MPPT Method for PV Systems, Electrical and Computer Engineering (CCECE). 2011, Canada.

[28] T. Bennett, A. Zilouchian, and R. Messenger, Perturb and Observe versus Incremental Conductance MPPT Algorithms, IEEE Transactions On Power Systems.

[29] R. Rawat and S.S.Chandel, Hill Climbing Techniques For Tracking Maximum Power Point In Solar Photovoltaic Systems-A Review, (IJSDGE), ISSN No.: 2315-4721, V-2, I-1, 2, 2013.

[30] U. R. Yaragatti, A. N. Rajkiran, and B. C. Shreesha, A Novel Method of Fuzzy Controlled Maximum Power Point Tracking in Photovoltaic Systems, in Proceedings of IEEE International Conference on Industrial Technology, pp. 1421-1426, 2005.

[31] A. M. Eltamaly, Modeling of Fuzzy Logic Controller for Photovoltaic Maximum Power Point Tracker,‖ Solar Future 2010 Conf. Proc., Istanbul, Turkey, pp. 4-9, Feb. 2010.

[32] C. Salah and M. Ouali, Comparison of Fuzzy Logic and Neural Network in Maximum Power Point Tracker for PV Systems , ‖ Electric Power Systems Research 81, pp. 43–50, 2011.

[33] H.E.A. Ibrahim and M. Ibrahim, Comparison Between Fuzzy and P&O Control for MPPT for Photovoltaic System Using Boost Converter, Journal of Energy Technologies and Policy, Vol.2, No.6, 2012.

[34] C.S. Chin, P. Neelakandan, H.P. Yoong, and K.T.K. Teo, Optimisation of Fuzzy based Maximum Power Point Tracking in PV System for rapidly changing solar irradiance, Transaction on Solar Energy and Planning, vol.2, June 2011.

[35] S.V. Dhople, A. Davoudi, and P.L Chapman, Dual Stage Converter to Improve Transfer Efficiency and Maximum Power Point Tracking Feasibility in Photovoltaic Energy-Conversion Systems, Applied Power Electronics Conference and Exposition (APEC), 2010 Twenty-Fifth Annual IEEE, March 2010, pp. 2138 - 2142.

[36] B.M. Hasaneen and A.A. Elbaset Mohammed, Design and Simulation of DC/DC Converter, Power System Conference, 2008. MEPCON 2008. 12th International Middle-East, July 2008, pp. 335 - 340.

[37] E. Koutroulis, K. Kalaitzakis, and N. C. Voulgaris, Development of A Microcontroller-Based Photovoltaic Maximum Power Point Tracking Control System, Transactions on Power Electronics, IEEE, vol. 16, August 2002, pp. 46 - 54.

[38] R. Song et al, VSC based HVDC and its Control Strategy, IEEE/PES Trans. and Distrb. Conference and Exhibition, 2005.

[39] J. Svensson, Synchronisation, Methods for Grid-Connected Voltage Source Converters, Proc. Inst. Electr. Eng.-Gener. Transm. Distrib. vol.148, no. 3, pp. 229–235, May 2001.

[40] C. Bajracharya, Control of VSC-HVDC for Wind Power, Specialization Project, NTNU, Jan. 2008.

[41] N. Mohan, T. M. Undeland, and W. P. Robbins, Power Electronics: Converters, Applications and Design, John Wiley and Sons Inc., November 2002.

[42] S.K. Chung, Phase-Locked Loop For Grid-Connected Three-Phase Power Conversion Systems, Proc. Inst. Electr. Eng-Electron. Power Appl.,vol.147, no. 3, pp. 213–219, May 2000.

[43] G. C. Hsieh and J. C. Hung , Phase- Lock Loop Techniques - A Survey IEEE Transaction on Industrial Electronics, Vol. 43, pp. 50- 60, December 1999.

[44] X. Zong. A Single Phase Grid Connected DC/AC Inverter with Reactive Power Control for Residential PV Application. Master's thesis, Department of Electrical and Computer Engineering University of Toronto, 2011.

[45] P. H Zope, P. G.Bhangale, P. Sonare, and S.R. Suralkar. Design and Implementation of Carrier Based Sinusoidal PWM Inverter. International Journal of Advanced Research in Electrical, Electronics and Instrumentation Engineering (IJAREEIE), ISSN: 2278 - 8875, Vol.1, No.4, pp 230-236, October, 2012.

[46] B. Majhi, Analysis of Single-Phase SPWM Inverter, Master's thesis, Department of Electrical Engineering National Institute of Technology, Rourkela May 2012.

[47] E. El-Saadany, Power Quality Improvement for Distribution Systems under Non-linear Conditions.PHD, Thesis, Waterloo, 1998.

[48] A. P. J. Rens and P. H. Swart, On Techniques for The Localization Of Multiple Distortion Sources in Three-Phase Networks: Time-Domain Verification, European Transactions on Electrical Power, 22 MAR 2007.

[49] IEEE Recommended Practice for Monitoring Electric Power Quality, IEEE Std. 1159-1995.

[50] M.H.J. Bollen, Understanding Power Quality Problems: Voltage Sags and Interruptions, Wiley-IEEE Press, 2000.

[51] G.W. Chang and P.F. Ribeiro. Harmonics Theory. Chapter 2, IEEE Tutorial on Harmonic Modeling, 1998.

[52] W. Xu, X. Liu, and Y. Liu, An Investigation on The Validity of Power Direction Method for Harmonic Source Determination. IEEE Power Engineering Review, IEEE Transactions, 2003, pp. 214 – 219.

[53] H. C. Seo, C. H. Kim, and Y. M. Yoon, C. S. Jung, Dynamics of Grid-Connected Photovoltaic System At Fault Conditions, Asia and Pacific Transmission & Distribution Conference & Exposition, 2009.

[54] BS EN 50160:2007, Voltage Characteristics of Electricity Supplied by Public Distribution System, CEI EN50160, February 2007.

[55] M. McGranaghan, D. Mueller, and M. Samotyj, Voltage Sags in Industrial System, Transactions on Industry Applications, vol. 29, no. 2, March-April 1993.

APPENDICES

APPENDICES

1.1 Appendix A

Data Sheet OF KYOCERA (KC200GT) High Efficiency Photovoltaic Module:

THE NEW VALUE FRONTIER

KYOCERA

KC200GT

HIGH EFFICIENCY MULTICRYSTAL
PHOTOVOLTAIC MODULE

LISTED

HIGHLIGHTS OF KYOCERA PHOTOVOLTAIC MODULES

Kyocera's advanced cell processing technology and automated production facilities produce a highly efficient multicrystal photovoltaic module.
The conversion efficiency of the Kyocera solar cell is over 16%.
These cells are encapsulated between a tempered glass cover and a pottant with back sheet to provide efficient protection from the severest environmental conditions.
The entire laminate is installed in an anodized aluminum frame to provide structural strength and ease of installation.
Equipped with plug-in connectors.

APPLICATIONS

KC200GT is ideal for grid tie system applications.

- Residential roof top systems
- Large commercial grid tie systems
- Water Pumping systems
- High Voltage stand alone systems
- etc.

QUALIFICATIONS

- **MODULE** : UL1703 certified
- **FACTORY** : ISO9001 and ISO 14001

QUALITY ASSURANCE

Kyocera multicrystal photovoltaic modules have passed the following tests.

- Thermal cycling test
- Thermal shock test
- Thermal / Freezing and high humidity cycling test
- Electrical isolation test
- Hail impact test
- Mechanical, wind and twist loading test
- Salt mist test
- Light and water-exposure test
- Field exposure test

LIMITED WARRANTY

- 1 year limited warranty on material and workmanship
- 20 years limited warranty on power output: For detail, please refer to "category IV" in Warranty issued by Kyocera

(Long term output warranty shall warrant if PV Module(s) exhibits power output of less than 90% of the original minimum rated power specified at the time of sale within 10 years and less than 80% within 20 years after the date of sale to the Customer. The power output values shall be those measured under Kyocera's standard measurement conditions. Regarding the warranty conditions in detail, please refer to Warranty issued by Kyocera)

ELECTRICAL CHARACTERISTICS

Current-Voltage characteristics of Photovoltaic Module KC200GT at various cell temperatures

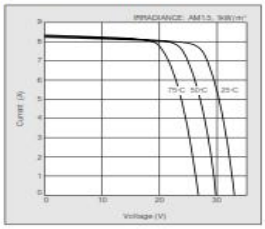

Current-Voltage characteristics of Photovoltaic Module KC200GT at various irradiance levels

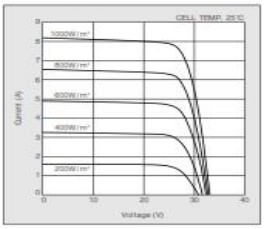

SPECIFICATIONS

KC200GT

■ Physical Specifications

Unit : mm (in.)

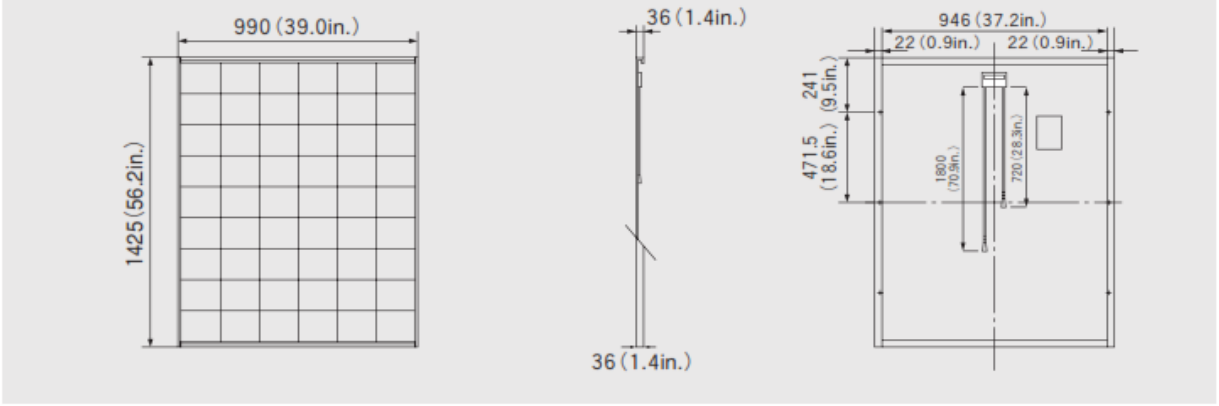

■ Specifications

■ Electrical Performance under Standard Test Conditions (*STC)	
Maximum Power (Pmax)	200W (+10%/−5%)
Maximum Power Voltage (Vmpp)	26.3V
Maximum Power Current (Impp)	7.61A
Open Circuit Voltage (Voc)	32.9V
Short Circuit Current (Isc)	8.21A
Max System Voltage	600V
Temperature Coefficient of Voc	-1.23×10^{-1} V/℃
Temperature Coefficient of Isc	3.18×10^{-3} A/℃

*STC : Irradiance 1000W/m², AM1.5 spectrum, module temperture 25℃

■ Electrical Performance at 800W/m², NOCT, AM1.5	
Maximum Power (Pmax)	142W
Maximum Power Voltage (Vmpp)	23.2V
Maximum Power Current (Impp)	6.13A
Open Circuit Voltage (Voc)	29.9V
Short Circuit Current (Isc)	6.62A

NOCT (Nominal Operating Cell Temperature) : 47℃

■ Cells	
Number per Module	54

■ Module Characteristics	
Length × Width × Depth	1425mm(56.2in)×990mm(39.0in)×36mm(1.4in)
Weight	18.5kg(40.7lbs.)
Cable	(+)720mm(28.3in),(-)1800mm(70.9in)

■ Junction Box Characteristics	
Length × Width × Depth	113.6mm(4.5in)×76mm(3.0in)×9mm(0.4in)
IP Code	IP65

■ Reduction of Efficiency under Low Irradiance	
Reduction	7.8%

Reduction of efficiency from an irrandiance of 1000W/m² to 200W/m² (module temperature 25℃)

Please contact our office for further information

KYOCERA

KYOCERA Corporation

■ KYOCERA Corporation Headquarters
CORPORATE SOLAR ENERGY DIVISION
6 Takeda Tobadono-cho
Fushimi-ku, Kyoto
612-8501, Japan
TEL:(81)75-604-3476 FAX:(81)75-604-3475
http://www.kyocera.com

● KYOCERA Solar, Inc.
7812 East Acoma Drive
Scottsdale, AZ 85260, USA
TEL:(1)480-948-8003 or (800)223-9580 FAX:(1)480-483-6431
http://www.kyocerasolar.com

● KYOCERA Solar do Brasil Ltda.
Av. Guignard 661, Loja A
22790-200, Recreio dos Bandeirantes, Rio de Janeiro, Brazil
TEL:(55)21-2437-8525 FAX:(55)21-2437-2338
http://www.kyocerasolar.com.br

● KYOCERA Solar Pty Ltd.
Level 3, 6-10 Talavera Road, North Ryde
N.S.W. 2113, Australia
TEL:(61)2-9870-3948 FAX:(61)2-9888-9588
http://www.kyocerasolar.com.au/

● KYOCERA Fineceramics GmbH
Fritz Muller strasse 107, D-73730 Esslingen, Germany
TEL:(49)711-93934-917 FAX:(49)711-93934-950
http://www.kyocerasolar.de/

● KYOCERA Asia Pacific Pte. Ltd.
298 Tiong Bahru Road, #13-03/05
Central Plaza, Singapore 168730
TEL:(65)6271-0500 FAX:(65)6271-0600

● KYOCERA Asia Pacific Ltd.
Room 801-802, Tower 1 South Seas Centre, 75 Mody Road,
Tsimshatsui East, Kowloon, Hong Kong
TEL:(852)2-7237183 FAX:(852)2-7244501

● KYOCERA Asia Pacific Ltd. Taipei Office
10 Fl., No.66, Nanking West Road, Taipei, Taiwan
TEL:(886)2-2555-3609 FAX:(886)2-2559-4131

● KYOCERA(Tianjin) Sales & Trading Corporation
19F, Tower C HeQiao Building 8A GuangHua Rd.,
Chao Yang District, Beijing 100026, China
TEL:(86)10-6583-2270 FAX:(86)10-6583-2250

LIE/109M0703-SAGKM

1.2 Appendix B

BOOST CONVERTERS

In our thesis, The main purpose of the DC/DC is to convert the DC input from the PV into a higher DC output. The maximum power point tracker uses the DC/DC converter to adjust the PV voltage at the maximum power point. The boost topology is used for stepping up the low voltage input from the PV. A boost type converter steps up the PV voltage to high voltage necessary for the inverter.

Figure C.1 shows the Boost converter. The DC input voltage is in series with an inductor L that acts as a current source. A switch T is in parallel with the current source that turns on and off periodically, providing energy from the inductor and the source to increase the average output voltage.

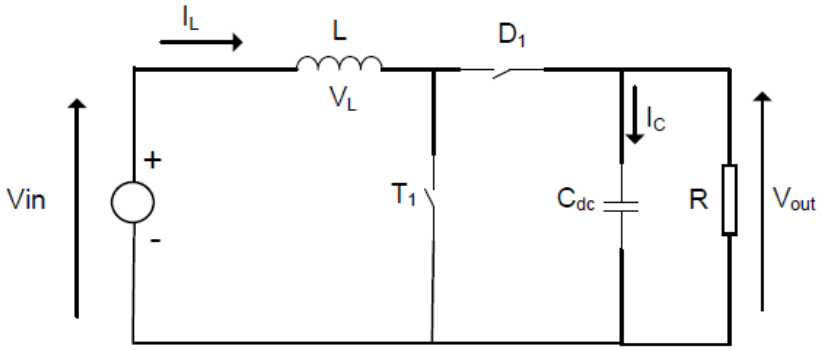

Fig.C.1: Topology of Boost converter.

The capacitor C_{dc} is large enough to keep a constant output voltage, and the inductor provides energy when the switch is open, boosting the voltage across the load. The duty cycle from the MPPT controller is to control the switch of the boost converter. It is a gate signal to turn on and off the switches by pulse width modulation.

In Figure C.2, The switch T1 is on and D1 is off, the circuit is split into two different parts: the source chargers the inductor on the left while the right has the capacitor, which is responsible for sustaining outgoing voltage via energy, stored previously. The current of inductor L is increased gradually.

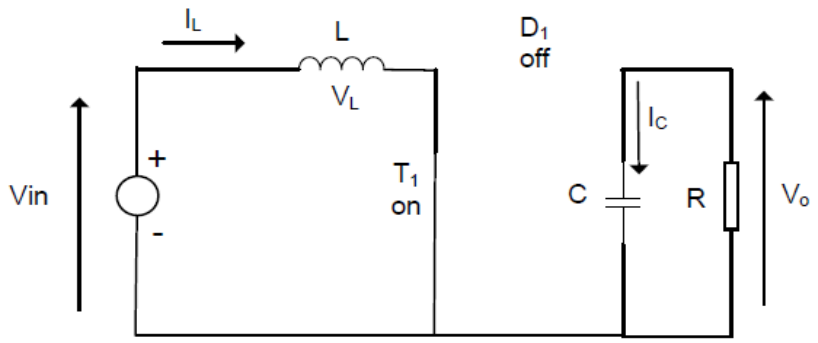

Fig.C.2: Circuit Diagram when switch T1 is on and D1 is off

In Figure C.3, the switch T1 is off and D1 is on, the energy along with the DC source that is stored within the inductor will help supplement power for the circuit that is on the right thereby resulting in a boost for the output voltage. Then, the inductor current discharges and reduces gradually. The output voltage could be sustained at a particular wanted level if the switching sequence is controlled.

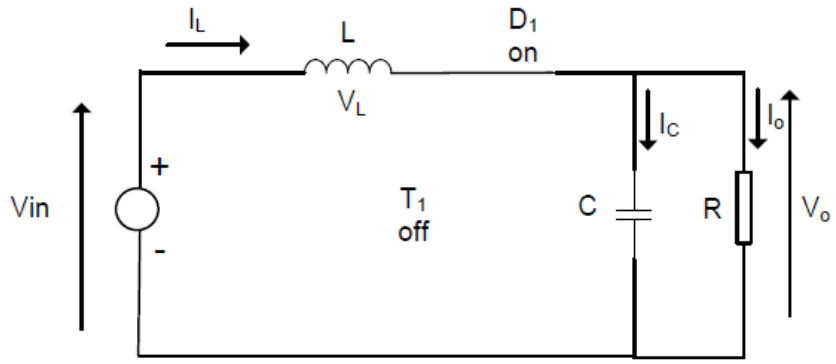

Fig.C.3: Circuit Diagram when switch T1 is off and D1 is on

Figure C.4 summarizes the currents and voltages for output in terms of the boost converter. The control switch for the voltage of control is shown. The switch turns ON and OFF for a period t_{on} and t_{off}. When the switch is on, the voltage across the switch is zero and once the switch is turned off, the voltage is V_{out}. The voltage across the inductor L is equal to the photovoltaic voltage during the on time of the transistor.

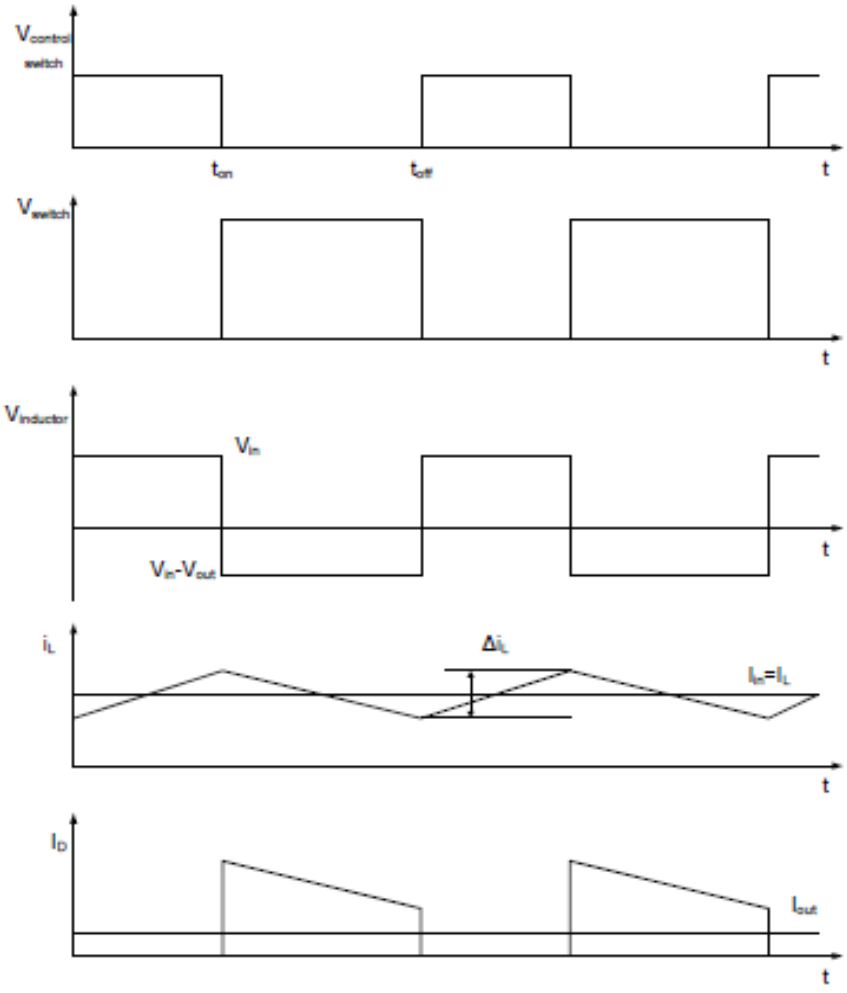

Fig.C.4: Output waveform of DC/DC Boost converter.

1.3 Appendix C

Park and Clark transformation system

The summary of the transformations are presented as follows.

Transformation	Transforms	Matrix for transformation
Clark transformation	from abc to αβ	$\frac{2}{3}\cdot\begin{pmatrix} 1 & -1/2 & -1/2 \\ 0 & \sqrt{3}/2 & -\sqrt{3}/2 \end{pmatrix}$
Inverse Clark transformation	from αβ to abc	$\begin{pmatrix} 1 & 0 \\ -1/2 & \sqrt{3}/2 \\ -1/2 & -\sqrt{3}/2 \end{pmatrix}$
Park transformation	from αβ to dq	$\begin{pmatrix} \cos\theta & \sin\theta \\ -\sin\theta & \cos\theta \end{pmatrix}$
Inverse Park transformation	from dq to αβ	$\begin{pmatrix} \cos\theta & -\sin\theta \\ \sin\theta & \cos\theta \end{pmatrix}$

1.4 Appendix D

SINUSOIDAL PULSE WIDTH MODULATIN ALGORITHM:

Three-phase VSCs cover the medium- to - high-power applications. The main purpose of these topologies is to provide three-phase voltage source, where the amplitude, phase, and frequency of the voltages should always be controllable. Although most of the applications require sinusoidal voltage waveforms (e.g., ASDs, UPSs, FACTS, VAR compensators), arbitrary voltages are also required in some emerging applications (e.g., active filters, voltage compensators). The standard three-phase VSC topology is shown in Figure.D.1

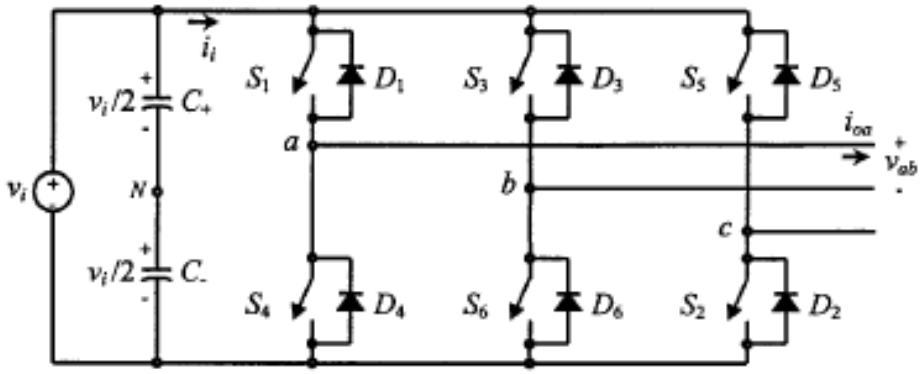

Fig.D.1: Three-phase VSC topology.

In this case and in order to produce 120° out-of-phase load voltages, three modulating signals that are 120°out of phase are used. Figure D.2 shows the ideal waveforms of three-phase VSC-SPWM. In order to use a single carrier signal and preserve the features of the PWM technique, the normalized carrier frequency m should be an odd multiple of 3. Thus, all phase voltages are identical but 120°out of phase. In this modulation technique there are multiple numbers of output pulses per half cycle and pulses are of different width. The width of each pulse is varying in proportion to the amplitude of a sine wave evaluated at the Centre of the same pulse. The gating signals are generated by comparing a sinusoidal reference signal with a high frequency triangular signal. The reference signal frequency determines the frequency of the inverter output voltage.

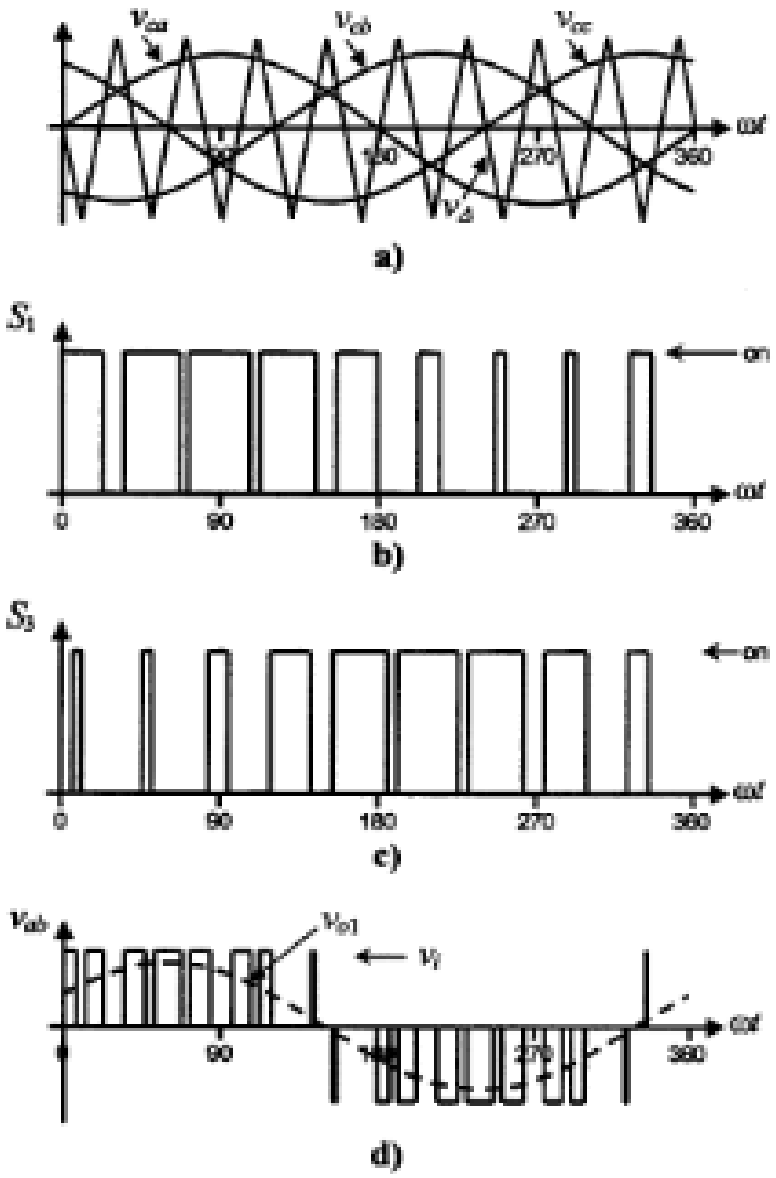

Fig.D.2: The three - phase VSC for the SPWM.

a. **Carrier and modulating signals**
b. **Switch S1 state**
c. **Switch S3 state**
d. **Ac output voltage**

1.5 Appendix E

MATLAB CODES:

E1: CODE OF PERTURB AND OBSERVE ALGORITHM.

```
function D  = PO(Param, Enabled, V, I)
%   increasing D = decreasing Vref
Di = Param(1);      %Initial value for D output
Dmax = Param(2);    %Maximum value for D
Dmin = Param(3);    %Minimum value for D
deltaD = Param(4);

%Increment value used to increase/decrease the duty cycle D

persistent Vo
           Po
           Do;

dataType = 'double';

if isempty(Vo)
    Vo=0;
    Po=0;
    Do=Di;
end
P= V*I;
deltaV= V - Vo;
deltaP= P - Po;

if deltaP ~= 0 & Enabled ~=0
    if deltaP < 0
        if deltaV < 0
            D = Do - deltaD;
        else
            D = Do + deltaD;
        end
    else
        if deltaV < 0
            D = Do + deltaD;
        else
            D = Do - deltaD;
        end
```

```
    end
else D=Do;
end

if D >= Dmax | D<= Dmin
    D=Do;
end

Do=D;
Vo=V;

% MPPT controller based on the Perturb & Observe algorithm.

% D output = Duty cycle of the boost converter (value between
   0 and 1)
%
% Enabled input = 1 to enable the MPPT controller

% V input = PV array terminal voltage (V)

% I input = PV array current (A)

load p_pv_po
load v_pv_po
load i_pv_po
power1';
current1';
voltage1';
close all
%-----------------------------------------------------------------
-----------------------------
F1=figure('Name','V,I and P  of PV array : Kyocera KC200GT of
8 series modules; 63 parallel strings');
figure(F1)
subplot(3,1,1)
a=voltage1';
plot(a(:,1),a(:,2))
ylabel('Voltage (V)')
xlabel('Time (S) ')
title(sprintf('PV Array : Kyocera KC200GT of 8 series modules;
63 parallel strings  %s'))
subplot(3,1,2)
b=current1';
```

```
plot(b(:,1),b(:,2))
ylabel('Current (A)')
xlabel('Time (S) ')
%title(sprintf('PV Array : Kyocera KC200GT of 8 series
modules; 63 parallel strings %s'))
%-----------------------------------------------------------------
-----------------------------


 subplot(3,1,3)
 c=power1';
 plot(c(:,1),c(:,2))
ylabel('Power (kW)')
xlabel('Time (S) ')
%title(sprintf('PV Array : Kyocera KC200GT of 8 series
modules; 63 parallel strings %s'))
%-----------------------------------------------------------------
-----------------------------
```

PUBLICATION OUT OF THIS THESIS

[1] Y. Abdelaziz, Hadi M. El-Helw and Basem Abdelhamed, 'Comparative Evaluation of Maximum Power Point Tracking Techniques for Grid Connected PV System', Proceedings of 11th International Conference on Modeling and Simulation of Electric Machines, Converters and Systems, ELECTRIMACS 2014, 19-22 May 2014, Valencia, Spain.

[2] A. Y. Abdelaziz, Hadi M. El-Helw and Basem Abdelhamed, 'Transient Analysis of Grid-Connected Photovoltaic System Based on Comparative Study of Maximum Power Point Tracking Techniques', International Journal of Advances in Power Systems (IJAPS), Vol. 1, No. 3, December 2013.

إستعراض الرسالة

الفصل الاول :

يعرض هذا الفصل مقدمة لموضوع البحث ، كما يعرض أهداف الرسالة ومكوناتها والخطوط العريضة لها.

الفصل الثانى :

يستعرض هذا الفصل بعض المبادئ الأساسية للطاقة الشمسية وخاصة الخلايا الضوئية وأنواعها والدوائر الكهربية وخصائص تلك الخلايا ، ومن خلال تلك الخصائص تتم معرفة أقصى نقطة تتبع لمجموعة الخلايا الضوئية.

الفصل الثالث :

يقدم هذا الفصل دراسة كيفية تتبع أقصى نقطة لمجموعة الخلايا الضوئية بالتفصيل وتوضيح الإختلاف بين مجموعة من الطرق المستخدمة. كما يقوم بتقييم أداء ثلاث تقنيات تتبع لنقطة القدرة العظمى لنظام التوليد بإستخدام الطاقة الضوئية والمتصلة بالشبكة الكهربية ومعرفة الفائدة من استخدام مقطع الجهد للتحكم فى الجهد المستمر الداخل الى دائرة العاكس فى الثلاث تقنيات المستخدمة.

الفصل الرابع :

يقدم هذا الفصل التعريف الخاص بجودة القدرة الكهربية والمصطلحات الخاصة بها وتفسيراتها الضرورية ، كما يقدم شرحا لكيفية حدوث بعض الظواهر التى تؤثر على جودة القدرة فى النظام الكهربى.

الفصل الخامس :

تم عمل نموذج كامل لأنظمة الخلايا الضوئية الموصلة مع الشبكة عن طريق المحاكاة الفعلية للنظام بإستخدام برنامج MATLAB ، ويعرض نتائج المحاكاة بالنسبة للثلاث تقنيات المستخدمة ، علاوة على ذلك تمت مقارنة المتحكم المبهم مع التقنيات التقليدية كذلك تمت دراسة تأثير الإضطرابات التى تحدث فى الشبكة الكهربية وتأثيرها على ملاحقة نقطة القدرة العظمى وتم دراسة مجموعة من هذه الاضطرابات وعمل دراسة مقارنة لتتبع الثلاث تقنيات المختلفة وتأثيرها على حالات جودة القدرة.

الفصل السادس :

يقدم هذ الفصل الإستنتاجات المستخلصة من الرسالة وتحليل النتائج التى تم الحصول عليها.

ملخص الرسالة

في الآونة الأخيرة، زاد استخدام أنظمة الطاقة الضوئية المتصلة بالشبكة و ذلك من أجل تلبية الطلب المتزايد على الطاقة. و التي تحتاج إلى تحسين المواد والطرق المستخدمة في تسخير هذا المصدر. و هناك العديد من الطرق المستخدمة من أجل تحقيق أقصى نقطة تتبع لمجموعة الخلايا الضوئية و منها الطرق التقليدية وطرق الذكاء الصناعى و من بين كل هذة التقنيات تلك التقنية المعتمدة على الذكاء الصناعى فهى فعالة جدا فى التتبع. وهذا المتحكم اما ان يكون من نوع تقليدى أو من نوع ذكى مثل المتحكمات المبهمة حيث أن للمتحكم المبهم مميزات مثل سهولة نسبية فى التصميم فهو لا يحتاج معرفة دقيقة عن المعادلات الرياضية التى تصف النظام المراد التحكم بة وهو يعمل بشكل أفضل مع الأنظمة الاخطية و من مميزات المنطق المبهم هو أن تعريف النظام اللغوي يصبح خوارزمي التحكم.

فى هذا البحث ، تم إستخدام نموذج لمحاكاة السلوك الفعلى لنظام الخلايا الضوئية و من ثم يتم تقيم أداء ثلاث تقنيات تتبع لنقطة القدرة العظمى لنظام التوليد بإستخدام الخلايا الضوئية و المتصلة بالشبكة الكهربية من أجل السيطرة على دائرة مغير الجهد المستمر. و التقنيات المستخدمة فى هذا البحث موضوع المقارنة و الدراسة هى ١- Perturb & Observe ٢- Incremental Conductance ٣- Fuzzy Logic Control
و من ثم تم استخدام مقطع الجهد للتحكم فى الجهد المستمر الداخل الى دائرة العاكس فى الثلاث تقنيات بحيث يظل الجهد ثابت مما يسهل من تحديد القيمة العظمى للنظام.

علاوة على ذلك، تم مقارنة المتحكم المبهم مع التقنيات التقليدية وأيضا تم دراسة الإضرابات التى تحدث فى الشبكة الكهربية وتأثير هذة الاضرابات على ملاحقة نقطة القدرة العظمى وتم دراسة مجموعة من هذة الاضرابات وعمل دراسة مقارنة لتتبع الثلاث تقنيات المختلفة و تم عمل نموذج كامل لأنظمة الخلايا الضوئية الموصلة مع الشبكة لمحاكاة الحياة الفعلية للنظام.

و قد اظهرت نتائج المحاكاة أن النظام المبهم يكشف أن الخوارزمية المقترحة تعطى تفوق واضح بالنسبة لتتبع النقطة العظمى من حيث السرعة ودقة الأداء ويعطى اقل تذبذب حول النقطة العظمى مقارنة بالأنظمة التقليدية و أيضا يعطى حاكم الدائرة العاكس استجابة سريعة للمتغيرات التى تحدث مما يسهل من عملية التتبع.

و إضافة الى ذلك فإن نتائج المحاكاة تحت ظروف الحالة المستقرة تظهر فاعلية النظام المبهم مقارنة بالأخرين، أما فى ظل الظروف العابرة تظهر أن القدرة المنتقلة الى الشبكة تظل تقريبا ثابتة مع استخدام المقترح المبهم مما يساعد على توصيل الخلايا الضوئية مع الشبكة الكهربية دون حدوث ضرر فى دائرة العاكس.

الاكاديمية العربية للعلوم و التكنولوجيا والنقل البحرى
كلية الهندسة و التكنولوجيا
قسم الهندسة الكهربية والتحكم

تحليل جودة الطاقة لأنظمة الخلايا الشمسية الموصلة مع الشبكة

رسالة الماجيستير

مقدمة من:

مهندس / باسم عبد الحميد رشاد عبدالرازق

للحصول على درجة الماجيستير فى الهندسة الكهربية و التحكم

تحت إشراف

أستاذ دكتور / المعتز يوسف عبد العزيز
مشرف

_____

دكتور / هادى ماجد الحلو
مشرف

_____

لجنة التحكيم

أستاذ دكتور /أحمد عبدالستار عبدالفتاح
ممتحن

_____

أستاذ دكتور /سعيد عبدالمنعم محمد وحش
ممتحن

_____

القاهرة ٢٠١٤

الاكاديمية العربية للعلوم و التكنولوجيا والنقل البحرى
كلية الهندسة و التكنولوجيا
قسم الهندسة الكهربية والتحكم

تحليل جودة الطاقة لأنظمة الخلايا الشمسية الموصلة مع الشبكة

رسالة الماجيستير

مقدمة من:

مهندس / باسم عبد الحميد رشاد عبدالرازق

للحصول على درجة الماجيستير فى الهندسة الكهربية و التحكم

تحت إشراف

أستاذ دكتور / المعتز يوسف عبد العزيز
قسم القوى الكهربية و الالات
كلية الهندسة
جامعة عين شمس

دكتور / هادى ماجد الحلو
قسم القوى الكهربية و التحكم
كلية الهندسة
الاكاديمية العربية للعلوم و التكنولوجيا والنقل البحرى

القاهرة ٢٠١٤